THE SLICHTER MODES IN A REALISTIC EARTH MODEL

ZHENGRONG PENG

National Library
of Canada

Acquisitions and
Bibliographic Services Branch

395 Wellington Street
Ottawa, Ontario
K1A 0N4

Bibliothèque nationale
du Canada

Direction des acquisitions et
des services bibliographiques

395, rue Wellington
Ottawa (Ontario)
K1A 0N4

Your file Votre référence

Our file Notre référence

NOTICE

The quality of this microform is heavily dependent upon the quality of the original thesis submitted for microfilming. Every effort has been made to ensure the highest quality of reproduction possible.

If pages are missing, contact the university which granted the degree.

Some pages may have indistinct print especially if the original pages were typed with a poor typewriter ribbon or if the university sent us an inferior photocopy.

AVIS

La qualité de cette microforme dépend grandement de la qualité de la thèse soumise au microfilmage. Nous avons tout fait pour assurer une qualité supérieure de reproduction.

S'il manque des pages, veuillez communiquer avec l'université qui a conféré le grade.

La qualité d'impression de certaines pages peut laisser à désirer, surtout si les pages originales ont été dactylographiées à l'aide d'un ruban usé ou si l'université nous a fait parvenir une photocopie de qualité inférieure.

Canada

The Slichter Modes in a Realistic Earth Model

© Zhengrong Peng (M. Sc.)

A thesis submitted to the School of Graduate

Studies in partial fulfillment of the

requirements of the degree of

Doctor of Philosophy

Department of Earth Sciences

Memorial University of Newfoundland

Octorber 1995

St. John's Newfoundland

TO MY PARENTS

Abstract

The density contrast across the inner core boundary is a critical parameter for evaluating the gravitational energy released from the segregation of the core material upon its cooling and solidification, a process which is one of the main contenders for the source of power of the geodynamo action in the Earth's fluid core. However, the density jump at the inner core boundary has so far not been well determined by conventional short-period seismology. It is known that the eigenperiods of the (not yet detected) Slichter modes critically depend on this density difference. The Slichter modes are the triplet of degree 1 long-period free oscillations of the Earth which involve translational vibration of the solid inner core in the surrounding liquid outer core. In this thesis, the eigenperiods of the Slichter modes for a realistic Earth model are computed by a variational principle based on the subseismic approximation and by a Galerkin method based on the two potential description of core dynamics. In this study, I have taken into account: (1) elastic deformation of the mantle and inner core, connected to liquid core dynamics via frequency-dependent internal load Love numbers; (2) retention of the self coupling of the displacement field in the solid parts of the Earth, and the Coriolis coupling up to degree 7 in the liquid core so as to ensure convergence; (3) elliptical stratification of the inner and outer cores (but not the mantle); (4) effects of a mushy inner core boundary. The research is a more comprehensive study of the Slichter oscillation than any previously undertaken, and is aimed to provide theoretical references for helping to determine the density contrast across the inner core boundary.

Key words: Free oscillation; Slichter modes; Love numbers; inner core.

Acknowledgements

I am grateful to my supervisor, Professor M. G. Rochester, for suggesting the topic and necessary revisions of the project from time to time, and for his constant guidance and support in carrying out this research, and during the writing of this thesis.

I would also like to thank the other members of my supervisory committee, Dr. J. Wright, Dr. C. Wright and Dr. L. Lines for their help.

Thanks are due also to Dr. W. Wu and Mr. B. Seyed-Mahmoud for helpful discussions during this research.

I would like to thank Dr. J. Rendell and K. Fagan, K. Munro, B. Ferguson, J. Rose, N. Earle, L. Detta, D. Casey, G. Bavington, G. Collins and V. Krishna of the MUN Writing Centre for their help in improving my written English.

I would like to acknowledge the use of facilities of the Department of Earth Sciences, Computing Services, and the Queen Elizabeth II Library of Memorial University of Newfoundland.

My graduate study was funded by Graduate Fellowships of the School of Graduate Studies of Memorial University of Newfoundland and from the NSERC research grant number A-1182, held by Professor Rochester.

Finally, I want to thank my parents and my brothers and sisters for their understanding and moral support, and my wife Zongshen Song and son Ruiqing Peng for their patience and encouragement.

Table of Contents

List of Tables

List of Figures

Glossary of Symbols and Abbreviations

Chapter 1 Introduction

1.1 Motivation for studying the Slichter Modes

For centuries people have been fascinated by the Earth's magnetic field and tried hard to seek its origin. It is now believed that the electrical current and flow patterns in the liquid core (LC) generate the geomagnetic field by dynamo action. A key issue is to find the source of the energy which drives the core flow. Earlier proposals of precession-driven flows or thermal convection were shown to be energetically impotent (Rochester *et al.*, 1975) or inefficient (Gubbins, 1977). Presently, the most favoured mechanism to power the dynamo is the gravitational differentiation of the inhomogeneous outer core fluid (Verhoogen, 1961; Braginskii, 1963). This compositional differentiation results in the formation and growth of the solid inner core (IC) through geological time.

A good indication of the inner core growth is the density contrast across the inner core boundary (ICB). It is evidence for a compositional difference between the two regions, and a measure of the gravitational potential energy released from the cooling and solidification process of the core material. It is now commonly accepted that the Earth's magnetic field has existed for at least 3.6 billion years (McElhinny *et al.*, 1980). If the core has been steadily crystallizing for the last 4 billion years, then the average ICB growth rate would be about 0.03 cm/year (Anderson & Young, 1988). The rate of energy release due to core growth would be about 2×10^{12} W, which is adequate to maintain a modest magnetic field of about 5×10^{-3} tesla (50 gauss) in the liquid core (Gubbins, 1977).

However, the density difference at the inner core boundary has so far not been very

well determined by conventional short-period seismology, indeed different data sources give quite different range of values for this density jump. The reflected P-wave at the inner core boundary ($PKiKP$) carries little energy, so they are therefore difficult to observe (Shearer & Masters, 1990). This makes the value of the density jump inferred from the amplitude ratio $PKiKP$ / PcP unreliable. The inhomogeneities near the core mantle boundary (CMB) inferred from complexities associated with the reflection of PcP wave also contribute to the poor determination of this parameter (Buchbinder *et al.*, 1973). A range of 1.3 - 1.6 $\times$ 10^3 kg m^{-3} is inferred from $PKiKP$ data (Souriau & Souriau, 1989). On the other hand, a set of short-period free oscillation data suggests that a range of 0.4 - 0.7 $\times$ 10^3 kg m^{-3} is more likely (Shearer & Masters, 1990).

For a better determination of this density jump, a seismological phenomenon which is critically dependent on this parameter has to be sought. There is an ideal candidate which can help to evaluate this parameter: it is the set of inner core translational modes (the Slichter modes), a special kind of long-period free oscillation of the Earth in which the solid inner core sloshes back and forth inside the fluid outer core. The eigenperiod of the Slichter mode (T) in a non-rotating Earth model is found to be critically dependent on the density jump at the ICB. The dependence can be approximately expressed as

$$T \sim k(\rho_{IC} - \rho_0)^{-1/2} \tag{1}$$

where k depends on the dimensions and densities of the inner and outer cores, and ρ_{IC} and ρ_0 are the densities of the inner and outer cores at the ICB respectively. To obtain the simple relation (1), it was assumed that the only restoring forces in the system are flow pressure on the inner core boundary and gravity on the entire inner core.

The Slichter modes were first predicted following the 1960 Chilean earthquake when an unusual gravity signal, showing a peak with a period of 86 min (amplitude of about 100 nanogals), was recorded on a LaCoste-Romberg earth-tide gravimeter. Slichter (1961) proposed that the observed signal could have been produced by the translational oscillation of the inner core in the surrounding fluid, like a pendulum swinging in the air. The mantle responds in a similar manner but with an opposite direction and a much smaller amplitude while the Earth's centre of mass remains fixed. Because of the Earth's rotation, a single mode is split into three different polarizations (a triplet): one axial and two equatorial (one retrograde and one prograde with respect to the sense of the Earth's rotation). Collectively these are called the Slichter *modes*. This splitting mechanism has great diagnostic significance for mode-identification. Knowing the frequency of one member of the triplet, those of the other two follow. Although Slichter's identification was later dismissed due to its unreasonably high amplitude and the lack of spatial and temporal supporting observations, it generated a significant impact on long period free oscillation research. Since then, a series of efforts, so far unsuccessful, have been made to detect these modes (Jackson & Slichter, 1974; Rydelek & Knopoff, 1984). However, recent studies (Crossley, 1988; Crossley *et al.*, 1991; Crossley, 1992) have concluded that, of the long-period (> 1 hr) normal modes (see §1.2), the Slichter modes are the most likely long-period core modes to be excited by a large deep earthquake. The seismic energy spreading from earthquakes flexes the core-mantle boundary and thus, sends a disturbance through the liquid core causing the inner core to oscillate. Another possible source of energy to joggle the inner core is from asymmetric crystallization of the liquid core material at the inner core boundary.

The detection of the Slichter modes requires the development of a satisfactory theory based on a realistic Earth model, without which one cannot be sure of correctly identifying the Slichter periods in the spectra of disturbances. The purposes of this thesis are to calculate the eigenperiods of the Slichter modes for a realistic Earth model, to estimate numerically the effects on the eigenperiods of various factors associated with the properties and the nature of the Earth, and to gain supporting evidence for the evaluation of the density change across the inner core boundary.

1.2 Free Oscillations and the Slichter Modes

The Slichter modes are the gravest (i.e. longest period) degree 1 free oscillations of the Earth. Like any other mechanical system, the planet Earth has its own natural oscillations which can be excited. Once it is set into vibration, the Earth can oscillate in an infinite number of normal modes for a long time (i.e. many days), ringing like a giant bell.

The study of free oscillations of an elastic body can be traced back to as early as 1829 when Poisson first investigated the vibration of a perfectly elastic sphere. Kelvin and Darwin later developed and applied the strain theory to an elastic sphere to study the tidal phenomena of the Earth (Bullen & Bolt, 1985). Lamb (1882) succeeded in separating the free vibration of a spherical body into two distinct types: the spheroidal type involving compression (or dilatation) and transverse motion, and the toroidal type involving twisting. The theories of elastic deformation and free oscillations have since been further developed for commonly used Earth models (Bullen & Bolt, 1985).

The identification of the free oscillations of the Earth was made for the first time follow-

ing the Kamchatka earthquake of November 1952, Richter magnitude M = 8.25 (Bullen & Bolt, 1985). However, globally distributed and independently confirmed recordings of free oscillations were not reported until the Chile earthquake of May 1960, M = 8.3 (Bullen & Bolt, 1985). Indeed, two types of oscillations were recorded following that earthquake: the spheroidal modes and the toroidal modes. It is known that only the radial component of the spheroidal modes is observable with a long period vertical instrument like gravimeters. The toroidal modes, which have no radial components, are best observed in the horizontal directions with clinometers or strainmeters.

Theoretical study and observations of the free oscillations of the Earth have led to a major advance in constructing new refined models of the Earth's interior and provide a further constraint on the inference of physical properties of the Earth from ray seismology (Haddon & Bullen, 1969; Dziewonski & Anderson, 1981). Recent Earth models, such as 1066A (Gilbert & Dziewonski, 1975), PREM (Dziewonski & Anderson, 1981) or CORE11 (Widmer *et al.*, 1988), have all used a large number of normal mode periods of free oscillations in conjunction with travel time observations.

It is now customary to further classify free oscillations of the Earth broadly into two groups: high-frequency normal modes (with periods shorter than an hour), familiar to seismologists as the above stated spheroidal and toroidal modes, and low-frequency normal modes (with periods longer than an hour). This classification is also based on the nature of the restoring forces sustaining the oscillations. The main restoring force for the high-frequency normal modes is the elasticity of the Earth, which is known to generate acoustic waves. Therefore, these modes are sometimes called 'acoustic modes' (Smylie & Rochester,

1981; Rochester, 1989). The restoring forces for the low-frequency normal modes are gravitational and Coriolis so these modes are called 'gravitational/inertial modes'. These long period normal modes can be important in a rotating fluid body (i.e. the liquid core) due to absence of rigidity.

Compared to the period of the Earth's rotation, the periods of the high-frequency normal modes are short enough that the effects of the Coriolis force can be considered as a small perturbation to the solutions of a non-rotating Earth model. Suppose ${}_l\omega_n^0$ is the eigenfrequency of a non-rotating Earth, then the eigenfrequencies of a rotating Earth could be calculated from the following formula

$$ {}_l\omega_n^m = {}_l\omega_n^0 + m\, {}_l\eta_l \Omega \tag{2} $$

where l, m and n are respectively the radial quantum number, order and degree of a mode, Ω is the steady rotational speed of the Earth, and ${}_l\eta_l$ is the splitting parameter (Bullen & Bolt, 1985). The perturbation caused by the Coriolis force removes the degeneracy of the eigenfrequencies associated with the azimuthal order m. A mode of degree n of a non-rotating Earth will now contain a $(2n + 1)$-fold multiplet if the rotation of the Earth is involved. It needs to be emphasized that the splitting formula (2) is valid only if the effect of the Coriolis splitting on a mode can be regarded as a small perturbation.

In the absence of rotation, the Earth can with considerable accuracy be regarded as spherically stratified due to self gravitation. The displacement field $\mathbf{u}$ and the gravitational perturbation V_l in this case can be most conveniently represented by the standard spherical harmonics

$$ \mathbf{u} = \sum_{l=-\infty}^{\infty} \sum_{n=0}^{\infty} \sum_{m=-n}^{n} \{ {}_l\mathbf{S}_n^m + {}_l\mathbf{T}_n^m \} \tag{3} $$

$$V_1 = \sum_{l=-\infty}^{\infty} \sum_{n=0}^{\infty} \sum_{m=-n}^{n} {}_l\Phi_n^m(r) Y_n^m(\theta, \phi) \tag{4}$$

where

$${}_l\mathbf{S}_n^m = [{}_l u_n^m(r)\hat{\mathbf{r}} + r \quad {}_l v_n^m(r)\nabla] Y_n^m(\theta, \phi)$$

$${}_l\mathbf{T}_n^m = {}_l\, t_n^m(r)\hat{\mathbf{r}} \times \nabla Y_n^m(\theta, \phi)$$

$$Y_n^m(\theta, \phi) = P_n^m(\cos\theta) e^{im\phi}.$$

Here ${}_l u_n^m$, ${}_l v_n^m$, ${}_l t_n^m$ and ${}_l\Phi_n^m$ are functions of radius r only, and P_n^m is the associated Legendre function. For a non-rotating Earth model, the orthogonal property of the spherical harmonics ensures that each spheroidal or toroidal field of a given degree n represents a single normal mode, with $(2n + 1)$-fold degeneracy in order m. The radial quantum number $l > $ or < 0 according as the mode in question is an overtone or undertone of the fundamental ($l = 0$). In a non-rotating Earth model, undertones are possible only if the fluid outer core is somewhere stably stratified.

However, the above treatments are no longer valid for low-frequency normal modes, such as gravitational/inertial modes, and the Slichter modes. The periods of these normal modes can be a significant fraction of half a day. Therefore, the Coriolis force can no longer be treated as a small perturbation. Instead, the Coriolis effect provides a restoring force for the toroidal modes, which in turn couples the spheroidal modes of different degrees into infinite chains of form

$${}_l\mathbf{S}_{|m|}^m + {}_l\,\mathbf{T}_{|m|+1}^m + {}_l\,\mathbf{S}_{|m|+2}^m + {}_i\,\mathbf{T}_{|m|+3}^m + \cdots \tag{5}$$

or

$$ {}_l\mathbf{T}^m_{|m|} + {}_l\mathbf{S}^m_{|m|+1} + {}_l\mathbf{T}^m_{|m|+2} + {}_l\mathbf{S}^m_{|m|+3} + \cdots . \tag{6} $$

The translational oscillation of the inner core is special in that it belongs neither to the conventional 'acoustic' modes, since its period is much longer than an hour and the main restoring force which sustains the oscillation is not elastic in nature; nor to the 'gravitational/inertial' modes, since its existence does not depend on any stable stratification of the liquid core or on the Earth's rotation. Of course the rotation, and even neutral radial stratification, would have a substantial influence on the Slichter modes. Crossley (1975) proposed that a Slichter mode should be regarded as a first undertone (period > 1 hour) of the $n = 1$ set of spheroidal modes, corresponding to a displacement field ${}_{-1}\mathbf{S}^m_1$, whereas Rochester & Peng (1993) argued that it should not be so classified since its existence does not require rotation or stable stratification of the liquid core. Note that conservation of linear momentum forbids the existence of a free mode $n = 1$, $l = 0$. The Slichter modes are now generally denoted as ${}_1\mathbf{S}^m_1$, i.e. the first overtone $l = 1$ of the degree $n = 1$ modes (Crossley *et al.*, 1992; Rochester & Peng, 1993). But due to Crossley's suggestion, the term 'Slichter-type oscillation' is used for the undertones of a longer period, which are possible when the liquid core is stably stratified. Since this thesis concentrates only on the Slichter modes themselves, I drop the index l from now on.

Therefore, the displacement field with rotational coupling, for the Slichter modes, will now read

$$ \mathbf{u} = \mathbf{S}^m_1 + \mathbf{T}^m_2 + \mathbf{S}^m_3 + \mathbf{T}^m_4 + \cdots . \tag{7} $$

i.e. a chain consisting of odd-degree spheroidal ($\mathbf{S}_n^m$) and even-degree toroidal ($\mathbf{T}_n^m$) displacement fields.

The coupling coefficients between successive terms in (5), (6) or (7) are proportional to $2\Omega/\omega$, where ω is the eigenfrequency of a vibration. At low frequencies, the amplitude of the coupling coefficient is close to 1, thus a longer coupling chain is needed for ensuring a convergence of numerical estimates of eigenfrequencies and eigenfunctions. This issue has been widely addressed by a number of authors (Smith, 1974; Haarden-Pedersen, 1975; Johnson & Smylie, 1977; Crossley & Rochester, 1980; Haarden-Pedersen & Bodri, 1980; Rochester, 1989; Rieutord, 1991), and appropriate methods have been sought to cope with this situation.

1.3 Previous Observational and Theoretical Studies

Crossley (1992) estimated that, for the PREM Earth model, the translational vibration of the inner core excited by a Chilean-type (1960) earthquake (with a focal depth of 25 km and a seismic moment of 10^{25} N m) could produce a gravity signal of about 0.5 nanogal at the Earth's surface. This is at the lower limit of detection by a superconducting gravimeter. Because of the extremely low magnitude of the signal, as much emphasis is placed on noise reduction of observation sites as on the sensitivity of the instruments. An ideal observing point for the Slichter modes is the south pole where the effects of diurnal tides and their higher harmonics (zero there on a spherical Earth) are minimized by distance from oceans, and which is seismically and culturally quiet. With a spring gravimeter at the south pole,

Jackson & Slichter (1974) achieved a noise level of 1 nanogal. If there were any translational modes with amplitude up to 1 nanogal excited during the period of observation (October 1970 - September 1971), it should have been recorded. The gradual establishment of a worldwide superconducting gravimeter network will play a major role in the observation and identification of the Slichter modes and the other core modes.

Busse (1974) was the first one to study the influence of the rotation and dimension of the liquid core on the Slichter mode. He concluded that the action of the Coriolis force on the motion of the fluid in the outer core, and the finite radius of the outer core may change the period of the mode by as much as 50 % from that predicted without taking these effects into account. He also found that the rotational splitting of the frequency was not symmetric. However, Busse's (1974) quantitative analysis was limited to the polar mode, the equatorial modes were studied qualitatively only. The Earth model used by Busse (1974) consists of a rigid sphere oscillating in a rotating incompressible homogeneous inviscid fluid. The fluid itself is contained within a concentric rigid spherical boundary.

In addition to considering the Earth's rotation, Crossley (1975) and Smith (1976) took into account the compressibility and radial stratification of the liquid core, as well as the elasticity of the inner core and mantle.

Smith (1976) also took into account the effects of the ellipticity of the Earth on the Slichter mode. He found that the rotational and elliptical splitting may vary the central period of the Slichter mode by about 10%, in which the main contribution to this splitting was from rotation. For an Earth model similar to that used by Busse (1974), the only difference being that the liquid core is radially stratified and the inner core is elastic, Smith

(1976) obtained a period of 7.653 hr for the polar mode, which is 20 % longer than Busse's result (6.397 hr). Both calculations used the same fractional density change ratio across the inner core interface ($\rho_{IC}/\rho_0 - 1 \approx 0.0328$).

Because the Coriolis coupling reduces the suitability of the spherical harmonic representation, numerical computations of eigenfrequencies and eigenfunctions of long period free oscillations had been severely limited before high-capacity computers became available. This led Crossley (1975) and Smith (1976) to retain only the first two terms in the expression (7) as their expansion of the displacement field of the liquid core. In solid parts of the Earth, Crossley (1975) restricted the coupling chain to the spheroidal field $\mathbf{S}_1^m$, whereas Smith (1976) extended it to the toroidal field $\mathbf{T}_2^m$. After much of the work reported in chapters 2 - 6 of this thesis had been done, Crossley (1992) extended the coupling chain much further, using different Earth models.

Dahlen & Sailor (1979) used a perturbation method to study the rotational and elliptical splitting of the free oscillations of the Earth. A convenient formula was developed there for calculating the amount of splitting. Their tabulated parameters include perturbations of second order in rotation and first order in ellipticity. The influence of the ellipticity on the Slichter modes is found not to exceed 0.1% for any member of the triplet.

Based on his theoretical prediction and analysis of the stacked super-conducting gravimeter data, Smylie (1992) claimed to have detected the Slichter triplet. However, the apparent discovery was nullified by his failure to recognize the frequency-dependent nature of the internal load Love numbers of degree 1, which are the key parameters relating the effects of the elastic inner core and mantle to the liquid core dynamics (Rochester & Peng, 1990; Crossley

et al., 1992; Rochester & Peng, 1993). Crossley *et al.* (1992) demonstrated that the Slichter eigenperiod lies very close to the resonance period of the ICB load Love numbers, therefore, it is essential to use the dynamic Love numbers for the Slichter modes. The use of the static load Love numbers also made Smylie's calculation of the amount of rotational splitting unrealistic. Even for a non-rotating Earth model, Smylie's prediction of the eigenperiods are roughly 40% shorter, and the Coriolis splitting of the triplet is about 60% narrower, than the correct values. The dependence of the load Love numbers on frequency will be further discussed in Chapter 3 of this thesis. On the other hand, Jensen *et al.* (1993) and Hinderer *et al.* (1993) argued on observational grounds that the peaks identified by Smylie (1992) were not significant, and indeed are barely above the noise level, and disappeared when more stringent processing tools were employed.

Taking a different approach than the direct integration method and the perturbation method, Rochester & Peng (1993) applied the subseismic approximation (SSA, details in Chapter 2) and a variational principle in the liquid core to compute the Slichter eigenperiods for a rotating, spherically stratified Earth model. The effects of the elastic inner core and mantle on the liquid core dynamics were transferred by the above discussed internal load Love numbers. Through a careful theoretical analysis, they identified and corrected a number of significant shortcomings in the recent treatments of the problem. Their result supports the conclusion of Rochester & Peng (1990) that the internal load Love numbers at the ICB and CMB are strongly frequency dependent. Serious errors would occur if the dynamical load Love numbers are replaced by the static ones.

Wu & Rochester (1994) examined the effects of melting/freezing at the ICB on the

eigenperiods of the Slichter modes. With a simple non-rotating Earth model, they regarded the ICB as a phase transition and ignored the possible existence of a mushy zone at the top of the ICB in the undeformed configuration. Using thermodynamic arguments, they demonstrated that the effects of melting and freezing at the ICB have a negligible effect on the Slichter eigenperiods.

The damping of the Slichter oscillation by various mechanisms has been further/newly studied recently by several authors. Crossley *et al.* (1991) investigated the damping of the Slichter mode (for a non-rotating Earth model) due to anelasticity, and found that the decay time is about a year. Smylie (1992) quantitatively estimated the kinematic viscosity of the liquid core fluid using the quality factor of the axial mode. Smylie & Qin (1992) used a boundary layer solution to calculate the drag that the inner core exerts on the outer core fluid, and the viscous dissipation in the boundary layer. However, quantitative estimate of damping time due to liquid core viscosity has not appeared in literature. Rochester (1994, unpublished) studied the thermal damping effects on the Slichter modes. He concluded that the damping time of a Slichter vibration of amplitude of about 1 cm, due to melting/freezing at the ICB, is several thousand years. Buffett & Goertz (1995) investigated the effects on the Slichter modes of Lorentz forces and ohmic dissipation associated with the magnetic field perturbation near the ICB. They found that the main effect is the damping of the oscillations, although the eigenperiods of the modes would also be affected. The time scale of magnetic damping can range from 150 days to 108 years, depending on the value of average radial magnetic field near the ICB used (0.5 - 1.0 $\times$ 10^{-3} tesla).

1.4 Scope of Research Reported in This Thesis

This thesis is divided into 11 chapters as described below:

Chapter 2 is a brief review of the subseismic approximation, and the associated advantages and disadvantages in applying it to core dynamics.

In Chapter 3, the internal load Love numbers at the ICB and CMB are derived. The frequency dependence of these Love numbers are correctly taken into account. Then a set of effective load Love numbers are developed to utilize the application of the SSA in a neutrally stratified liquid core.

In Chapter 4, a variational principle is constructed using the effective load Love numbers to solve the subseismic wave equation (SSWE). The variational principle is an alternative to the direct integration of the ordinary differential equations (ODE) with a Runge-Kutta method. The latter process has been widely used in free oscillation literature (Smith, 1974; Smith, 1976; Crossley, 1975; Wahr, 1981). However, it is shown that a variational principle for the SSWE alone exists only if the liquid core is neutrally stratified. Therefore, I computed the Slichter eigenperiods in Chapter 4 only for a modified PREM model (so as to have an exactly neutral liquid core). The resonance character of the internal load Love numbers and effective load Love numbers are discussed in this chapter, along with the spurious roots found near the eigenperiods of the Slichter modes. I also calculated and plotted the eigenfunctions of the Slichter modes using the SSA. Due to the application of the SSA in the liquid core, and the use of the natural boundary conditions in the variational principle, the eigenfunctions so calculated exhibit some kind of distortion at the outer core boundaries, as well as in the mantle. The discussion regarding this feature is presented at the end of Chapter 4. Some

results of this chapter were published in Rochester & Peng (1993).

Chapter 5 describes the application of the exact two-potential description (TPD) of core dynamics (Wu & Rochester, 1990) in Slichter modes modelling. A brief review of the formulation of the TPD and some shortcomings of the method are given in this chapter.

Chapter 6 outlines the Galerkin method, based on the TPD, which is constructed to calculate the eigenperiods of the Slichter modes for a rotating Earth model. The Galerkin method is an alternative approach to a variational principle, by which the stringent restrictions for the latter are relaxed. The results using the TPD for a neutrally stratified liquid core provided a test of the accuracy of the SSA applied earlier in this thesis. The computations show that the TPD method can easily handle both the neutral/non-neutral stratification of the liquid core. At the end of Chapter 6, I discuss the calculations and plot the eigenfunctions of the Slichter modes using the TPD. A comparison of these figures with those in Chapter 5 clearly shows that while the eigenperiods of the Slichter modes are obtained correctly using the SSA, its use brings certain errors to the eigenfunctions so calculated, especially to those of the mantle.

Chapters 7, 8 and 9 describe the evaluation of the effects of the centrifugal force and the ellipticity of the inner and outer cores on the Slichter modes. This was the first time that the spheroidal load Love numbers were developed and used to evaluate these effects. The method introduced here provides an alternative to the perturbation theory used by Dahlen & Sailor (1979).

At the beginning of Chapter 7, I briefly review the different approaches used by Smith (1976) and Dahlen & Sailor (1979) to tackle this problem. As I discussed earlier, Smith

(1976) only kept a two-term expansion in the liquid core displacement field and used a direct integration method, while Dahlen & Sailor (1979) applied a perturbation theory in their investigation. It is not known in advance if these treatments would yield satisfactory results. The calculations in this and subsequent chapters (8 and 9) may provide a test of the accuracy of these treatments. However, because the presence of the ellipticity of the Earth and centrifugal force makes the coupling of the spheroidal field of degree 1 to that of degree 3, it is expected that the perturbation theory will give a more complete treatment of the problem than using only a two-term expansion. The assumption for using the perturbation theory or a heavily truncated coupling chain of the displacement field in the direct-integration method is that the eigenfrequency of the mode in question is much higher than 2Ω.

In the rest of Chapter 7, I shall first discuss how to handle the eigenvalue problem for an ellipsoidal Earth model in a consistent way both in the interior and near boundaries. Two different approaches are discussed: Smith's (1974) approach, and an improvement on Smith's approach. However, without losing much accuracy, as well as for computational efficiency, I will use Smith's (1974) approach in the final computation to formulate the governing differential equations for the ellipsoidal inner core and appropriate continuity conditions at the outer boundaries. These governing equations and boundary conditions are then used in Chapter 8 to calculate the effect of the inner core on the outer core dynamics in terms of the spheroidal load Love numbers. The coefficient matrix of this equation set is given in Appendix A.

Chapter 8 presents the calculations of the internal spheroidal load Love numbers at the ICB including the effects of the centrifugal force and ellipticity of the inner core. The first

part of this chapter illustrates the derivation of the starting solutions of the 14th order ordinary differential equations at the geocentre. The second part illustrates the formulation of the appropriate continuity conditions at the ellipsoidal liquid core boundaries. The details of the formulation of the boundary conditions are presented in Appendix B. Here I retain the effects of the ellipticity only to first order, the effects of rotation to second order at least, and the elliptical/Coriolis coupling to a toroidal field $\mathbf{T}_2^m$ and a spheroidal field $\mathbf{S}_3^m$.

Chapter 9 is used to find Galerkin solutions of the two-potential description in an ellipsoidally stratified liquid core. In this ellipsoidal fluid shell, the full effects of the Coriolis /elliptical /centrifugal coupling are taken into account by employing the Galerkin method based on the TPD which has then been modified accordingly. That only the elliptical stratification of the outer and inner cores are taken into consideration, relies on the fact that the Slichter modes are apparently dominated by the degree 1 spheroidal displacement field of the inner core.

In Chapter 10, I will investigate the effects of a mushy inner core boundary on the Slichter modes for a simple Earth model (rotating, spherical configuration). The mushy inner core boundary has been discussed by several researchers (Cummins & Johnson, 1988; Shearer & Masters, 1990), but this is the first time that a mushy zone on the top of the inner core is incorporated into the Slichter modes computation.

Chapter 11 is the summary of the thesis.

Chapter 2 The Subseismic Approximation

2.1 Introduction

As I discussed in §1.2, the perturbation method may not yield satisfactory results for long period free oscillations. On the other hand, a heavy truncation of the coupling chain of the displacement field in the direct-integration method may raise serious questions about convergence. In an attempt to overcome these difficulties in long period normal modes calculation, Smylie & Rochester (1981) proposed an approximation. They called it the 'subseismic' approximation since it is applicable only to low-frequency (less than 300 μHz) vibrations. By neglecting the contribution of the Eulerian flow pressure to compression, in comparison with the contribution of transport through the hydrostatic pressure gradient, the SSA effectively removes the acoustic modes from the free oscillation eigenspectrum. Mathematically, the SSA is used to convert the entire free oscillation problem from the simultaneous solution of a fourth-order coupled system of partial differential equations in four variables, to the solution of a single second order partial differential equation in one scalar variable. However the utility of the SSA is greatly reduced by the fact that the boundary conditions to be satisfied still involve solutions of the Poisson equation (Rochester, 1989).

2.2 The Subseismic Approximation

Assuming an equilibrium configuration in which the Earth is at rest in a steadily-rotating reference frame, free oscillations of the liquid core without dissipative mechanism are governed by a set of six equations (three scalar equations and three components of a vector equation) which express the conservation of entropy (equation of state), mass, momentum and gravitational flux respectively:

$$\frac{p_1}{\rho_0} = -\alpha^2 \nabla \cdot \mathbf{u} - \mathbf{u} \cdot \mathbf{g}_0 \tag{8}$$

$$\rho_1 = -\nabla \cdot (\rho_0 \mathbf{u}) \tag{9}$$

$$-\omega^2 \mathbf{u} + 2i\omega\Omega \hat{\mathbf{k}} \times \mathbf{u} = -\frac{1}{\rho_0}\nabla p_1 + \nabla V_1 + \frac{\rho_1}{\rho_0}\mathbf{g}_0 \tag{10}$$

$$\nabla^2 V_1 = -4\pi G \rho_1 \tag{11}$$

where (10) is a vector equation which is equivalent to three scalar equations. Here α is the compressional wave speed, p_1 is the Eulerian flow pressure, ρ_0 and $\mathbf{g}_0$ are the density of the liquid core and the gravitational acceleration respectively at equilibrium, ρ_1 is the Eulerian density increment, ω is the vibration frequency, and $\hat{\mathbf{k}}$ is the unit vector aligned with the Earth's rotation axis. The SSA suggests that the following inequality holds

$$\left|\frac{p_1}{\rho_0}\right| \ll |\mathbf{u} \cdot \mathbf{g}_0|, \tag{12}$$

and it simplifies the equation of state (8) as

$$\nabla \cdot \mathbf{u} = -\frac{\mathbf{u} \cdot \mathbf{g}_0}{\alpha^2}. \tag{13}$$

Smylie & Rochester (1981) show how to reduce these six governing equations (8) - (11) to a pair of partial differential equations; the Poisson equation and the 'subseismic wave equation' (SSWE), based on only two scalar potential quantities V_1 and χ:

$$\frac{1}{4\pi G\rho_0}\nabla^2 V_1 = \frac{1}{B}\mathbf{C}\cdot\nabla\chi \tag{14}$$

$$\nabla\cdot(f\mathbf{\Gamma}\cdot\nabla\chi) = 0 \tag{15}$$

where

$$\chi = \frac{p_1(\mathbf{r})}{\rho_0} - V_1(\mathbf{r}) \tag{16}$$

$$B = \frac{\alpha^2\omega^2}{\beta}(1-\mu^2) + g_0^2 - \mu^2(\hat{\mathbf{k}}\cdot\mathbf{g}_0)^2 \tag{17}$$

$$\mathbf{C} = \mu^2\hat{\mathbf{k}}\hat{\mathbf{k}}\cdot\mathbf{g}_0 - \mathbf{g}_0 + i\mu\hat{\mathbf{k}}\times\mathbf{g}_0 \tag{18}$$

$$\mathbf{\Gamma} = \mathbf{1} - \mu^2\hat{\mathbf{k}}\hat{\mathbf{k}} - \frac{\mathbf{C}\cdot\mathbf{C}}{B} + i\mu\hat{\mathbf{k}}\times\mathbf{1} \tag{19}$$

$$\mu = \frac{2\Omega}{\omega} \tag{20}$$

where $\mathbf{1}$ is a unit tensor, and f (which Smylie *et al.* (1992) termed the 'decompression factor') was first introduced by Friedlander (1988):

$$f = \exp\left(\int_{ICB}^{W_0}\frac{1}{\alpha^2}dW_0\right) \tag{21}$$

with W_0 representing the equilibrium geopotential. The stability parameter β was first used by Pekeris and Accad (1972), and it satisfies the following relation

$$\nabla\rho_0 = (1-\beta)\frac{\rho_0\mathbf{g}_0}{\alpha^2}. \tag{22}$$

Note that in this thesis, μ and β are also used to denote rigidity and shear wave speed respectively in the solid parts of the Earth. Fortunately, they do not appear at the same time and should not be confused.

The stability parameter measures the departure of the Earth's equilibrium density profile from that due to purely adiabatic compression of a chemically homogeneous material. Therefore, it is a key to understanding the thermal state of the liquid core - which is also critical to the geodynamo theory - and its interaction with the lower mantle. Specifically, the sign of β is associated with the state of stratification: negative, zero or positive values everywhere correspond to a gravitationally stable, neutral or unstable stratification of the liquid core respectively. Unfortunately, like the density contrast at the ICB, the stability parameter has so far also not been well determined by conventional short period seismology. It is hoped that the observation of long period 'gravity' modes will shed light on the evaluation of β. The gravity wave may be possible only if at least part of the liquid core is stably stratified (Smylie, 1974).

The estimate of the stability parameter so far has been mostly based on thermodynamics. Earlier work of Higgins & Kennedy (1971) had ruled out the possibility of whole-liquid-core radial convection. Kennedy & Higgins (1973) suggested that it is unstable and convective near the inner core boundary, and neutral or stable in the rest of the liquid core. Fearn & Loper (1981) argued that the liquid core is unstably stratified throughout except for a thin layer which may be stably stratified, some 70 km deep below the core mantle boundary, and made up of light material segregated as the inner core grows. Gubbins *et al.* (1982) agreed with a stable layer at the top of the liquid core, but argued that the layer is growing

downwards from the core mantle boundary, due to the Earth's slow cooling, reaching a thickness of 100 - 1000 km. Loper (1984) offered an alternative mechanism which suggests that the stable layer grows downwards from the CMB due to a chemical interaction there. The uncertainty of the parameter has led some researchers to assume, for simplicity in their modelling, that it is a constant (Pekeris & Accad, 1972; Smylie, 1974; Crossley, 1975). Since the Slichter modes are not sensitive to the stability parameter (Smith, 1976; Wu & Rochester, 1994), I will not pursue it any further in this thesis. It is sufficient to note that the density profile of the PREM Earth model, which is used throughout this thesis, delineates a slightly unstable region near the ICB, and a slightly stable region near the CMB. The rest of the liquid core is nearly neutrally stratified in this model (Peng, 1990).

In principle, once the SSWE is solved, the solution χ can be substituted in the Poisson equation to obtain V_1. Then the displacement $\mathbf{u}$ and the perturbation in density ρ_1 and pressure p_1 and are obtained from the other relevant equations.

For a neutrally stratified liquid core, $\beta = 0$ and $B \to \infty$, $\mathbf{\Gamma}$ of (19) reduces to the Poincaré tensor

$$\mathbf{\Gamma}_p = \mathbf{1} - \mu^2 \hat{\mathbf{k}}\hat{\mathbf{k}} + i\mu\hat{\mathbf{k}} \times \mathbf{1} \tag{23}$$

and the SSWE reduces to

$$\nabla \cdot (\rho_0 \mathbf{\Gamma}_p \cdot \nabla\chi) = 0 \tag{24}$$

with f replaced by $\rho_0(\mathbf{r})$. The Poisson equation (14) reduces to the Laplace equation

$$\frac{1}{4\pi G\rho_0}\nabla^2 V_1 = 0. \tag{25}$$

2.3 Restrictions to the Application of the Subseismic Approximation

The SSA has been extensively used in long period free oscillation calculations (Smylie & Rochester, 1981; Shen, 1983; Smylie *et al.*, 1984; Smylie & Rochester, 1986a, 1986b; Friedlander, 1987; Dehant, 1988; Smylie, 1988; Wu & Rochester, 1988; Rochester, 1989; Peng, 1990; Smylie *et al.*, 1990; Wu & Rochester, 1990; Crossley, 1992; Crossley & Rochester, 1992; Crossley *et al.*, 1992; de Boeck *et al.*, 1992; Smylie *et al.*, 1992; Webb, 1992; Crossley, 1993; Rochester & Peng, 1993; Wu, 1993; Wu & Rochester, 1993, 1994). While the full potential and advantages of the SSA were explored, some disadvantages also became apparent.

A variational principle for the the SSWE alone could be constructed only for an Earth model with spherical rigid-fixed outer core boundaries, or deformable boundaries but with a strictly neutral liquid core. Otherwise, the Hermitean property of the subseismic operator, as in (15), is violated (Rochester, 1989; Wu & Rochester, 1990; Crossley & Rochester, 1992; Rochester & Peng, 1993). This failure arises from a requirement in the boundary conditions at the ICB and CMB that the Poisson equation has to be solved simultaneously with the SSWE. Hence the main advantage of the SSA is lost. Whereas if the liquid core is neutrally stratified, the Poisson equation reduces to a Laplace equation with a single potential field V_1 only, which then can be solved independently. The match of continuity conditions at the ICB and CMB for solving the SSWE alone in a neutral liquid core are to be implemented by a set of 'effective' load Love numbers, which I shall discuss in Chapter 3.

While applying the SSA in the body of the liquid core gives satisfactory results (eigenfre-

quencies are obtained correctly), it fails badly near a boundary which does not move much, such as the CMB. The mantle has a much higher rigidity and a larger volume compared to those of the liquid core (Crossley & Rochester 1992). This fact grossly violates the inequality (12), which is the backbone of the SSA. Consequently, extending computations of the eigenfunctions from the liquid core to the solid parts of the Earth, especially to the mantle, is jeopardized. More specifically, it seems that conservation of the linear momentum across the CMB is violated. I will further discuss this problem in Chapter 4 with computations of the eigenfunctions.

In short, it can be concluded that the best use of the SSA is to find the eigenfrequencies of long period free oscillation modes for a relatively simple Earth model (e.g. spherical, rotating Earth with a neutral liquid core and deformable ICB and CMB). The results so obtained are close approximations to that of a more realistic Earth model, where non-neutral stratification of the liquid core and/or elliptical stratification of the Earth may be present. With these results as reference values, an exact calculation of the eigenvalue problem may be performed using more stringent methods, such as the two-potential description of core dynamics (TPD, Wu & Rochester, 1990), or extended direct integration. This indeed is the path this thesis follows, for the Slichter modes.

Chapter 3 Love Numbers at Spherical Core Boundaries

3.1 Introduction

Due to absence of rigidity, the response of the liquid core to deformation at long period is potentially more complicated than that of the solid inner core and mantle. For this reason, it is often convenient to centre the analysis of long-period normal modes around the dynamics of the liquid core, and treat the accompanying vibrations of the solid inner core and mantle as their response to the deformation of the ICB and CMB. Based on this viewpoint, the linearity of the relations between displacement, elastic stress and gravitational force suggests that the deformation of the solid side of a physical interface can be expressed as a linear function of the disturbing effects acting from the fluid side. The coefficients of such a function, at each of the core boundaries, can easily be made dimensionless. By analogy with the tidal Love numbers, which express the relation of the deformation of the Earth's surface to the tidal force potential acting there, these coefficients are called internal load Love numbers. This is the way I adopt in this thesis to describe the dynamics of the Earth.

It is known that the inner core translational motion involves a large S_1^m of the IC spheroidal field. However, it is difficult to decide *a priori*, for a given Earth model, how many terms in the coupling chain of the displacement field $\mathbf{u}$ should be retained in a numerical computation. Because of the enormous mass of the mantle, which accounts for 68 % of the Earth, its displacement in responding to that of the inner core for conserving the

linear momentum of the system is much smaller than the latter, so is its contribution to the Slichter oscillation. For this reason and also due to a much higher rigidity of the inner core and mantle compared to those of the liquid core, it is reasonable for simplicity to ignore the toroidal displacement fields generated by Coriolis coupling in the solid parts of the Earth. Such a treatment has also been justified by calculation; the effects of coupling to $\mathbf{T}_2^m$ changes the load Love numbers by no more than 0.0001% (Rochester & Peng, 1993). Therefore in this and the subsequent chapters I consider the Coriolis coupling only within the same degree (self-coupling) in the inner core and mantle, but will include the coupling of $\mathbf{T}_2^m$ from $\mathbf{S}_1^m$ to $\mathbf{S}_3^m$ in Chapter 7, where the ellipticity of the inner and outer cores are taken into account. In the liquid core, the use of the SSA enables a much longer chain of coupled spheroidal and toroidal fields to be used, for the same computational effort. The degree of truncation of the trial function series in the liquid core will be decided experimentally for ensuring a convergent eigenperiod.

The influence of the elasticity of the inner core and mantle on the liquid core dynamics are represented by the frequency-dependent internal load Love numbers at the ICB and CMB. To fully utilize the SSA when the core boundaries are deformable, a set of effective load Love numbers appropriate to a neutral liquid core will be introduced in this chapter. These effective load Love numbers are combinations of the ordinary load Love numbers at the ICB and CMB.

3.2 Internal Load Love Numbers at the Inner and Outer Core Boundaries

The governing system of differential equations for an elastic sphere or an elastic spherical shell with only the first order Coriolis self-coupling taken into account is most conveniently expressed in AJP notations (Alterman, Jarosch & Pekeris, 1959):

$$\frac{d\underline{y}}{dr} = \mathcal{A}\,\underline{y} \tag{26}$$

where

$$\underline{y} = (y_1\ y_2 \cdots y_6)^T$$

$y_1(r)$ and $y_3(r)$ are the radial parts (functions of r only) of the normal and transverse displacement fields. Referring to the definitions (3) of Chapter 1, they are defined as

$$y_1(r) = u_n^m(r) \tag{27}$$

$$y_3(r) = v_n^m(r). \tag{28}$$

$y_2(r)$ and $y_4(r)$ are the radial parts of the normal and shear stress fields,

$$y_2 = \lambda\left(\frac{du_n^m}{dr} + \frac{2u_n^m - n(n+1)v_n^m}{r}\right) + 2\mu\frac{du_n^m}{dr} \tag{29}$$

$$y_4 = \mu\left(\frac{dv_n^m}{dr} - \frac{v_n^m - u_n^m}{r}\right) \tag{30}$$

where λ and μ are two of the Earth's property parameters: the Lamé parameter and rigidity, respectively. Referring to the definition (4) of Chapter 1, $y_5(r)$ is the radial part of the additional gravitational potential field

$$y_5(r) = \Phi_n^m(r) \tag{31}$$

and $y_6(r)$ is the gravitational flux

$$y_6 = \frac{d\Phi_n^m}{dr} - 4\pi G\rho_0 u_n^m. \tag{32}$$

The matrix $\mathcal{A}$ in (26) consists of coefficients of y_i's of the governing equations, and they are functions of radius r, frequency ω, azimuthal order m and/or degree n. The nonzero elements of $\mathcal{A}$ are:

$$\mathcal{A}_{1,1} = -\frac{2\lambda}{(\lambda+2\mu)r}$$

$$\mathcal{A}_{1,2} = \frac{1}{\lambda+2\mu}$$

$$\mathcal{A}_{1,3} = \frac{n(n+1)\lambda}{(\lambda+2\mu)r}$$

$$\mathcal{A}_{2,1} = -\rho_0\omega^2 - \frac{4\rho_0 g_0}{r} + \frac{4\mu(3\lambda+2\mu)}{(\lambda+2\mu)r^2}$$

$$\mathcal{A}_{2,2} = -\frac{4\mu}{(\lambda+2\mu)r}$$

$$\mathcal{A}_{2,3} = 2m\rho_0\omega\Omega + \frac{n(n+1)\rho_0 g_0}{r} - \frac{2\mu n(n+1)(3\lambda+2\mu)}{(\lambda+2\mu)r^2}$$

$$\mathcal{A}_{2,4} = \frac{n(n+1)}{r}$$

$$\mathcal{A}_{2,6} = -\rho_0$$

$$\mathcal{A}_{3,1} = -\frac{1}{r}$$

$$\mathcal{A}_{3,3} = \frac{1}{r}$$

$$\mathcal{A}_{3,4} = \frac{1}{\mu}$$

$$\mathcal{A}_{4,1} = \frac{1}{n(n+1)}\mathcal{A}_{2,3}$$

$$\mathcal{A}_{4,2} = -\frac{1}{n(n+1)}\mathcal{A}_{1,3}$$

$$\mathcal{A}_{4,3} = -\rho_0\omega^2 + \frac{2\mu}{(\lambda+2\mu)r^2}[\lambda(2n^2+2n-1) + 2\mu(n^2+n-1)] + \frac{2m\rho_0\omega\Omega}{n(n+1)}$$

$$\mathcal{A}_{4,4} = -\frac{3}{r}$$

$$\mathcal{A}_{4,5} = -\frac{\rho_0}{r}$$

$$\mathcal{A}_{5,1} = 4\pi G\rho_0$$

$$\mathcal{A}_{5,6} = 1$$

$$\mathcal{A}_{6,3} = -4\pi G\rho_0\frac{n(n+1)}{r}$$

$$\mathcal{A}_{6,5} = \frac{n(n+1)}{r^2}$$

$$\mathcal{A}_{6,6} = -\frac{2}{r}.$$

These expressions of matrix $\mathcal{A}$ are analogous to those given by Crossley & Rochester (1980), except they also included the Coriolis coupling to the toroidal field $\mathbf{T}^m_{n-1}$ and $\mathbf{T}^m_{n+1}$.

System (26) can be integrated numerically by a Runge-Kutta method through the inner core to obtain solutions at the ICB, and through the mantle to obtain solutions at the surface of the Earth. Since the geocentre is a regular singular point of the sixth order differential system (26), only three of the six fundamental solutions are regular there, and care must be taken in selecting the starting values of these solutions at the geocentre. To start integration, Pekeris (1966) suggested using a power series expansion near the geocentre, whereas Takeuchi and Saito (1971) used analytic solutions in a homogeneous sphere of small radius. Crossley (1975) introduced a variable transformation to reduce the singularity from second order to

first order, and showed how to select solutions that are finite at the geocentre (also see Haardeng-Pedersen, 1975). This technique was used by Smylie *et al.* (1990) to compute the static load Love numbers, and is used in this thesis to compute the dynamic load Love numbers at the ICB. The latter result was reported in Rochester and Peng (1993). Wu and Rochester (1994) give detailed starting values at or near the geocentre for Crossley's method or Pekeris' method respectively. For the sixth order differential system here, either method yields the same load Love numbers. However, for a more realistic Earth model which includes the ellipticity of strata, I shall start the integration a little distance away from the geocentre to avoid possible computational instabilities.

Now define the dimensionless radius

$$x = \frac{r}{R} \tag{33}$$

where R is the radius of the Earth. By defining the dimensionless AJP variables as $\bar{y}_i$'s, the dimensioned y_i's are expressed in terms of these dimensionless ones according to the following relation

$$y_i = a\bar{y}_i\{\delta_{i1} + \delta_{i3} + g_0(a)[\rho_0(a_+)(\delta_{i2} + \delta_{i4}) + \delta_{i5} + \frac{1}{a}\delta_{i6}]\} \tag{34}$$

where $\delta_{ij} = 1$ if $i = j$, and $\delta_{ij} = 0$ otherwise. Then the fundamental solutions at the geocentre can be represented as the following, which are equivalent to those of Crossley (1975) except for the presence of Ω here, or that of Wu & Rochester (1994):

$$\bar{y}_1 = Ax^{n-1} + A'x^{n+1} + \cdots \tag{35}$$

$$\bar{y}_2 = Bx^{n-2} + \zeta B'x^n + \cdots \tag{36}$$

$$\bar{y}_3 = Cx^{n-1} + C'x^{n+1} + \cdots \tag{37}$$

$$\bar{y}_4 = Dx^{n-2} + \zeta D' x^n + \cdots \tag{38}$$

$$\bar{y}_5 = Ex^n + \gamma E' x^{n+2} + \cdots \tag{39}$$

$$\bar{y}_6 = \nu F x^{n-1} + \gamma \nu F' x^{n+1} + \cdots \tag{40}$$

where

$$\zeta = \frac{\mu(0)}{R\rho_0(a_+)g_0(a)} \tag{41}$$

$$\gamma = \frac{4\pi G\rho_0(0)R}{g_0(a)} \tag{42}$$

$$\nu = a/R \tag{43}$$

where $\mu(0)$ and $\rho_0(0)$ are the rigidity and density of the inner core at the geocentre, a is the radius of the ICB, and $\rho_0(a_+)$ the density of the liquid core just above the ICB. Note that hereafter for convenience in writing, I will drop $\bar{}$ on the dimensionless y_i's. Whenever the dimensioned y_i's arise, they will be referred to explicitly.

Of twelve coefficients listed in (35) - (40), only three of them are independent. I choose C, E and A' as the independent coefficients which will enable the case $n = 0$ (purely radial deformation) to be handled easily - no separate treatment is needed. All the other coefficients are expressed in terms of these three as the following:

$$A = nC \tag{44}$$

$$B = 2n(n-1)\zeta C \tag{45}$$

$$D = 2(n-1)\zeta C \tag{46}$$

$$F = n(E - \gamma C) \tag{47}$$

$$C' = \frac{1}{p_1 - np_2}\{p_2 A' + \frac{R}{\nu\beta_0^2}[g_0(a)\nu F + (\omega^2 - 2m\omega\Omega + (3-n)\frac{4\pi}{3}G\rho_0(0))aA]\} \tag{48}$$

$$D' = A' + nC' \tag{49}$$

$$B' = q_2 D' - q_1 C' \tag{50}$$

$$E' = \frac{1}{2(2n+3)}[(n+3)A' - n(n+1)C'] \tag{51}$$

$$F' = (n+2)E' - A' \tag{52}$$

$$p_1 = 2n\,[n(n+2)\frac{\alpha_0^2}{\beta_0^2} - (n+1)^2] \tag{53}$$

$$p_2 = n\,[(n+3)\frac{\alpha_0^2}{\beta_0^2} - (n+1)] \tag{54}$$

$$q_1 = 2n\,[(n+2)\frac{\alpha_0^2}{\beta_0^2} - (n+3)] \tag{55}$$

$$q_2 = (n+3)\frac{\alpha_0^2}{\beta_0^2} - 4 \tag{56}$$

where α_0 and β_0 are the compressional and shear wave velocities at the center of the Earth respectively. If one chooses to start the integration at a point away from the geocentre, Wu & Rochester (1994) demonstrated that it is adequate to keep only two terms in the above power expansion, provided that the starting point is very close to, e.g. a few kilometres from, the centre.

The general solutions in terms of these three independent constants have a form of

$$\underline{y} = C\underline{y}^{(1)} + E\underline{y}^{(2)} + A'\underline{y}^{(3)} \tag{57}$$

where $\underline{y}^{(k)}$ are the fundamental solutions. At the inner core boundary, the solutions

$$\underline{y}(a_-) = C\underline{y}^{(1)}(a_-) + E\underline{y}^{(2)}(a_-) + A'\underline{y}^{(3)}(a_-) \tag{58}$$

must satisfy the necessary boundary conditions, namely the continuity of normal displacement $\hat{\mathbf{n}} \cdot \mathbf{u}$, incremental gravitational potential V_1, normal stress $\hat{\mathbf{n}} \cdot \tau$, and gravitational flux $\hat{\mathbf{n}} \cdot [\nabla V_1 - 4\pi G\rho_0 \mathbf{u}]$, where $\hat{\mathbf{n}}$ is the unit normal pointing out of liquid core (therefore $\hat{\mathbf{n}}=-\hat{\mathbf{r}}$ at the ICB, and $\hat{\mathbf{n}}=\hat{\mathbf{r}}$ at the CMB), τ is the additional stress due to the disturbance of deformation.

By the definitions (4), (7), (27) and (31)

$$\hat{\mathbf{n}} \cdot \mathbf{u} = \sum_{n=|m|}^{\infty} y_1(r) Y_n^m \tag{59}$$

$$V_1 = \sum_{n=|m|}^{\infty} y_5(r) Y_n^m. \tag{60}$$

Therefore, the first two boundary conditions mean that y_1 and y_5 are continuous across the ICB. Note that for simplicity, the notation for the y_i's adopted here for calculating the load Love numbers will not explicitly include their dependence on frequency and on azimuthal order number m, nor their dependence on degree n.

Before proceeding further, it is necessary to look at the expression of the radial component of the normal stress (denoted as τ_{rr}) at the liquid side of the ICB. First, the reduced pressure χ may be represented by the superposition of a radial function and the standard spherical harmonics

$$\chi = \sum_{n=|m|}^{\infty} \chi_n^m(r) Y_n^m. \tag{61}$$

Referring to equations (8) and (16) of Chapter 2, the normal stress in the liquid core can be written as

$$\tau_{rr} = \lambda \nabla \cdot \mathbf{u} = -\rho_0(\mathbf{u} \cdot \mathbf{g}_0 + \chi + V_1)$$

$$= -\rho_0 \sum_{n=|m|}^{\infty} [-g_0(r)y_1(r) + \chi_n^m(r) + y_5(r)]Y_n^m. \tag{62}$$

At the point just above the ICB, the normal stress expressed in AJP notations is

$$\lambda \nabla \cdot \mathbf{u} = \sum_{n=|m|}^{\infty} y_2(a_+)Y_n^m. \tag{63}$$

As defined in equation (34), all AJP field variables of the inner core in the boundary conditions can also be expressed in terms of the corresponding dimensionless quantities. Therefore, with dimensioned quantities replaced by dimensionless ones, the condition of a continuous normal stress across the ICB, $y_2(a_+) = y_2(a_-)$, can then be simplified as:

$$y_1(a_-) - y_5(a_-) - y_2(a_-) = \frac{\chi_n^m(a_+)}{a g_0(a)} \tag{64}$$

where the fully dimensioned quantity $\chi_n^m(a_+)$ is the radial part of the potential χ just above the ICB.

For an inviscid liquid core, the shear stress vanishes at the ICB

$$y_4(a_-) = 0. \tag{65}$$

Finally, the continuity of the gravitational flux across the ICB gives

$$\frac{4\pi G \rho_0(a_+)a}{g_0(a)} y_1(a_-) + y_6(a_-) = \frac{1}{g_0(a)}\left(\frac{dy_5}{dr}\right)_{r=a_+}. \tag{66}$$

Note that $\left(\frac{dy_5}{dr}\right)_{r=a_+}$ of the liquid core remains a fully dimensioned quantity.

Equations (64), (65) and (66) are seen to depend on χ_n^m and dy_5/dr of the liquid side of the ICB only. Guided by this dependence, the internal load Love numbers can be defined in such a way that

$$y_1(a) = h_1(a)\frac{\chi_n^m(a_+)}{ag_0(a)} + k_1(a)\frac{1}{ag_0(a)}\left(r\frac{dy_5}{dr}\right)_{r=a_+} \tag{67}$$

$$y_5(a) = h_5(a)\frac{\chi_n^m(a_+)}{ag_0(a)} + k_5(a)\frac{1}{ag_0(a)}\left(r\frac{dy_5}{dr}\right)_{r=a_+} \tag{68}$$

where the load Love numbers h_1 and h_5 are the solutions y_1 and y_5 when

$$\frac{\chi_n^m(a_+)}{ag_0(a)} = 1, \qquad \left(\frac{dy_5}{dr}\right)_{r=a_+} = 0 \tag{69}$$

and k_1 and k_5 are those solutions when

$$\chi_n^m(a_+) = 0, \qquad \frac{1}{ag_0(a)}\left(r\frac{dy_5}{dr}\right)_{r=a_+} = 1. \tag{70}$$

With the above conditions, the coefficients C, E and A' can be obtained, hence the internal load Love numbers:

$$h_1 \ or \ k_1 = C\,y_1^{(1)} + E\,y_1^{(2)} + A'\,y_1^{(3)} \tag{71}$$

$$h_5 \ or \ k_5 = C\,y_5^{(1)} + E\,y_5^{(2)} + A'\,y_5^{(3)}. \tag{72}$$

The internal load Love numbers at the CMB can be obtained with the same procedure as that at the ICB (Rochester & Peng, 1993), subject to the boundary conditions at the free surface of the Earth:

$$y_2(R_-) = 0 \tag{73}$$

$$y_4(R_-) = 0 \tag{74}$$

$$\frac{n+1}{R}\, y_5(R_-) \;+\; y_6(R_-) \;=\; 0 \tag{75}$$

and similar boundary conditions as (65), (64) and (66) at the CMB, but with $\chi_n^m(a_+)$ and $g_0(a)$ replaced by $\chi_n^m(b_-)$ and $g_0(b)$. The radial displacement and additional gravitational fields at the CMB are now expressed in terms of the mantle load Love numbers $h_1(b)$, $h_5(b)$, $k_1(b)$ and $k_5(b)$ at the CMB and the quantities $\chi_n^m(b_-)$ and $(r\ dy_5/dr)_{r=b_-}$ just below the CMB:

$$y_1(b) \;=\; h_1(b)\frac{\chi_n^m(b_-)}{bg_0(b)} \;+\; k_1(b)\frac{1}{bg_0(b)}\left(r\,\frac{dy_5}{dr}\right)_{r=b_-} \tag{76}$$

$$y_5(b) \;=\; h_5(b)\frac{\chi_n^m(b_-)}{bg_0(b)} \;+\; k_5(b)\frac{1}{bg_0(b)}\left(r\,\frac{dy_5}{dr}\right)_{r=b_-}. \tag{77}$$

Note that I have kept the inertial term $\omega^2\mathbf{u}$ and the self-coupling contribution from the Coriolis term $2i\omega\Omega\hat{\mathbf{k}}\times\mathbf{u}$ in the original equation of momentum conservation, as well as in the course of deriving the AJP governing system (26) and the starting solutions of the integration at the geocentre. Similar care has been taken in deriving the load Love numbers at the CMB. By doing so I correctly take into account the dependence of the internal load Love numbers on frequency ω and azimuthal order number m.

It is shown, in the numerical computation, that the load Love numbers of degree 1 at outer core boundaries display long period resonances (Table 1), which are natural frequencies of the Earth's subsystem. The reason for this occurrence is that the main restoring force for degree 1 deformation of the inner core is gravitation (rather than elasticity). These 'poles' of Table 1, especially that of the ICB, are so close to the eigenperiods of the Slichter modes that the load Love numbers at such periods are highly frequency dependent (dynamical), even for a non-rotating Earth model. Therefore, in long period free oscillation modelling

(e.g. the Slichter modes), serious error may arise if the dynamical load Love numbers are replaced by the static ones (Crossley *et al.*, 1992; Rochester & Peng, 1993). This closeness of the resonance frequency of the load Love numbers to the eigenfrequency of the mode under investigation is to signal that it is important to take into account inertial (including Coriolis self- coupling) effects in the solid parts of the Earth when computing the eigenfrequency of that mode.

In other words, the load Love numbers can be regarded as independent of frequency only in those frequency ranges which are far from these poles. For deformations of degree $n \geq 2$, the vibrational resonances of the solid inner core and mantle are all at period below 1 hour due to their high rigidity. Little error would incur by treating the response of the inner core and mantle, to disturbances from the liquid core, as essentially static. However, this is no longer a case for $n = 1$ where the poles of the load Love numbers, especially that of the ICB, are at periods not far from the Slichter modes themselves.

Table 1: Resonance periods (hr) of the degree 1 load Love numbers at the ICB and CMB for the PREM model with a neutral liquid core. The azimuthal number m=0, 1, -1 represents the axial, retrograde and prograde equatorial mode respectively.

	non-rotating	rotating		
		m=0	m=1	m=-1
ICB	4.56962	4.56962	3.77971	5.52462
CMB	1.02800	1.02800	0.9944	1.06281

3.3 Effective Load Love Numbers

The whole purpose of adopting the SSA is to avoid having to solve the Poisson equation simultaneously with the momentum conservation equation. Instead one solves the SSWE (15) first and then returns to solve the Poisson equation (14). It is necessary to incorporate in the solution of the SSWE the continuity conditions at the deformable core boundaries, expressed by the load Love numbers just derived. However, to use these boundary conditions requires knowledge of dy_5/dr at $r = a_+$ and at $r = b_-$, i.e. the Poisson equation needs to be solved first! There appears to be no consistent way of doing this, i.e. of taking full advantage of the SSA, except in the special case when the liquid core is neutrally stratified. For then, as already observed, the Poisson equation reduces to the Laplace equation, its solution can be written *a priori* as

$$y_5(r) = A_n(\frac{r}{b})^n + B_n(\frac{a}{r})^{n+1} \tag{78}$$

where A_n and B_n are to-be-determined coefficients, a and b are the radii of the ICB and CMB respectively.

Taking the first derivative of (78), one can arrive at

$$\frac{dy_5}{dr} = \frac{n}{b}(\frac{r}{b})^{n-1}A_n - \frac{n+1}{a}(\frac{a}{r})^{n+2}B_n. \tag{79}$$

Since V_1 is continuous across the outer core boundaries, (78) and (79) can be substituted into the load Love number condition (68) at the ICB and its equivalent at the CMB, which then become:

$$C_{11}(\frac{a}{b})^n A_n + C_{12}B_n = h_5(a)\chi_n^m(a_+) \tag{80}$$

$$C_{21}A_n + C_{22}(\frac{a}{b})^{n+1}B_n = h_5(b)\chi_n^m(b_-) \tag{81}$$

where

$$C_{11} = 1 - nk_5(a) \tag{82}$$

$$C_{12} = 1 + (n+1)k_5(a) \tag{83}$$

$$C_{21} = 1 - nk_5(b) \tag{84}$$

$$C_{22} = 1 + (n+1)k_5(b). \tag{85}$$

Now the constants A_n and B_n are solved from equations (80) and (81):

$$A_n = -\frac{C_{22}}{C_{21}P'}(\frac{a}{b})^{n+1}h_5(a)\chi_n^m(a_+) + [\frac{1}{C_{21}} + \frac{C_{11}C_{22}}{C_{21}^2P'}(\frac{a}{b})^{2n+1}]h_5(b)\chi_n^m(b_-) \tag{86}$$

$$B_n = \frac{1}{P'}[h_5(a)\chi_n^m(a_+) - \frac{C_{11}}{C_{21}}(\frac{a}{b})^n h_5(b)\chi_n^m(b_-)] \tag{87}$$

where

$$P' = C_{12} - \frac{C_{11}C_{22}}{C_{21}}(\frac{a}{b})^{2n+1}. \tag{88}$$

Then the derivatives dy_5/dr at the ICB and CMB are expressed in terms of the load Love numbers, the radial functions $\chi_n^m(a_+)$ just above the ICB, and $\chi_n^m(b_-)$ just below the CMB. Finally, substituting the latter into the load Love number condition (67) at the ICB and its equivalent at the CMB, y_1 at these boundaries will be obtained

$$y_1(a) = H_{IC}^e\chi_n^m(a_+) + K_{IC}^e\chi_n^m(b_-) \tag{89}$$

$$y_1(b) = H_M^e\chi_n^m(b_-) + K_M^e\chi_n^m(a_+) \tag{90}$$

where H^e_{IC}, K^e_{IC}, H^e_M and K^e_M are the effective load Love numbers at the ICB and CMB respectively:

$$H^e_{IC} = h_1(a) - \frac{k_1(a)h_5(a)}{C_{21}P'}[(n+1)C_{21} + nC_{22}(\frac{a}{b})^{2n+1}] \tag{91}$$

$$K^e_{IC} = (\frac{a}{b})^n \frac{k_1(a)h_5(b)}{C_{21}P'}[nC_{12} + (n+1)C_{11}] \tag{92}$$

$$H^e_M = h_1(b) - \frac{k_1(b)h_5(b)}{C_{21}P'}[(n+1)C_{11}(\frac{a}{b})^{2n+1} + nC_{12}] \tag{93}$$

$$K^e_M = -(\frac{a}{b})^{n+1} \frac{k_1(b)h_5(a)}{C_{21}P'}[nC_{22} + (n+1)C_{21}]. \tag{94}$$

These final results of $y_1(a)$ and $y_1(b)$ enable the continuity conditions $\hat{\mathbf{n}} \cdot \mathbf{u}$ at the ICB and at the CMB to be expressed in terms of χ^m_n only. It needs to be emphasized that the effective load Love numbers can be used only if the liquid core is neutrally stratified.

Chapter 4 Variational Solution of the Subseismic Wave Equation

4.1 Introduction

Applying the SSA in a neutrally stratified liquid core, the equation of momentum conservation and the SSWE can be written in compact forms:

$$\omega^2(1-\mu^2)\mathbf{u} = \mathbf{\Gamma}_p \cdot \nabla\chi \tag{95}$$

$$\mathcal{L}_p\chi = 0 \tag{96}$$

where $\mathbf{\Gamma}_p$ is the Hermitean tensor given in (23), and $\mathcal{L}_p$ stands for the linear operator in (24).

A conventional approach to solving equation (96) is along the following lines: First, use a spherical harmonic representation of χ to reduce (96) to a set of first-order ordinary differential equations. This equation set is built up from subsets of ordinary differential equations corresponding to a particular degree n, and their coupled companions of degree $n-2$ and $n+2$ due to the Coriolis effects. Then, a decision is made to truncate the coupling chain at a certain degree. Finally, the resulting set of ordinary differential equations are integrated numerically by a Runge-Kutta method.

An alternative to such direct integration of the governing differential equations is to use a variational principle. A variational principle exists if one can construct a functional which becomes extremal (usually a minimum) only when the dependent variables of this functional satisfy the governing differential equations throughout the physical body of interest. The

functional, in this case, is a volume integral with integrand a quadratic function of the dependent variables. In applying the variational principle, a set of trial functions, which are linear combinations of simple basis functions that are linearly independent of (e.g. orthogonal to) one another, can be chosen to represent the dependent variables. Thus the burden of satisfying the governing differential equations by these dependent variables is shifted onto the coefficients of these combinations. Finally, a set of algebraic equations linear in these coefficients is produced by requiring the functional to be extremal. Usually the trial functions are made to satisfy all necessary boundary conditions *a priori*, but it is always possible to generalize the extremal property, by adding surface integrals to the functional, so that it guarantees that the boundary conditions, as well as the governing differential equations, are satisfied. Clearly the accuracy to which the equations and boundary conditions are satisfied will depend on the number, and possibly the particular character, of trial functions used to approximate each dependent variable.

In this thesis, I will take advantage of the existence of the variational principle for the SSWE which can be constructed using the effective load Love numbers. A trial function for χ needs to be chosen in this approach. I will also take advantage that the boundary conditions on $\hat{\mathbf{n}} \cdot \mathbf{u}$ in the present case are so called 'natural' boundary conditions. This will allow for adding appropriate surface integrals containing these boundary conditions to the functional, which then can be made extremal. Hence the extra effort is no longer needed to make the trial functions satisfy the boundary conditions *a priori*. With these natural boundary conditions, the second derivative of the trial function in a functional will be eliminated upon proper choice of weight functions in the surface integrals. However, a price has to be paid for

these conveniences: the eigenfunctions so computed will exhibit slight discontinuities across the inner and outer core boundaries where they should be continuous.

4.2 Variational Principle Based on the Subseismic Wave Equation

Guided by (61), I construct a trial function χ:

$$\chi(r,\theta,\phi) = \sum_{n=1}^{N} \chi_{2n-1}^{m}(r) P_{2n-1}^{m}(\cos\theta) e^{im\phi} \tag{97}$$

where

$$\chi_{2n-1}^{m}(r) = \sum_{p=1}^{2(L-1)} c_{pn} (\frac{r}{z})^{\nu}. \tag{98}$$

Here the constants c_{pn} are coefficients of the radial trial function, L and N are experimentally-decided integers specifying the truncation levels: $2(L-1)$ for the radial function and $2N-1$ for the associated Legendre functions. z is introduced for scaling and the integer ν will be given below. In writing (97), I have taken advantage of the fact that the Coriolis coupling gives rise only to odd degree terms of χ, therefore adds only odd-degree harmonics to the fundamental degree 1 field, and the computations involving even-degree harmonics thus can be avoided.

When the liquid core is homogeneous and incompressible, and rotation is neglected, χ satisfies the Laplace equation (Peng, 1990; Rochester & Peng, 1993), and its solution does not contain a constant term or the term with a power of -1. This proves to be true also for the more general core model treated here. Without losing generality, it can be assumed that

the coefficients c_{pn} are real, and they can be replaced by a set of new coefficients d_k with only a single suffix number k based on 1-1 correspondence (the exact relation will be shown below). Then the trial function χ will be written in a more convenient form:

$$\chi = \sum_{k=1}^{2(L-1)N} d_k (\frac{r}{z})^{\nu} P_{2n-1}^{m} e^{im\phi} \tag{99}$$

where

$$k = p + 2(L-1)(n-1), \qquad n = 1, 2, \cdots, N$$

$$\nu = p - (L+1), \quad z = a, \quad \text{for } 1 \leq p \leq L-1$$

$$\nu = p - (L-1), \quad z = b, \quad \text{for } L \leq p \leq 2L-2.$$

Note that the choice of scaling factor z as above ensures that r/z is always less than 1, which then prevents the value of the radial trial function from being too large.

First, a functional based on the SSWE can be defined in a neutral liquid core

$$F_1 = \int_{LC} \chi^* \mathcal{L}_p \chi dV \tag{100}$$

where the integral is over the volume of the liquid core. Using the divergence theorem, the Hermitean property of Γ_p, and the equation of the momentum conservation (95), the first variation in F_1 is given by

$$\delta F_1 - \int_{LC} [\delta\chi^* \mathcal{L}_p \chi + (\delta\chi^* \mathcal{L}_p \chi)^*] dV$$

$$= \omega^2(1-\mu^2) \int_{ICB+CMB} \rho_0 (\chi^* \hat{\mathbf{n}} \cdot \delta\mathbf{u} - \delta\chi \hat{\mathbf{n}} \cdot \mathbf{u}^*) dS \tag{101}$$

where $\hat{\mathbf{n}}$ is the unit normal pointing out of the liquid core. It is clear that, for rigid outer core boundaries, a variational principle exists if F_1 is stationary in the domain of interest,

i.e. $\delta F_1 = 0$ for an arbitrary $\delta\chi$, then χ must satisfy the SSWE. Whereas for deformable boundaries, (101) suggests that surface integrals accommodating continuity of the normal displacement field $\hat{\mathbf{n}} \cdot \mathbf{u}$ across these boundaries could be added to the functional F_1.

Now, let a new functional F be defined by adding to F_1 the surface integrals containing the natural boundary conditions $\hat{\mathbf{n}} \cdot \mathbf{u}$ at the outer core boundaries:

$$F = \int_{LC} \chi^* \mathcal{L}_p \chi dV + \int_{ICB+CMB} \psi_i^* \hat{\mathbf{n}} \cdot (\mathbf{u} - \mathbf{u}_s) dS \tag{102}$$

where χ^*, ψ_i^* (i=1 or 2 referring to the ICB or CMB) are weighting functions, and $\mathbf{u}_s$ is the displacement field of the solid parts of the Earth, i.e. $\mathbf{u}_{IC}$ of the inner core, or $\mathbf{u}_M$ of the mantle. Generally, χ^*, ψ_1^* and ψ_2^* are independent and the latter two are arbitrary, but it may be advantageous if they are related in some manner. This point will become apparent later.

The first variation now can be performed on the functional (102), which leads to:

$$\begin{aligned} \delta F = & \int_{LC} [\delta\chi^* \mathcal{L}_p \chi + \chi^* \mathcal{L}_p \delta\chi] dV \\ & + \int_{ICB+CMB} [\delta\psi_i^* \hat{\mathbf{n}} \cdot (\mathbf{u} - \mathbf{u}_s) + \psi_i^* \hat{\mathbf{n}} \cdot (\delta\mathbf{u} - \delta\mathbf{u}_s)] dS. \end{aligned} \tag{103}$$

Equation (103) can be re-arranged into the following form

$$\begin{aligned} & \delta F - \int_{LC} [\delta\chi^* \mathcal{L}_p \chi + (\delta\chi^* \mathcal{L}_p \chi)^*] dV \\ & - \int_{ICB+CMB} \{\delta\psi_i^* \hat{\mathbf{n}} \cdot (\mathbf{u} - \mathbf{u}_s) + [\delta\psi_i^* \hat{\mathbf{n}} \cdot (\mathbf{u} - \mathbf{u}_s)]^*\} dS \\ & = \int_{LC} [\chi^* \mathcal{L}_p \delta\chi - \delta\chi (\mathcal{L}_p \chi)^*] dV \\ & + \int_{ICB+CMB} [\psi_i^* \hat{\mathbf{n}} \cdot (\delta\mathbf{u} - \delta\mathbf{u}_s) - \delta\psi_i \hat{\mathbf{n}} \cdot (\mathbf{u} - \mathbf{u}_s)^*] dS. \end{aligned} \tag{104}$$

Clearly, if the RHS of (104) vanishes for an arbitrary $\delta\chi$, then F is stationary in the domain of interest and χ must satisfy the SSWE and the associated boundary conditions.

Using the momentum conservation equation (95) and the Hermitean property of $\mathbf{\Gamma}_p$, the RHS of equation (104) can be written as:

$$\text{RHS of (104)} = \int_{LC}[\nabla\cdot(\chi^{*}\rho_0\mathbf{\Gamma}_p\cdot\nabla\delta\chi) - \nabla\cdot(\delta\chi\rho_0\mathbf{\Gamma}_p^{*}\cdot\nabla\chi^{*})]dV$$

$$+\int_{ICB+CMB}[\psi_i^{*}\hat{\mathbf{n}}\cdot(\delta\mathbf{u}-\delta\mathbf{u}_s) - \delta\psi_i\hat{\mathbf{n}}\cdot(\mathbf{u}-\mathbf{u}_s)^{*}]dS. \tag{105}$$

Applying the divergence theorem and equation (95) again, the above equation can be expressed as:

$$\text{RHS of (104)} = \omega^2(1-\mu^2)\int_{ICB+CMB}\rho_0\chi^{*}\hat{\mathbf{n}}\cdot\delta\mathbf{u}dS$$

$$-\omega^2(1-\mu^2)\int_{ICB+CMB}\rho_0\delta\chi\hat{\mathbf{n}}\cdot\mathbf{u}^{*}dS$$

$$+\int_{ICB+CMB}[\psi_i^{*}\hat{\mathbf{n}}\cdot(\delta\mathbf{u}-\delta\mathbf{u}_s) - \delta\psi_i\hat{\mathbf{n}}\cdot(\mathbf{u}-\mathbf{u}_s)^{*}]dS. \tag{106}$$

Obviously, if I choose

$$\psi_1^{*} = \psi_2^{*} = -\omega^2(1-\mu^2)\rho_0\chi^{*} \tag{107}$$

the surface integrals in (106) associated with $\hat{\mathbf{n}}\cdot\delta\mathbf{u}$ and $\hat{\mathbf{n}}\cdot\mathbf{u}^{*}$ will be cancelled out, and (106) is then simplified as:

$$\text{RHS of (104)} = \omega^2(1-\mu^2)\int_{ICB}\rho_0[-\chi^{*}\hat{\mathbf{r}}\cdot\delta\mathbf{u}_{IC} + \delta\chi\hat{\mathbf{r}}\cdot\mathbf{u}_{IC}^{*}]dS$$

$$+\omega^2(1-\mu^2)\int_{CMB}\rho_0[\chi^{*}\hat{\mathbf{r}}\cdot\delta\mathbf{u}_M - \delta\chi\hat{\mathbf{r}}\cdot\mathbf{u}_M^{*}]dS. \tag{108}$$

From (59),

$$\hat{\mathbf{n}} \cdot \mathbf{u}_{IC} = \sum_{n=|m|}^{\infty} y_1(a) Y_n^m \tag{109}$$

$$\hat{\mathbf{n}} \cdot \mathbf{u}_{M} = \sum_{n=|m|}^{\infty} y_1(b) Y_n^m \tag{110}$$

where $y_1(a)$ and $y_1(b)$ are computed from equations (89) and (90), using the effective load Love numbers and the liquid core quantities χ_n^m. Note that $y_1(a)$ and $y_1(b)$ in (89) and (90) are dimensionless quantities, while they are dimensioned in (108). The relation between the dimensioned and dimensionless quantities is given by (34). Therefore,

$$\hat{\mathbf{r}} \cdot \delta\mathbf{u}_{IC} = \frac{1}{g_0(a)} \sum_{n=|m|}^{\infty} [H_{IC}^e \delta\chi_n^m(a) + K_{IC}^e \delta\chi_n^m(b)] Y_n^m \tag{111}$$

$$\hat{\mathbf{r}} \cdot \delta\mathbf{u}_{M} = \frac{1}{g_0(b)} \sum_{n=|m|}^{\infty} [H_{M}^e \delta\chi_n^m(b) + K_{M}^e \delta\chi_n^m(a)] Y_n^m. \tag{112}$$

Note that nothing is lost by omitting the subscripts '+' and '−' of a and b in equations (111) and (112).

Using the orthogonality properties of spherical harmonics, and substituting (111) and (112), (108) can be re-written as:

$$\text{RHS of (104)} = \omega^2(1-\mu^2)\frac{4\pi(-1)^m}{2(n+1)!}\frac{\rho_0 a^2}{g_0(a)}$$

$$\times \sum_{n=|m|}^{\infty} \{\frac{\rho_0(b_-) g_0(a) b^2}{\rho_0(a_+) g_0(b) a^2} K_M^e + K_{IC}^e\} [\delta\chi_n^m(a)\chi_n^{m*}(b) - \delta\chi_n^m(b)\chi_n^{m*}(a)]. \tag{113}$$

Using the ordinary load Love numbers, the quantity in the curly brackets of (113) is seen to be proportional to

$$\Delta = \frac{\rho_0(b_-) b\, k_1(b)}{g_0(b) h_5(b)} - \frac{\rho_0(a_+) a\, k_1(a)}{g_0(a) h_5(a)}. \tag{114}$$

It can be shown that Δ vanishes to within 1×10^{-6}, an error much less than that of the SSA itself (Rochester & Peng, 1993). Therefore, it can be concluded that the chosen trial function χ, which makes the functional F extremal and is not constrained in advance by the boundary conditions, will satisfy the SSWE and associated boundary conditions.

By substituting ψ_1^* and ψ_2^* of equation (107) into the functional F of (102), and by using the divergence theorem, the final form of the functional F is as below:

$$F = -\int_{LC} \rho_0 \nabla \chi^* \cdot \Gamma_p \cdot \nabla \chi dV + \omega^2(1-\mu^2) \int_{ICB+CMB} \chi^* \rho_0 \hat{\mathbf{n}} \cdot \mathbf{u}_s dS. \tag{115}$$

Substituting (99) into the RHS of (115) makes the latter take the form of

$$F = \sum_{k=1}^{2(L-1)N} \sum_{l=1}^{2(L-1)N} G_{kl} d_k d_l. \tag{116}$$

For F to be stationary, the choice of d_1, d_2, $\cdots$, d_k, $\cdots$ is constrained by the requirement that

$$\frac{\partial F}{\partial d_k} = 0, \quad k = 1, \cdots\cdots 2(L-1)N. \tag{117}$$

This set of equations can be put into a matrix form:

$$(\underline{G} + \underline{G}^T)\, \underline{D} = \underline{0} \tag{118}$$

where G_{kl} is the k,lth component of the LHS of equation (117), and

$$\underline{D} = (d_1\ d_2\ \cdots\ d_k\ \cdots)^T. \tag{119}$$

All integrals in G_{ij} can be evaluated analytically because a neutrally stratified liquid core has been assumed. Then the eigenperiods are found from the requirement

$$Det(\ \underline{G} + \underline{G}^T\ ) = 0 \tag{120}$$

which guarantees that a non-trivial $\underline{D}$ exists.

Once the eigenperiod is found, the coefficients of the trial function can be obtained from the eigenperiod condition (118) and (120). From analytic solutions of a simple Earth model (Peng 1990), it is known that d_k, at least when $k = j$, does not vanish when the corresponding power of r of the radial trial function $\nu = j-(L+1) = -2$ or $\nu = j-(L-1) = 1$. Suppose $d_q \neq 0$ (it can be chosen arbitrarily, e.g. $d_q = 1$ for convenience), then (118) can be written as

$$\sum_{k\neq q} Q_{pk}(\frac{d_k}{d_q}) = -Q_{pq}, \qquad p = 1, 2, \cdots, 2(L-1)N-1 \tag{121}$$

where

$$\underline{Q} = \underline{G} + \underline{G}^T. \tag{122}$$

Note that the upper limit of p is $2(L-1)N-1$, because one equation needs to be dropped for solving that number of d_k/d_q, with $k \neq q$ (for k=1, 2, $\cdots\cdots$, $2(L-1)N-1$). A complete set of coefficients consists of d_k's (for k=1, 2, $\cdots\cdots$, $2(L-1)N-1$) and $d_q = 1$. When these coefficients are found, the eigenfunction χ of the liquid core follows. Then, the ordinary load Love numbers and the eigenfunction χ at the ICB and CMB can be used to compute A_n and B_n of equations (86) and (87). Consequently, y_5 is found from equation (78), and y_2 is found from equation (13) according to definition (63). The radial and transverse displacement y_1 and y_3 are found from the displacement field $\mathbf{u}$ of equation (95):

$$y_1^n = u_n^m(r) = u_r^{m,n}. \tag{123}$$

If $m = 0$,

$$y_3^n = v_n^m(r) = -\frac{1}{(n+1)J_n^m}[u_\theta^{m,n-1} - (n-2)H_{n-2}^m y_3^{n-2}] \tag{124}$$

and if $m \neq 0$,

$$y_3^n = \frac{1}{m}[u_\phi^{m,n} + L_n^m y_7^{n+1}] \tag{125}$$

where $L_n^m = (n+2)J_n^m$ if $n = 1$, or $L_n^m = -(n+1)H_{n+1}^m$ otherwise, with

$$J_n^m = \frac{(n+m)}{2n+1} \tag{126}$$

$$H_n^m = \frac{(n+1-m)}{2n+1}. \tag{127}$$

The quantity y_7^{n+1} in equation (125) is the coefficient of the toroidal field of the liquid core displacement **u**

$$y_7^{n+1} = t_n^m(r) = \frac{1}{F_{n+1}^m}[u_\theta^{m,n+1} - D_n^m u_\phi^{m,n} - E_{n+2}^m u_\phi^{m,n+2}] \tag{128}$$

where

$$F_n^m = \frac{1}{m}[n(n+2)J_{n+1}^m H_n^m + (n-1)(n+1)H_{n-1}^m J_n^m] + m \tag{129}$$

$$D_n^m = \frac{n\, H_n^m}{m} \tag{130}$$

$$E_n^m = -\frac{(n+1)J_n^m}{m} \tag{131}$$

and $u_r^{m,i}$, $u_\theta^{m,i}$ and $u_\phi^{m,i}$ are the radial, polar and azimuthal components of the displacement field **u** of the liquid core respectively. Finally, $y_4 = 0$ in the liquid core, and y_6 is found from its definition

$$y_6 = \frac{dy_5}{dr} - 4\pi G\rho y_1. \tag{132}$$

4.3 Eigenperiods and Eigenfunctions: Numeral Results Using the Subseismic Approximation

I adopt the PREM Earth model for my numerical test in this thesis. The model consists of an elastic inner core, an elastic mantle, and a non-neutrally stratified, inviscid, compressible liquid core. The whole system is spherical in shape, and rotates at a steady angular velocity Ω. The density contrast of this model at the ICB lies in the range preferred by the free oscillation data examined by Shearer & Masters (1990), namely 0.4 - 0.7 $\times$ 10^3 kg m^{-3}. For applying the SSA in this chapter and the comparisons of the computational results in the subsequent chapters, I assume an exactly neutrally stratified liquid core (Peng, 1990), and use a modified density profile with $|\beta| < 1 \times 10^{-6}$. Other physical property data, such as seismic wave velocities, density profiles in the inner core and mantle, as well as the dimensions of the Earth's subsystems, are retained from the original PREM model. However, the water layer at the surface of the Earth is replaced with a solid layer, provided that the mass, moment of inertia and P-wave transit time are preserved (Rochester & Peng 1993). This modification simplifies the computation by avoiding handling a fluid layer in the mantle, and its effects on the computed load Love numbers at the CMB should be negligible. Here I also take advantage of the fact that the physical properties of the PREM model are given as polynomials, which makes it possible to evaluate all volume integrals in (115) analytically, though it may result in less precision than if I use the tabulated data at discrete radii.

I started to search for the roots of the $Det(\underline{G} + \underline{G}^T)$ from 1 hour to 10 hours with the number $L = 3$ and degree $N = 2$ for each member of the triplet (i.e. $\Omega = 0$, m=0; $\Omega \neq 0$,

m=0, +1, -1), and narrowed the search range under the guidance of the roots found from the first round of computation. Then L and N were increased until convergent roots were obtained. The convergence was ensured by requiring the difference of eigenperiods between two successive computations with different L and N be less than 1×10^{-5} hr. Table 2 tabulates the eigenperiods of the triplet associated with different L and N. The results show that $N = 2$ or 3 are adequate for a convergent eigenperiod in this case, and confirm Crossley's (1992) eigenperiods, achieved using coupling chain up to $N = 3$: 5.3172 hr ($m = 0$), 4.7733 hr ($m = 1$) and 5.9872 hr ($m = -1$). This means that the Coriolis coupling of a spheroidal field in the liquid core need not be extended further than $\mathbf{S}_3^m$ or $\mathbf{S}_5^m$, which is a factor $2\Omega/\omega$ or $(2\Omega/\omega)^3$ respectively beyond the calculations by Dahlen & Sailor (1979). Note that I did not take the coupling to toroidal field $\mathbf{T}_2^m$ in the solid parts of the Earth, whereas the latter authors did.

Table 2: Eigenperiods (hr) of the Slichter modes for PREM with a neutral liquid core using a variational principle based on the SSA. L and N are the integers specify the truncation level of the radial function and the degree of the spherical harmonics of the trial function χ. Therefore, χ contains $2(L-1)$ direct and inverse powers of radius, and $2N-1$ members of the spherical harmonics. The spurious root is also listed at the bottom of the table.

	non-rotating			rotating	
(L, N)		(L, N)	m=0	m=1	m=-1
(3, 1)	5.41190				
		(3, 2)	5.30168	4.75933	5.96971
(5, 1)	5.41190	(5, 3)	5.30168	4.75936	5.96972
		(7, 4)	5.30168	4.75936	5.96972
Spurious root	5.76485		5.76464	4.54077	7.31700

Two poles, and a spurious root, are also found close to the eigenperiods of the triplet (see bottom of Table 2). A close examination shows that the poles are identical to the resonance periods of the effective load Love numbers of degree 1, which in turn result from the resonance character of the ordinary load Love numbers (Table 1). Table 3 displays the resonance periods of the effective load Love numbers of degree 1 for the PREM model with a neutral liquid core. Again, the resonance character of these effective load Love numbers suggests that they are strongly frequency-dependent, at least for degree 1. The spurious root is an artifact of the SSA: a solution by direct integration of the governing equations for a non-rotating Earth model shows that it is absent when the SSA is not invoked, but appears from a very long period as the SSA is gradually applied, finally stopping at 5.76485 hr (Rochester & Peng, 1993). The latter test is achieved by multiplying the terms, which will be omitted if the SSA is applied, with a factor changing from 1 to 0. However, with the spurious root present, the real eigenperiod can still be easily identified by tracking it down from the known eigenperiod for a non-rotating Earth model, as the rotation rate Ω is gradually increased from zero to its proper size. This can be achieved by multiplying the functional F of (115) with Ω^2.

Table 3: Resonance periods (hr) of the degree 1 effective load Love numbers for the PREM model with a neutral liquid core.

non-rotating	rotating		
	m=0	m=1	m=-1
5.04588	5.04588	4.09303	6.22055
4.20360	4.20360	3.52967	5.00523

Next, I examined the effect of higher degree self-coupling of the displacement field in the inner core on the Slichter periods (assuming a rigid-fixed mantle, i.e. a rigid mantle fixed in the steadily rotating reference frame), and the effect of mantle elasticity (retaining odd-degree spheroidal self-coupling of the displacement field of the mantle). The data in Table 4 and Table 5 show that the effects of higher (than one) degree displacement field in the inner core and the effects of mantle elasticity are relatively small. Both are of the same order, amounting only to about one part in a thousand. It is apparent that the net effect of these influences is to lengthen the eigenperiods of the Slichter modes slightly, because they reduce the effective gravitational restoring force that sustains the vibration. Note that the modification to the eigenperiods of the Slichter modes by these effects are also slightly different for each mode. The increment of the eigenperiod of the prograde mode (m=-1) is slightly larger than that of the polar mode, and the increment of the retrograde mode (m=1) is slightly less than that of the polar mode. This may be due to the nature of the Earth's rotation. The eastward travelling waves are enhanced, whereas the westward travelling waves are diminished. This is the same mechanism that causes uneven splitting of the mode.

Table 4: Comparison of the eigenperiods (hr) for cases:
1. homogeneous elastic inner core, only the degree 1 displacement field is taken into account;
2. elastic inner core, the spheroidal self-coupling of the degree 5 displacement field is taken into account. A rigid-fixed mantle is assumed for both cases.

	non-rotating	rotating		
		m=0	m=1	m=-1
1.(degree 1)	5.39946	5.28990	4.74922	5.95462
2.(self-coupling)	5.40589	5.29592	4.75412	5.96220
Difference	0.00643	0.00602	0.00490	0.00758
Increment	0.119%	0.114%	0.103%	0.127%

Table 5: Effects of a deformable CMB and the elasticity of the mantle on the eigenperiods (hr) of the Slichter modes:
1. Rigid-fixed mantle, elastic inner core, spheroidal self-coupling of displacement field is retained in the inner core;
2. Elastic mantle and inner core, spheroidal self-coupling of displacement field is retained in both the mantle and inner core.

	non-rotating	rotating		
		m=0	m=1	m=-1
1.(rigid-fixed mantle)	5.40589	5.29592	4.75412	5.96220
2.(elastic mantle)	5.41190	5.30168	4.75935	5.96972
Difference	0.00601	0.00576	0.00523	0.00752
Increment	0.111%	0.109%	0.110%	0.126%

The eigenfunctions of the mantle are obtained upon integrating the mantle governing differential equations. Following procedures in §3.3, the corresponding effective load Love numbers at the CMB for field variables y_2, y_3, y_4, y_5, and y_6 can be readily obtained. Then the starting solutions of these variables at the CMB will be calculated using those effective load Love numbers and the eigenfunctions $\chi(a_+)$ and $\chi(b_-)$ of the ICB and CMB ($y_1(b)$ has been calculated in §3.3). Crossley (1993, unpublished) has shown that the mantle eigenfunctions have two disturbing features: y_5 is about twice as large as it should be, and **u** is reversed in sign from the correct motion (Rochester & Peng 1993). The $n = 1$ part of the eigenfunctions produced here show the same features (Fig. 1 - Fig. 8). The former can be clearly seen by comparing Fig. 1 - Fig. 4 with Fig. 9 - Fig. 12, and the latter was shown in Fig. 5 - Fig. 8, which are the enlarged portions of the plots of the mantle eigenfunction y_1. Note that y_1 of the mantle has the correct sign only for the retrograde ($m = 1$) mode (Fig. 7). The feature of y_1 having a wrong sign in the mantle indicates a violation of the conservation of the linear momentum across the CMB. As I discussed in Chapter 2, this unusual behaviour of the eigenfunctions across the CMB and in the mantle arises from the fact that the basic assumption of the SSA, the inequality (12), is violated. On the other hand, in the case of a neutrally stratified liquid core, the SSA removes the sources of V_1 to the core boundaries by reducing the Poisson equation to a Laplace equation. This distortion of V_1 in the liquid core is probably responsible for starting y_5 off with the wrong value at the bottom of the mantle. Without actually solving the Laplace equation, the solution of y_5 is assumed from the nature of the Laplace equation, and computed from the quantities purely derived from the SSWE alone. This latter character may also contribute to the larger amplitude of y_5 in

the mantle. Note that even if the conditions of $y_4 = 0$ and y_3 being discontinuous at the outer core boundaries are met, all other y_i's have shown some kind of discontinuity at the ICB and CMB, where they are supposed to be continuous. This discrepancy may well be related to the approximating nature of the variational method and the use of the natural character of the continuity condition $\hat{\mathbf{n}} \cdot \mathbf{u}$, and to the fact that the trial functions do not satisfy the boundary condition *a priori* or *a posteriori* at the outer core boundaries. Indeed the procedure used here only ensures that the trial function satisfies the SSWE and the boundary conditions in some average sense. Choosing to make the trial function satisfy the boundary conditions *a priori* would have reduced the number of independent d_k's in (99).

Figure 1: Eigenfunctions of the polar mode computed using SSA
For non-rotating PREM with a neutral LC
m=0, T=5.41190 hr, N=1

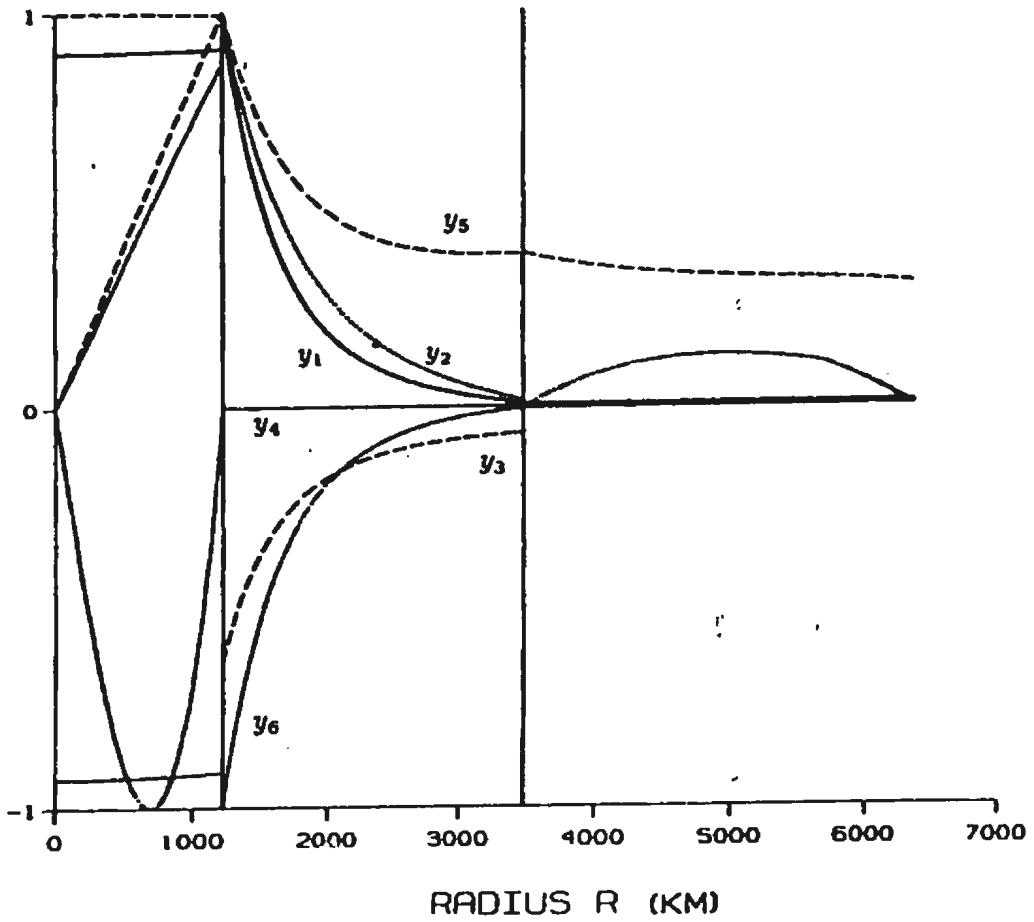

Figure 2: Eigenfunctions of the polar mode computed using SSA
For rotating PREM with a neutral LC
m=0, T=5.30168 hr, N=1

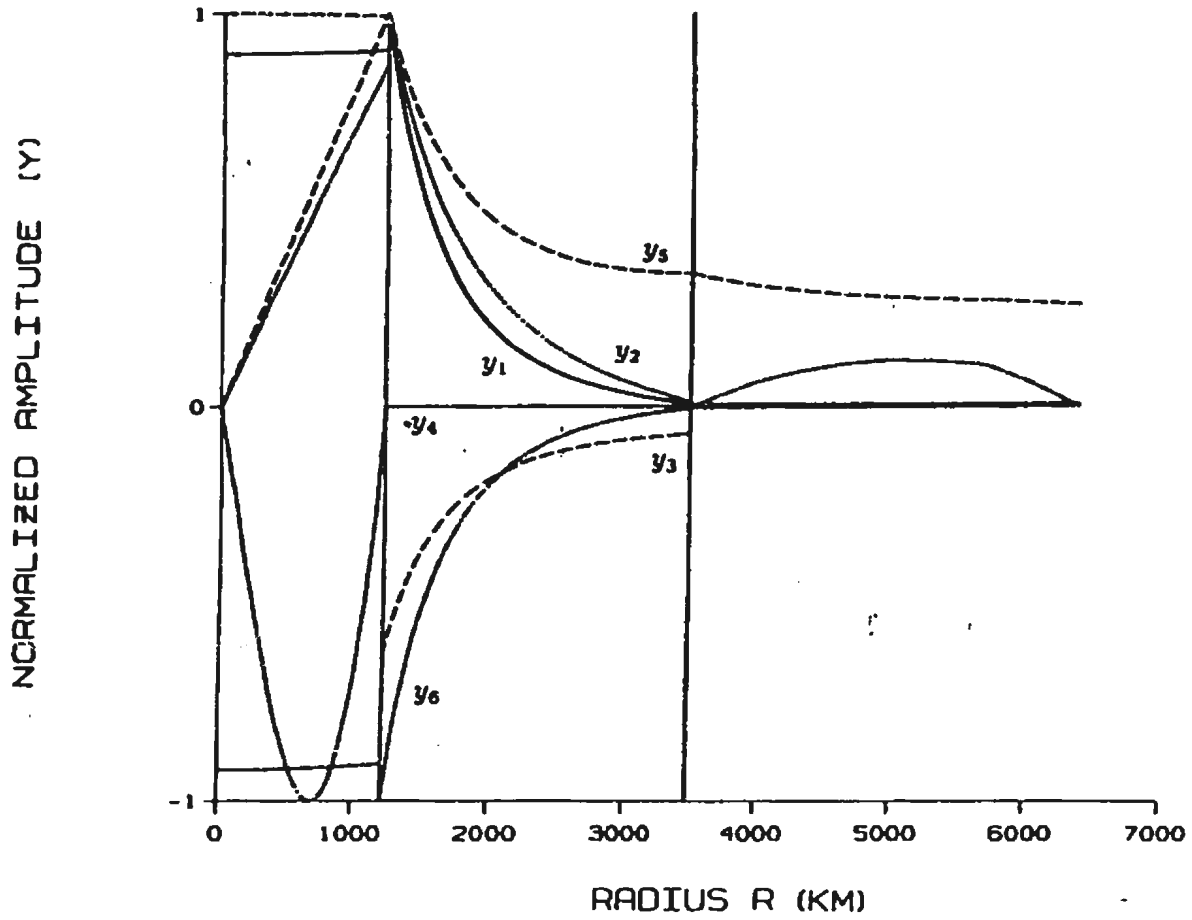

Figure 3: Eigenfunctions of the retrograde mode computed using SSA
For rotating PREM with a neutral LC
m=1, T=4.75935 hr, N=1

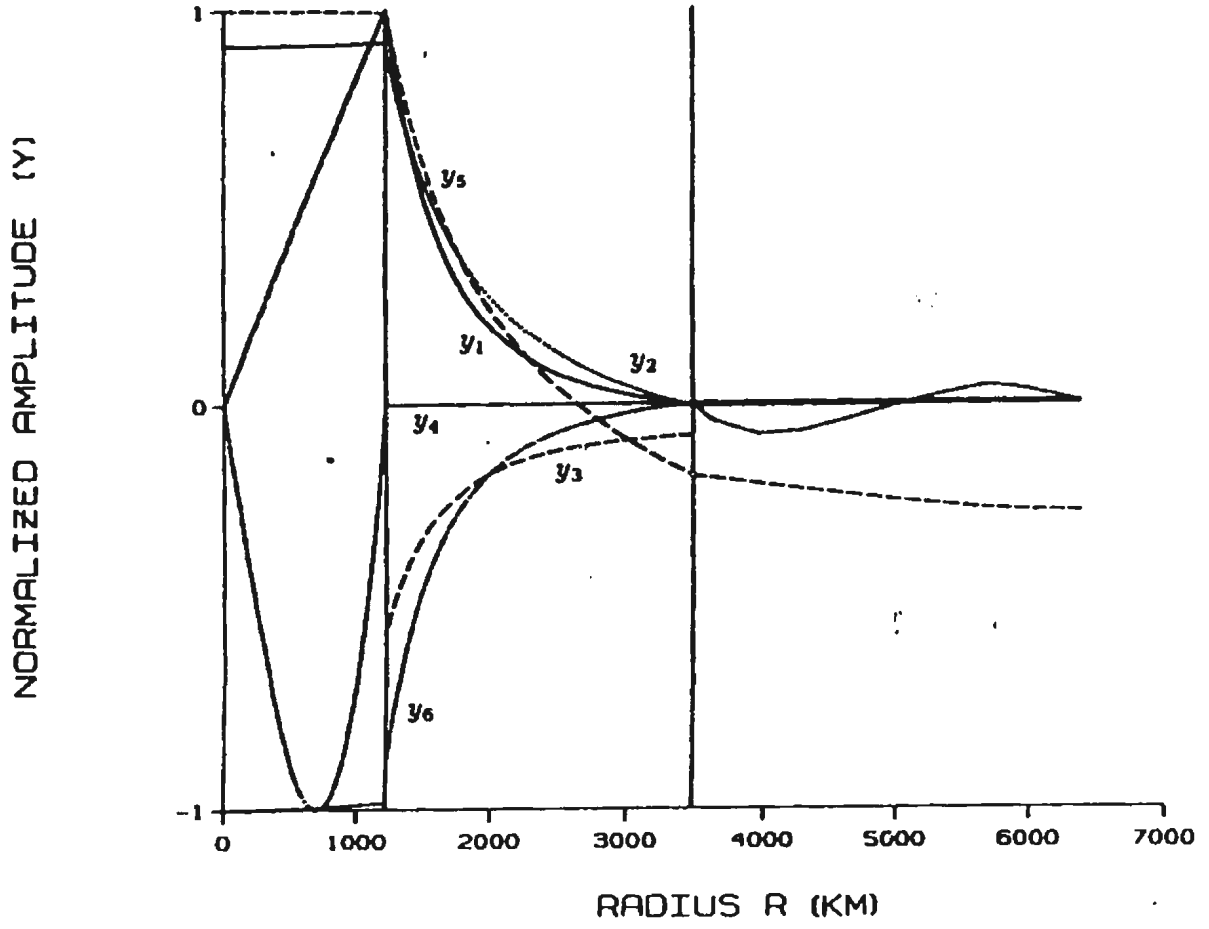

Figure 4: Eigenfunctions of the protrograde mode computed using SSA
For rotating PREM with a neutral LC
m=-1, T=5.96972 hr, N=1

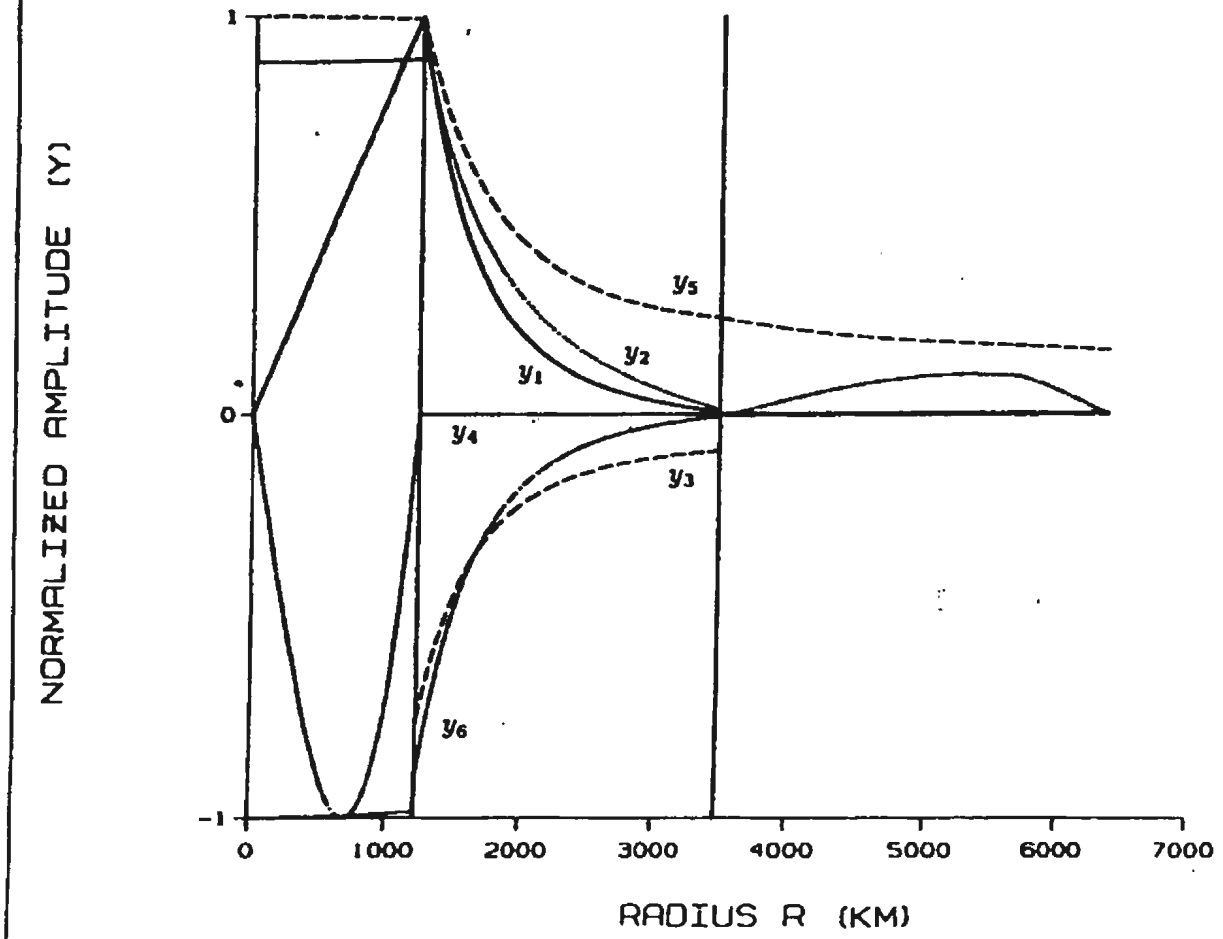

Figure 5: Eigenfunction y_1 of the mantle for the polar mode computed using SSA for a non-rotating PREM with a neutral LC
m=0, T=5.41190 hr, N=1

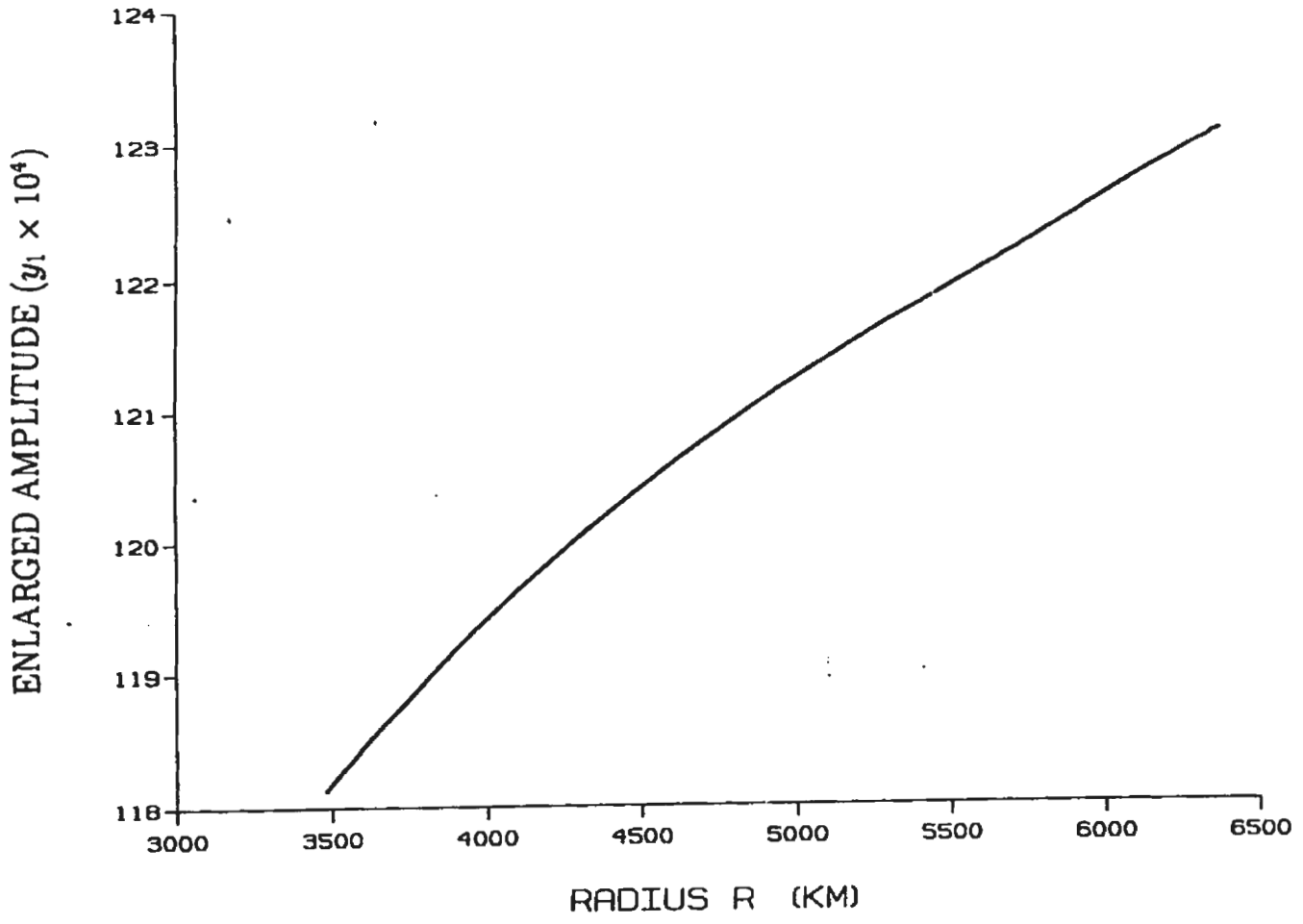

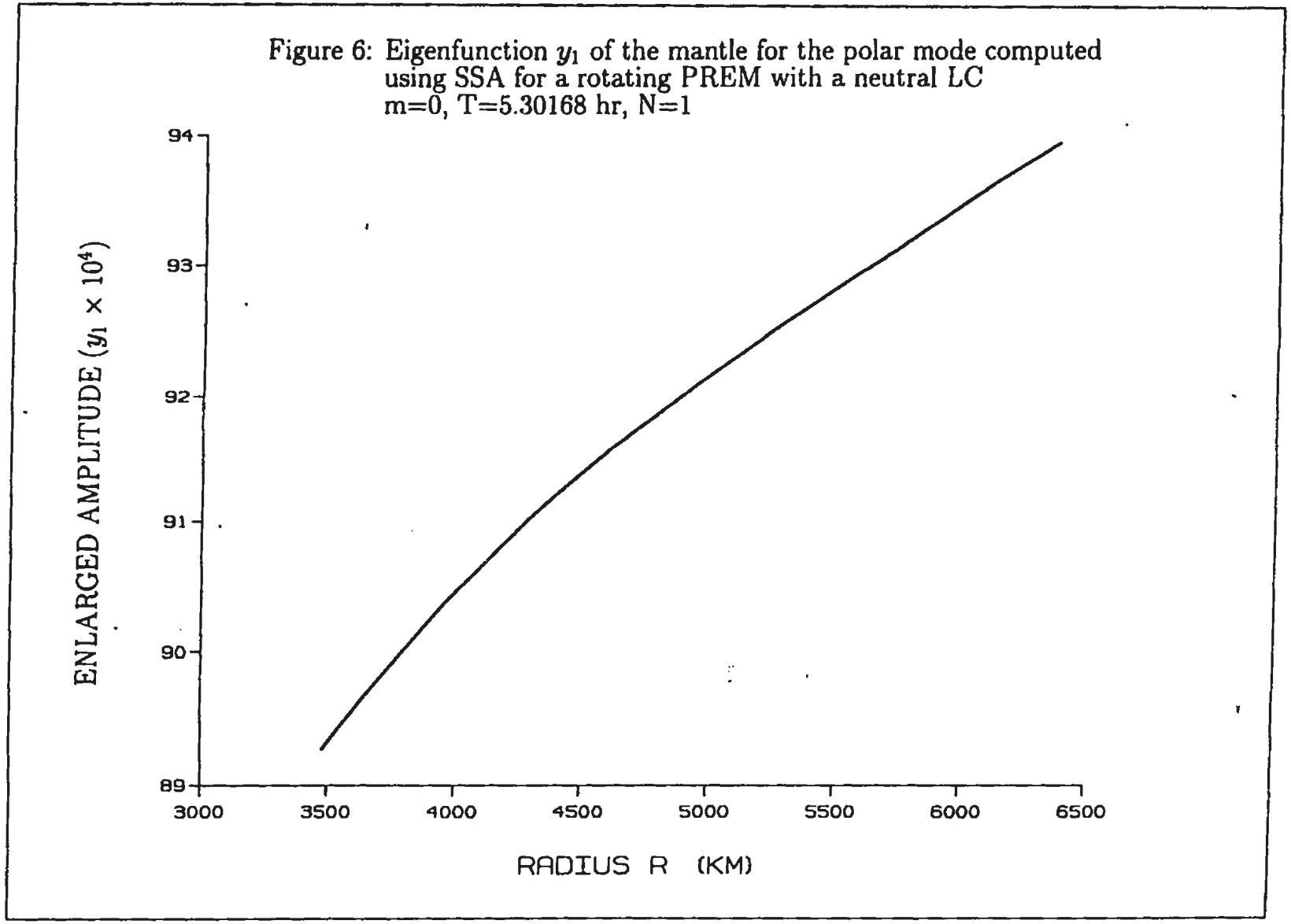

Figure 6: Eigenfunction y_1 of the mantle for the polar mode computed using SSA for a rotating PREM with a neutral LC
m=0, T=5.30168 hr, N=1

Figure 7: Eigenfunction y_1 of the mantle for the retrograde mode computed using SSA for a rotating PREM with a neutral LC m=1, T=4.75935 hr, N=1

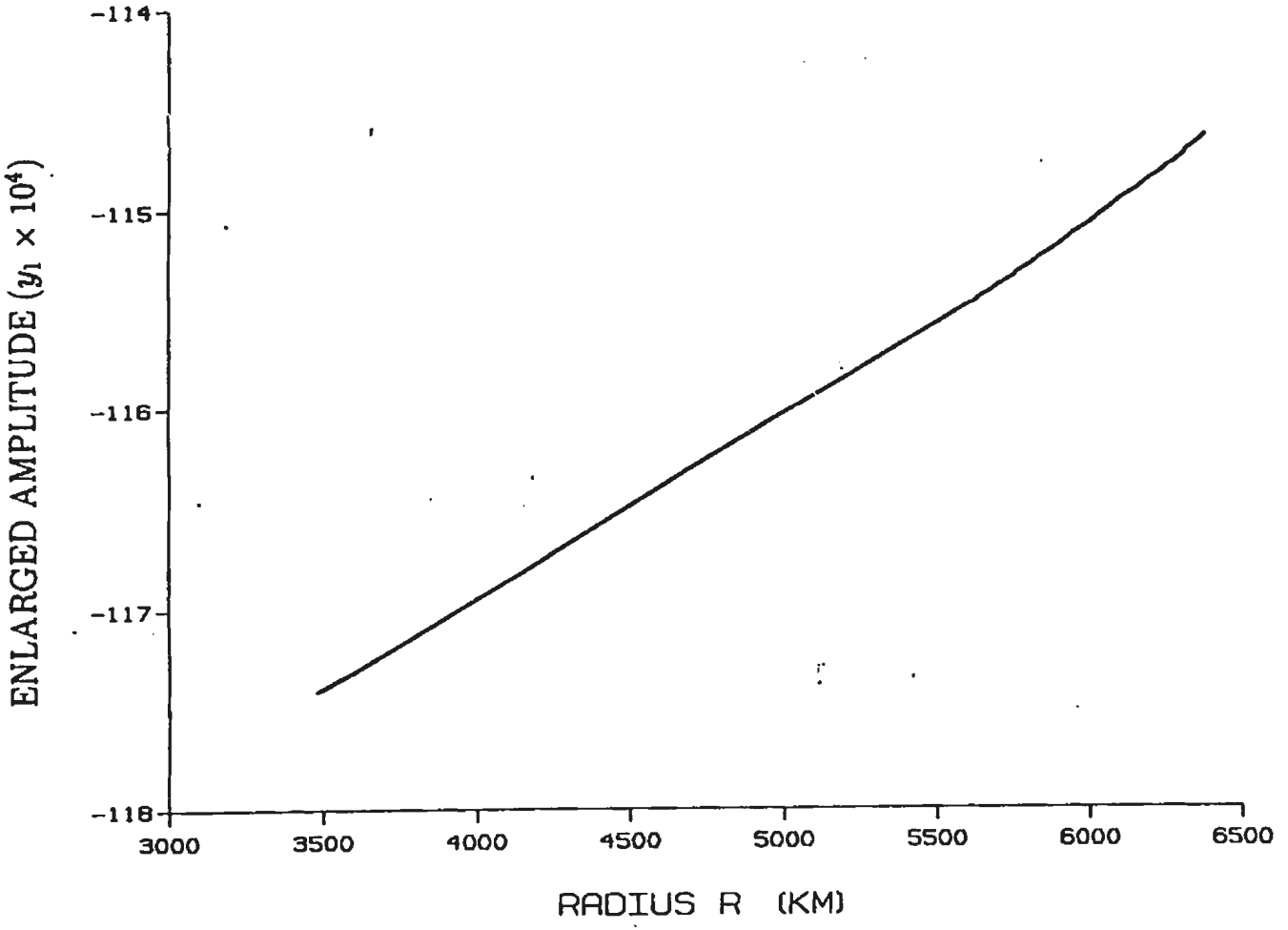

Figure 8: Eigenfunction y_1 of the mantle for the prograde mode computed using SSA for a rotating PREM with a neutral LC m=-1, T=5.96972 hr, N=1

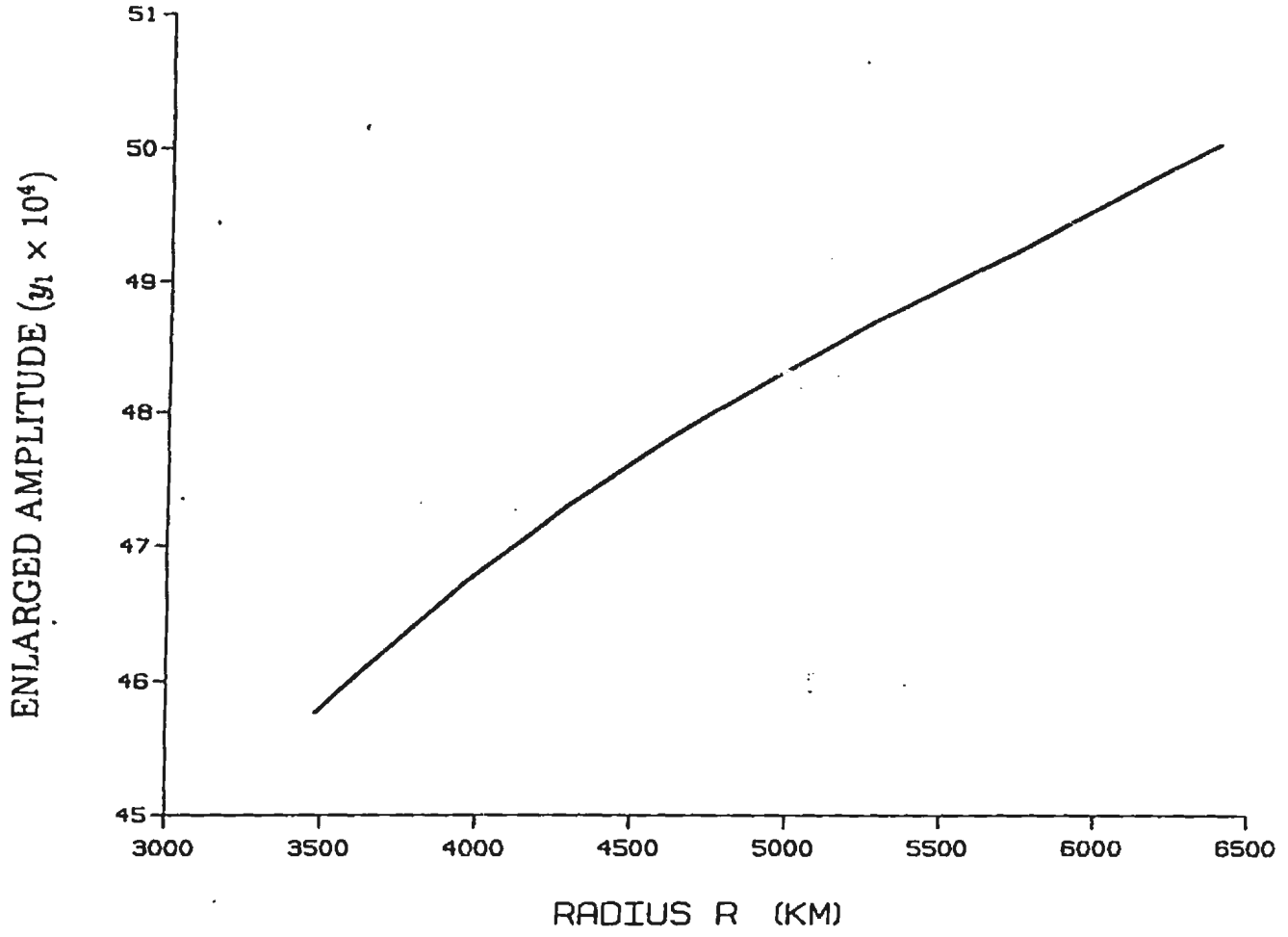

Chapter 5 Two-Potential Description of Core Dynamics

5.1 Introduction

I have discussed and tested in Chapter 2, 3 and 4 the problems associated with application of the SSA. The primary one was that the deformable core boundaries made it impossible, except in the artificial case of a strictly neutral liquid core, to solve the resulting SSWE for the scalar potential χ without simultaneously solving the Poisson equation for the scalar potential V_1. This difficulty greatly reduces the utility of the SSA, and at the same time stimulates searches for the possibility of an exact description of dissipationless core dynamics using the two scalar potential χ and V_1. Wu & Rochester (1990) showed that this is possible. The two-potential description of core dynamics they discovered indeed achieves the latter goal. This description is an improvement on the conventional treatment of exact core dynamics using the spheroidal and toroidal displacement field with the potential field V_1, since it reduces four field variables (three vector components and one scalar) to two, both of which are scalars requiring similarly simple mathematical representation. The spheroidal-toroidal field representation of conventional normal mode theory is simply bypassed and computational effort is thereby considerably reduced.

In this thesis, I intend to show the application of this two-potential description to solve the Slichter modes eigenproblem, for a spherical Earth model in this chapter, and for an ellipsoidal Earth model in Chapter 7, 8 and 9. The comparison of results obtained in this

chapter with that obtained using the SSA and direct integration will also show the advantage of the TPD Note that the bulk of this work using the TPD was completed before the appearance of Crossley's (1992) alternative exact calculation.

5.2 Governing Equations in the Two-Potential Description of Core Dynamics

Wu & Rochester (1990) showed that the governing system (8), (9), (10) and (11) can be reduced, without invoking any approximation, to a coupled pair of second order linear partial differential equations based on exactly two scalar potential fields χ and V_1. With χ defined in (16), they started from decoupling the mass conservation equation (9) by substituting ρ_1 from that equation in (10) and (11). Then they used (16) to eliminate p_1 from (8) and (10). Finally invoking equation (22), six equations in the governing system were reduced to five: namely the equation of momentum conservation (vector), the Poisson (scalar) and the entropy equations (scalar)

$$\omega^2\mathbf{u} - 2i\omega\Omega\hat{\mathbf{k}}\times\mathbf{u} = \nabla\chi + [\nabla\cdot\mathbf{u} + \frac{(1-\beta)}{\alpha^2}(\chi + V_1 + \mathbf{u}\cdot\mathbf{g}_0)]\,\mathbf{g}_0 \tag{133}$$

$$\nabla^2 V_1 = -4\pi G\nabla\cdot(\rho_0\mathbf{u}) \tag{134}$$

$$\nabla\cdot\mathbf{u} = -\frac{(\chi + V_1 + \mathbf{u}\cdot\mathbf{g}_0)}{\alpha^2}. \tag{135}$$

Substituting (135) into (133) and (134), the latter pair become:

$$\omega^2\mathbf{u} - 2i\omega\Omega\hat{\mathbf{k}}\times\mathbf{u} = \nabla\chi - \beta\mathbf{g}_0\frac{(\chi + V_1 + \mathbf{u}\cdot\mathbf{g}_0)}{\alpha^2} \tag{136}$$

$$\nabla^2 V_1 = -4\pi G\rho_0 \frac{(\chi + V_1 + \beta \mathbf{u}\cdot\mathbf{g}_0)}{\alpha^2}. \tag{137}$$

Now the displacement field $\mathbf{u}$ can be solved directly from (136) as long as $|\omega| \neq 2\Omega$

$$\omega^2(1-\mu^2)\mathbf{u} = \mathbf{\Gamma}\cdot\nabla\chi + \omega^2(1-\mu^2)(\chi + V_1)\frac{\mathbf{C}^*}{B} \tag{138}$$

where $\mathbf{\Gamma}$, $\mathbf{C}$, B and μ are defined in (19), (18), (17) and (20).

Finally substituting $\mathbf{u}$ from (138) in the entropy and Poisson equations (135) and (137) to obtain two coupled second-order partial differential equations in only two potential variables χ and V_1:

$$\nabla\cdot[\mathbf{\Gamma}\cdot\nabla\chi + \omega^2(1-\mu^2)(\chi+V_1)\frac{\mathbf{C}^*}{B}]$$

$$-\frac{\omega^2(1-\mu^2)}{\beta B}[\mathbf{C}\cdot\nabla\chi - \omega^2(1-\mu^2)(\chi+V_1)] = 0 \tag{139}$$

$$\frac{1}{4\pi G}\nabla^2 V_1 - \rho_0\{\frac{\mathbf{C}\cdot\nabla\chi}{B} - [\frac{1-\beta}{\alpha^2} + \frac{\omega^2(1-\mu^2)}{B}](\chi+V_1)\} = 0. \tag{140}$$

In a neutrally stratified liquid core ($\beta = 0$), this pair of equations becomes

$$\nabla\cdot(\rho_0\mathbf{\Gamma}_p\cdot\nabla\chi) + \omega^2(1-\mu^2)\frac{\rho_0(\chi+V_1)}{\alpha^2} = 0 \tag{141}$$

$$\nabla^2 V_1 + 4\pi G\frac{\rho_0(\chi+V_1)}{\alpha^2} = 0. \tag{142}$$

Note that a negative β will introduce additional liquid core resonances of gravity wave type to the Slichter modes eigen-spectrum. With a non-zero β, the possibility exists that $B \to 0$ in some frequency range somewhere in the liquid core, which leads the equations

(139) and (140) to become improper. This point becomes more clear if the Brunt-Väisäilä frequency N is used in (17) according to the relation

$$N^2 = -\frac{\beta g_0^2}{\alpha^2}. \tag{143}$$

Then whenever $B \to 0$, the following criterion from (17) holds

$$N^2[1 - \mu^2 \frac{(\dot{\mathbf{k}} \cdot \mathbf{g}_0)^2}{g_0^2}] = \omega^2(1 - \mu^2). \tag{144}$$

That is to say that difficulties will arise in either the following period range:

(i) $T >$ larger of (T_{BV}, 12 hr)

(ii) smaller of (T_{BV}, 12 hr) $> T > \frac{T_{BV}}{[1+(\frac{T_{BV}}{12})^2]^{1/2}}$

where the Brunt-Väisäilä period $T_{BV} = 2\pi/N$. For a non-neutrally stratified liquid core, the period of the slowest core gravity mode is at least $6 \sim 8$ hours, based on Masters' (1979) estimate of the core stability parameter β (Crossley, 1984).

To use the TPD in case of $B \to 0$, (139) and (140) can be modified with $(\beta B)^2$ and βB to yield

$$(\beta B)^2 \nabla \cdot \{\mathbf{\Gamma}_p \cdot \nabla\chi - \frac{\mathbf{C}}{B}[\mathbf{C} \cdot \nabla\chi - \omega^2(1 - \mu^2)(\chi + V_1)]\}$$

$$- \omega^2(1 - \mu^2)\,\beta B\,[\mathbf{C} \cdot \nabla\chi - \omega^2(1 - \mu^2)(\chi + V_1)] = 0 \tag{145}$$

$$\frac{1}{4\pi G}\beta B \nabla^2 V_1 - \rho_0\{\beta \mathbf{C} \cdot \nabla\chi - [\frac{1 - \beta}{\alpha^2}\beta B + \beta\omega^2(1 - \mu^2)](\chi + V_1)\} = 0. \tag{146}$$

Equations (145) and (146) are the forms of the governing equations suitable for a numerical search for eigenperiods in a frequency range for which B may vanish somewhere in the liquid core. These equations will be used in Chapter 6.

An improvement on the two-potential description, which avoids the complexity of the equations required when B may vanish, and retains the advantages of a variational principle, was recently discovered by Rochester (unpublished ms; Seyed-Mahmoud, 1994). However, the discovery of this three-potential description came at such a late stage in my calculations that it seemed unnecessary to incorporate it into this thesis.

Chapter 6 Galerkin Solution of the Two-Potential Description

6.1 Introduction

An alternative approach to solve the reformulated two-potential equations (145) and (146) is the Galerkin method. This weighted residual procedure allows the trial functions to satisfy the governing partial differential equations in a weighted mean sense. The difference between the Galerkin method and other residual methods is that the former takes the trial functions themselves as the weighting functions. The resulting expressions from substituting the trial functions into the governing equations are orthogonal to the respective set of trial functions. In principle, one can require the trial functions, χ and V_1 in the case of the two-potential description, to satisfy the associated boundary conditions *a priori*. But again, one can take advantage of the natural character of the boundary conditions on χ and V_1, and relax the latter requirement by adding necessary surface integrals containing these boundary conditions to the resulting Galerkin equations.

Suppose the two equations of the TPD (145) and (146) are written in a compact form

$$\underline{\mathcal{L}}\ \underline{\chi} = \underline{0} \tag{147}$$

where $\underline{\mathcal{L}}$ is constructed from the linear operators in these two equations:

$$\underline{\mathcal{L}} = (\mathcal{L}_1\ \ \mathcal{L}_2)^T \tag{148}$$

and

$$\underline{\chi} = (\chi\ \ V_1)^T. \tag{149}$$

At the outer core boundaries, $\underline{\chi}$ are required to satisfy continuity conditions

$$\underline{\mathcal{K}}\ \underline{\chi}\ =\ \underline{0} \tag{150}$$

where $\underline{\mathcal{K}}$ are also linear operators in the associated boundary conditions:

$$\underline{\mathcal{K}}\ =\ (\mathcal{K}_1\ \ \mathcal{K}_2)^T. \tag{151}$$

Then the compact form of the Galerkin equations incorporating the natural boundary conditions is

$$\int_{LC} \underline{\chi}^*\underline{\mathcal{L}}\ \underline{\chi}\ dV + \int_{ICB+CMB} \underline{\Psi}^*\underline{\mathcal{K}}\ \underline{\chi}\ dS = \underline{0} \tag{152}$$

where $\underline{\Psi}^*$ are independent weighting functions

$$\underline{\Psi}\ =\ (\Psi_1\ \ \Psi_2)^T. \tag{153}$$

6.2 Two-Potential Galerkin Equations

Guided by (99), the trial function for the potential field V_1 can be constructed in a similar fashion

$$V_1(r,\theta,\phi)\ =\ \sum_{k=1}^{(2L-2)N} c_k(\frac{r}{z})^\nu P_{2n-1}^m e^{im\phi}. \tag{154}$$

For convenience, χ and V_1 can also be written in an alternative form

$$\chi = \sum_{k=1}^{M} d_k\chi_k e^{im\phi} \tag{155}$$

$$V_1 = \sum_{j=1}^{M} c_k V_{1,j} e^{im\phi}. \tag{156}$$

where χ_k and $V_{1,j}$ are functions of radius r and the polar angle θ. As $M \to \infty$, the trial function set in a Galerkin method shall represent any function satisfying boundary conditions. This is the so-called 'completeness' requirement (Zienkiewicz & Morgan, 1982).

Now using the definition (138) for the displacement $\mathbf{u}$, I will explicitly write the Galerkin equations constructed in (152) as

$$\begin{aligned}
&\omega^2(1-\mu^2)\int_{LC}\chi_l^*(\beta B)^2\nabla\cdot\mathbf{u}dV \\
&-\omega^2(1-\mu^2)\int_{LC}\chi_l^*(\beta B)[\mathbf{C}\cdot\nabla\chi-\omega^2(1-\mu^2)(\chi+V_1)] \\
&+\int_{ICB+CMB}\Psi_{1,l}^*\hat{\mathbf{n}}\cdot(\mathbf{u}-\mathbf{u}_s)dS \;=\; 0
\end{aligned} \tag{157}$$

$$\begin{aligned}
&\frac{1}{4\pi G}\int_{LC}(\beta B)\,V_{1,l}^*\nabla^2V_1dV-\int_{LC}\rho_0\beta V_{1,l}^*\mathbf{C}\cdot\nabla\chi dV \\
&+\int_{LC}\rho_0V_{1,l}^*[\frac{(1-\beta)}{\alpha^2}\beta B+\omega^2(1-\mu^2)\beta](\chi+V_1)dV \\
&+\int_{ICB+CMB}\Psi_{2,l}^*[\hat{\mathbf{n}}\cdot(\nabla V_1-4\pi G\rho_0\mathbf{u})-\hat{\mathbf{n}}\cdot(\nabla V_1^s-4\pi G\rho_0^s\mathbf{u}_s)]dS \;=\; 0
\end{aligned} \tag{158}$$

where χ_l^*, $\Psi_{1,l}^*$, $\Psi_{2,l}^*$ and $V_{1,l}^*$ are weighting functions, ρ_0^s, $\mathbf{u}_s$ and V_1^s are the density, displacement and additional gravitational potential fields in the solid parts of the Earth.

Using the divergence theorem and equation (138) again, it is clear that if I choose

$$\Psi_{1,l}^* \;=\; -\omega^2(1-\mu^2)\chi_l^*(\beta B)^2 \tag{159}$$

$$\Psi_{2,l}^* \;=\; -\frac{1}{4\pi G}(\beta B)V_{1,l}^* \tag{160}$$

equations (157) and (158) will be changed into

$$-\int_{LC}\nabla[\chi_l^*(\beta B)^2]\cdot\{\mathbf{\Gamma}_p\cdot\nabla\chi-\frac{\mathbf{C}^*}{B}[\mathbf{C}\cdot\nabla\chi-\omega^2(1-\mu^2)(\chi+V_1)]\}dV$$

$$- \omega^2(1-\mu^2)\int_{LC} \chi_i^*(\beta B)[\mathbf{C}\cdot\nabla\chi - \omega^2(1-\mu^2)(\chi+V_1)]dV$$

$$+ \int_{ICB+CMB} \omega^2(1-\mu^2)\chi_i^*(\beta B)^2\hat{\mathbf{n}}\cdot\mathbf{u}_s dS \;=\; 0 \tag{161}$$

$$- \frac{1}{4\pi G}\int_{LC}[\beta B\,\nabla V_{1,l}^*\cdot\nabla V_1 + V_{1,l}^*\nabla(\beta B)\cdot\nabla V_1]dV$$

$$- \int_{LC}\rho_0\beta V_{1,l}^*\mathbf{C}\cdot\nabla\chi dV \;+\; \int_{LC}\rho_0 V_{1,l}^*[\frac{(1-\beta)}{\alpha^2}(\beta B)+\omega^2(1-\mu^2)\beta](\chi+V_1)dV$$

$$+ \frac{1}{4\pi G}\int_{ICB+CMB}(\beta B)\,V_{1,l}^*[4\pi G(\rho_0-\rho_0^s)\hat{\mathbf{n}}\cdot\mathbf{u} + \hat{\mathbf{n}}\cdot\nabla V_1^s]dS \;=\; 0. \tag{162}$$

Upon substituting trial functions (99) and (154) into equations (161) and (162) and using the continuity conditions at the ICB and CMB, they may be written in a matrix form

$$\underline{G}\;\underline{D} \;=\; 0 \tag{163}$$

where

$$\underline{G} = (G_1\;\; G_2)^T \tag{164}$$

$$\underline{D} \;=\; (d_1\; d_2\; \cdots\; d_k \cdots\; c_1\; c_2\; \cdots\; c_k\; \cdots)^T. \tag{165}$$

$G_{1,ij}$ and $G_{2,ij}$ are the i,jth component of the LHS of equations (161) and (162)

$$G_{1,ij} = -\int_{r,\theta}\nabla(\chi_i^*(\beta B)^2)\cdot\{\Gamma_p\cdot\nabla\chi_j$$

$$- \frac{\mathbf{C}^*}{B}[\mathbf{C}\cdot\nabla\chi_j - \omega^2(1-\mu^2)(\chi_j+V_{1,j})]\}r^2\sin\theta dr d\theta$$

$$- \omega^2(1-\mu^2)\int_{r,\theta}\chi_i^*(\beta B)[\mathbf{C}\cdot\nabla\chi_j - \omega^2(1-\mu^2)(\chi_j+V_{1,j})]r^2\sin\theta dr d\theta$$

$$- \omega^2(1-\mu^2)\int_{\theta}\chi_i^*(\beta B)^2 y_1^j(a)a^2\sin\theta d\theta$$

$$+ \omega^2(1-\mu^2)\int_\theta \chi_i^-(\beta B)^2 y_1^j(b) b^2 \sin\theta d\theta \tag{166}$$

$$\begin{aligned}
G_{2,ij} = & -\int_{r,\theta} \rho_0 \beta V_{1,i}^- \mathbf{C}\cdot\nabla\chi_j r^2\sin\theta dr d\theta \\
& + \int_{r,\theta}\rho_0 V_{1,i}^-[\frac{(1-\beta)}{\alpha^2}(\beta B) + \omega^2(1-\mu^2)\beta](\chi_j + V_{1,j}) r^2\sin\theta dr d\theta \\
& - \frac{1}{4\pi G}\int_{r,\theta}[\beta B\,\nabla V_{1,i}^-\cdot\nabla V_{1,j} + V_{1,i}^-\nabla(\beta B)\cdot\nabla V_{1,j}] r^2\sin\theta dr d\theta \\
& - \frac{1}{4\pi G}\int_\theta (\beta B) V_{1,i}^-[4\pi G\rho_0(a) y_1^j(a) + y_6^j(a)] a^2\sin\theta d\theta \\
& + \frac{1}{4\pi G}\int_\theta (\beta B) V_{1,i}^-[4\pi G\rho_0(b) y_1^j(b) + y_6^j(b)] b^2\sin\theta d\theta .
\end{aligned} \tag{167}$$

Note that $y_1^j(a)$, $y_1^j(b)$, $y_6^j(a)$, and $y_6^j(b)$ in $G_{1,ij}$ and $G_{2,ij}$ are dimensioned quantities of the inner core and mantle, and they are readily computed from the corresponding dimensionless quantities.

6.3 Eigenperiods and Eigenfunctions: Numerical Results Using the Two-Potential Description

In numerical computations, the volume integrals in $G_{l,ij}$ can be evaluated analytically for a neutral liquid core, whereas numerical integration with respect to r is required if the stratification of the liquid core is not neutral. The θ component of the integration is evaluated analytically for any spherical stratification using the orthogonality relation of the associated Legendre functions. Due to the use of the TPD, the resulting matrix of the determinant is twice as large in size compared to that which results from using the SSA for the same level of truncation.

Among these computed results, I compared the eigenperiods of the Slichter modes for a neutral liquid core calculated using the TPD, with that obtained from using the SSA. The first part of the Table 6 lists the results of this comparison. In examining the accuracy of both the SSA and TPD, I also compared (in the second part of Table 6) the results from the SSA and those from the direct integration method. Note that the latter is limited to a non-rotating Earth model only.

Generally speaking, the error brought into the eigenperiod calculation by using the SSA is small. From the above comparison, it seems that the maximum difference appears in prograde mode ($m = -1$) and the minimum difference appears in retrograde mode ($m = 1$), with a shift of 0.043% and 0.006% respectively. The difference between the results from the TPD and the results from the direct integration is much smaller than the difference between the results from the SSA and the results from the direct integration, by a factor of about

3 or so. Note that a difference of 0.00045 hr between the result from the TPD and that from the direct integration is still large, whereas in principle they should be very small. This discrepancy may well be related to the fact that, in this thesis, the trial functions in the Galerkin method based on the TPD only satisfy the governing equations and the associated boundary conditions in a weighted average sense. If the trial functions satisfy the boundary conditions exactly, this discrepancy should be very small.

Table 6: Comparison of the eigenperiods (hr) from the TPD with those from the SSA for the PREM model with a neutrally stratified LC.

	non-rotating	rotating		
		m=0	m=1	m=-1
SSA-VP	5.41190	5.30168	4.75935	5.96972
TPD-Galerkin	5.41367	5.30333	4.75960	5.97230
Difference	0.00177	0.00165	0.00027	0.00259
Percentage	0.033 %	0.031 %	0.006 %	0.043 %
Direct integ.	5.41322			
Diff. to SSA	0.00132			
Diff. to TPD	0.00045			

Table 7 compares the eigenperiods of the Slichter modes for the original PREM model, with those for the modified PREM model with an exactly neutrally stratified liquid core. Both these results are calculated using the Galerkin method based on the TPD. It is shown that if the core is exactly neutrally stratified, the Slichter periods are shorter than those of the non-neutral liquid core. The largest decrease of 0.126% occurs in the non-rotating case, and a decrease of 0.101%, 0.102% and 0.097% occur for the polar, prograde and retrograde modes respectively. It is known that gravity modes with periods longer than the Slichter modes would exist if the part of the liquid core is stably stratified. Therefore, it is expected that, even though the existence of the Slichter modes does not depend on stable stratification of the liquid core, the non-neutral stratification of it will lengthen the Slichter eigenperiods.

Table 7: Comparison of the eigenperiods (hr) of the Slichter modes for an exactly neutral liquid core with those for a non-neutral liquid core models. Both results are obtained using the TPD.

	non-rotating	rotating		
		m=0	m=1	m=-1
Original PREM Model	5.42050	5.30871	4.76426	5.97838
Modified PREM Model	5.41367	5.30333	4.75960	5.97230
Difference of Eigenperiods	0.126%	0.101%	0.097%	0.102%

Next I compared the results obtained here for the original PREM model with those obtained by Crossley (1992) and Wu & Rochester (1994), for both the non-rotating and rotating Earth models. Crossley (1992) used ICB and CMB Love numbers but a direct integration method and the spheroidal-toroidal field representation to solve the coupled ordinary differential equations in the liquid core for the discrete data version of the PREM. Wu & Rochester (1994) used the TPD and a Galerkin method for a polynomial data version of PREM, as used in this thesis, but with the boundary conditions being satisfied *a priori* by the trial functions. Table 8 displays these three groups of eigenperiods of the Slichter modes respectively. In order to be consistent with Crossley (1992), I only retained five significant figures in the results of Wu & Rochester (1994) and those of this thesis. The line W-P in Table 8 shows that while there is an exact agreement between the eigenperiod calculated in this thesis and that of Wu & Rochester (1994) for the non-rotating case, the eigenperiods of the polar mode, retrograde mode and prograde mode of this thesis are 0.030%, 0.048% and 0.010% shorter than those obtained by Wu & Rochester (1994). These discrepancies may also arise from the different ways we handle the boundary conditions: Wu & Rochester (1994) made the trial functions satisfy the boundary conditions exactly, whereas I used the natural character of these boundary conditions so that the trial functions only satisfy them approximately. The line C-W in Table 8 shows that there are very small differences between the results of Crossley (1992) and those of Wu & Rochester (1994), only amounting to 0.002% - 0.003%. These little differences may be caused by their use of different data versions: discrete vs. polynomial data versions. It is clear that the differences shown in the line C-P indicate a superposition of two sources of errors: one is due to my use of the natural

boundary conditions in the Galerkin method based on the TPD, and one is due to my use of the polynomial data version of the PREM.

Table 8: Comparison of the eigenperiods (hr) of the Slichter modes obtained by different authors using different approaches.
C: Crossley's (1992) results, using the direct integration and the spheroidal-toroidal field representation in the liquid core;
W: Wu & Rochester's (1994) results, using the TPD and a Galerkin method in the liquid core with the boundary conditions satisfied *a priori*;
P: Peng (1995), the results of this thesis using the TPD and a Galerkin method in a liquid core with the boundary conditions not satisfied *a priori*.
C-W, W-P and C-P are percentage differences between these authors' results.

	non-rotating	rotating		
		m=0	m=1	m=-1
C	5.4206	5.3104	4.7667	5.9792
W	5.4205	5.3103	4.7666	5.9790
P	5.4205	5.3087	4.7643	5.9784
C-P	0.002%	0.032%	0.050%	0.012%
W-P	0.000%	0.030%	0.048%	0.010%
C-W	0.002%	0.002%	0.002%	0.003%

After the eigenperiods have been obtained, the coefficients of the trial functions χ and V_1 were calculated using the same procedure as described in Chapter 4. Here I only needed to use the ordinary load Love numbers at the CMB for extending the eigenfunctions to the mantle, since V_1 is explicitly involved in the liquid core now. For comparison with the eigenfunctions obtained in Chapter 4 using the SSA, here I plotted in Fig. 9 - Fig. 16 only the eigenfunctions of degree 1 obtained using the TPD for a neutrally stratified liquid core. In contrast to those obtained using the SSA, these graphs in Fig. 9 - Fig. 16 look like those obtained by direct integration, i.e. the abandonment of the SSA has restored the mantle eigenfunctions to their correct amplitudes (particularly y_5) and sign (particularly y_1, see Fig. 13 - Fig. 16). I conclude that the use of the SSA is responsible for the distortion of the eigenfunctions in the mantle.

Note that the discontinuities of the eigenfunctions y_1, y_2, y_5 and y_6 at the ICB and CMB are still present. Again, the particular way in which I applied the Galerkin method, i.e. using the natural character of the boundary conditions to avoid making the trial functions satisfy these boundary conditions precisely, may be responsible for these jumps at the outer core boundaries. To explain this more clearly, let me present a brief review of just how these eigenfunctions of degree 1 are obtained in the solid parts of the Earth, e.g. in the mantle. Once the numerical solutions are found, values of χ_1^m and dy_5/dr on the liquid side of the CMB are obtained from now-determined trial functions χ and V_1. Using these quantities and the exact load Love numbers, the starting values of y_1, y_2, y_5 and y_6 on the solid side of the CMB are obtained ($y_4 = 0$ and y_3 discontinuous there). These are the quantities that ought to be continuous with the corresponding values of these AJP variables on the liquid

side of the CMB. However, the quantities of the AJP variables on the liquid side of the CMB are calculated from the numerical solutions for χ_1^m and y_5 given by equations (99) and (154) respectively. With $\chi_1^m(b_-)$ and $y_5(b_-)$ so obtained, $y_1(b_-)$ can be calculated from equation (138). Then $y_2(b_-)$ will be given by

$$y_2(b_-) = \rho_0(b_-)[g_0(b)y_1(b_-) - \chi_1^m(b_-) - y_5(b_-)] \tag{168}$$

and finally $y_6(b_-)$ is computed from y_1 and dy_5/dr. All these quantities on the liquid side of the CMB are based on the coefficients of the trial functions χ and V_1 of equations (99) and (154), which are not required to satisfy the boundary conditions exactly. Therefore, one should not expect to see that the quantities computed on the liquid side of the CMB are continuous with the corresponding quantities computed on the solid side of the CMB. That is the price to be paid for taking advantage of the natural character of the boundary conditions, and indicates that future applications of a variational or Galerkin method should use trial functions satisfying the boundary conditions *a priori*.

Figure 9: Eigenfunctions of the polar mode computed using TPD
For non-rotating PREM with a neutral LC
m=0, T=5.41367 hr, N=1

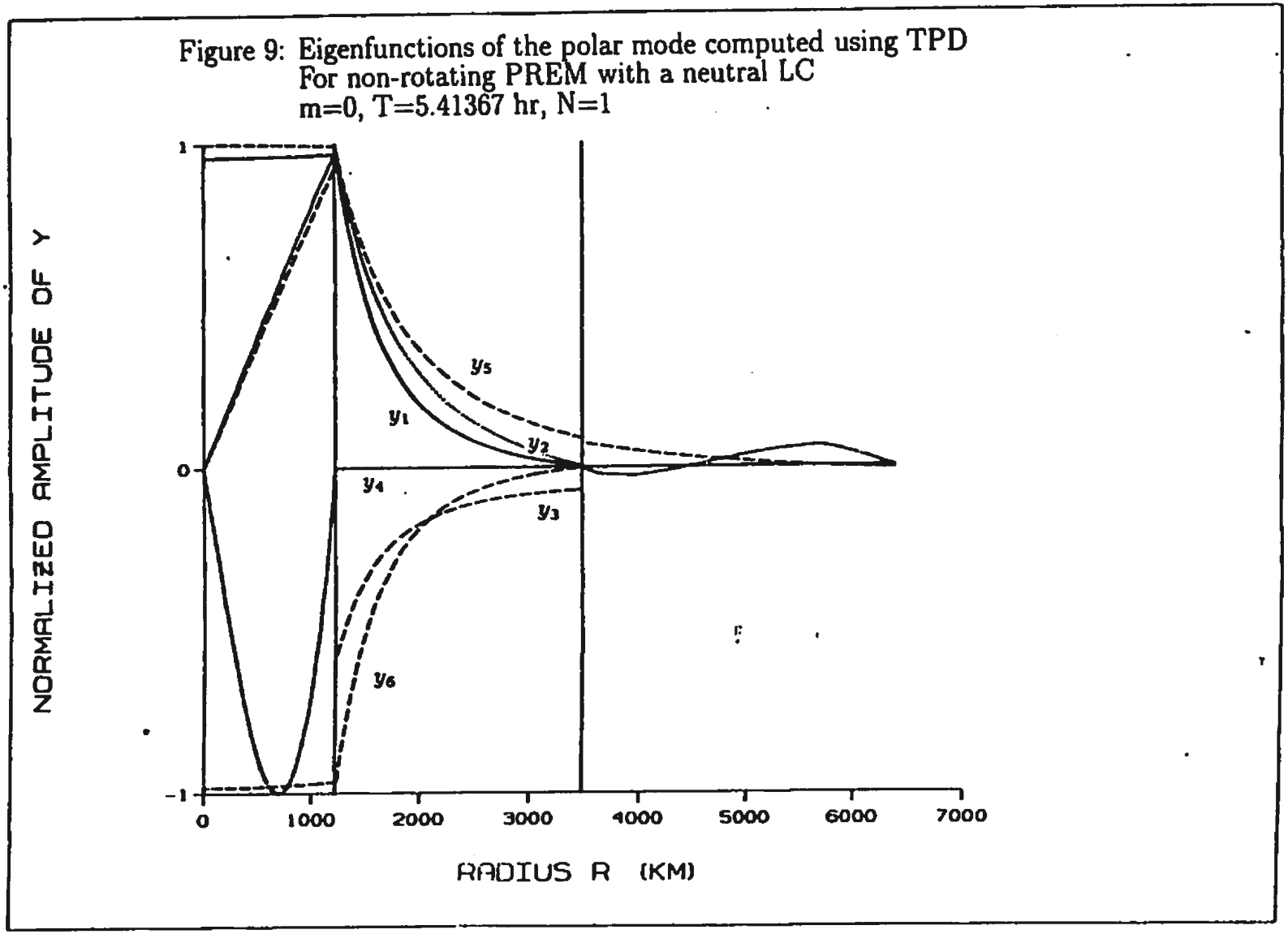

Figure 10: Eigenfunctions of the polar mode computed using TPD
For rotating PREM with a neutral LC
m=0, T=5.30334 hr, N=1

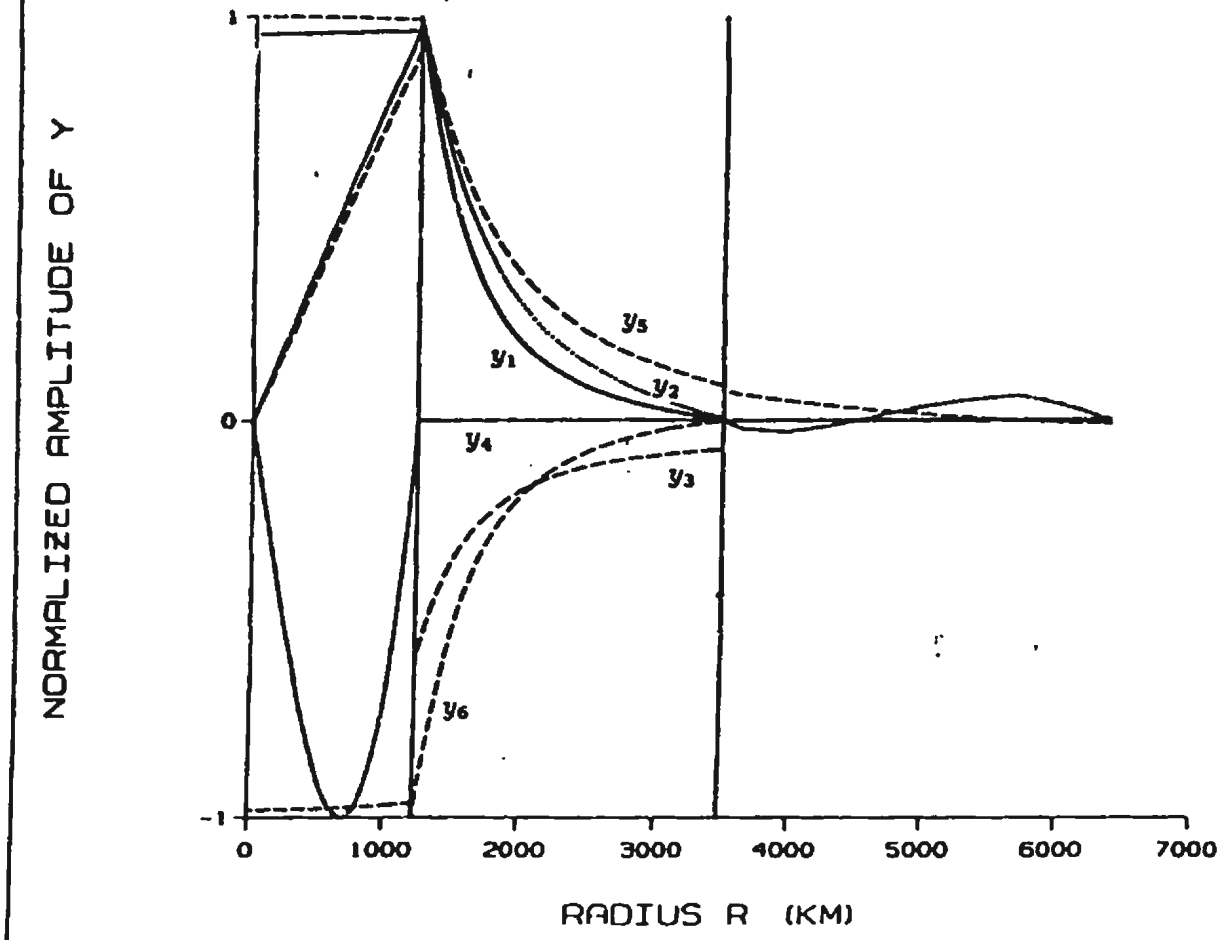

Figure 11: Eigenfunctions of the retrograde mode computed using TPD
For rotating PREM with a neutral LC
m=1, T=4.75960 hr, N=1

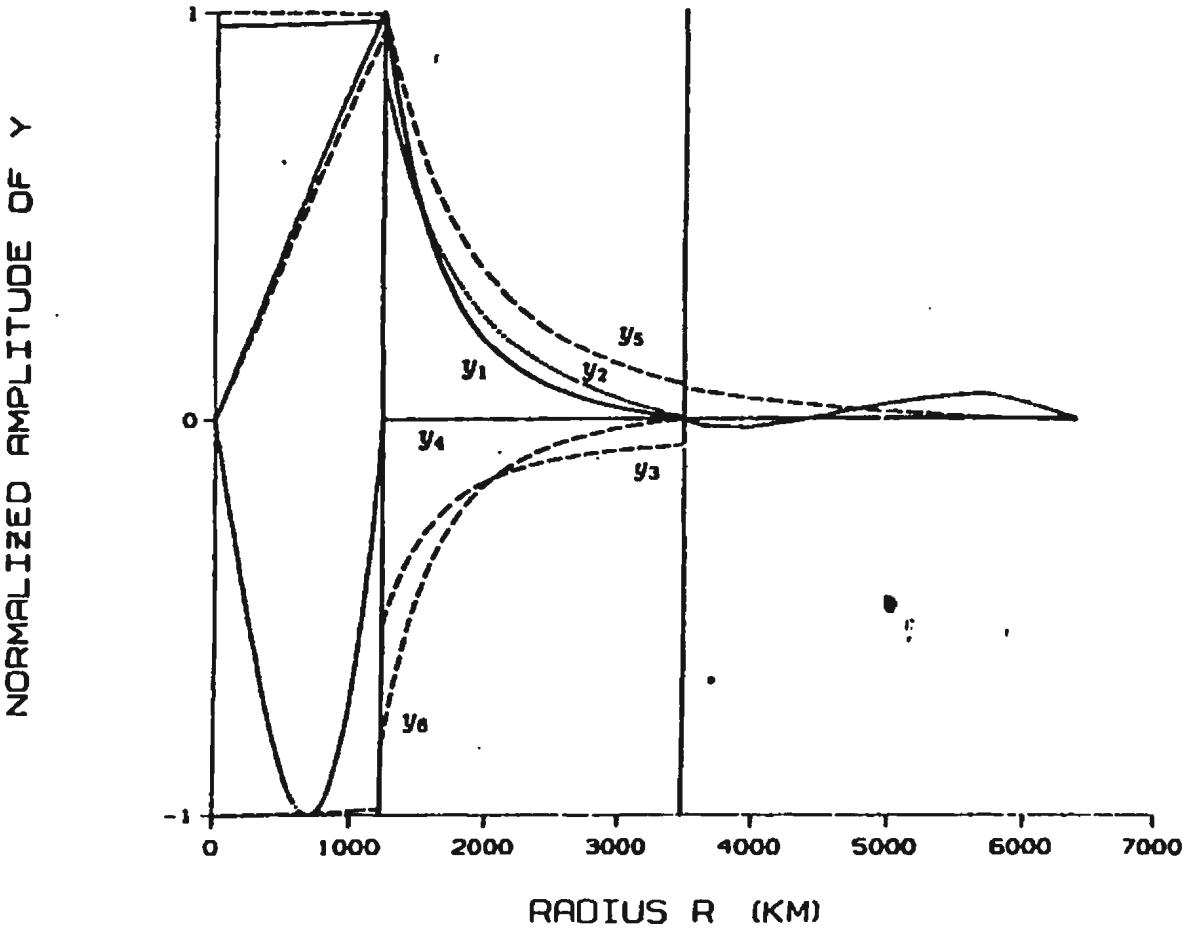

Figure 12: Eigenfunctions of the protrograde mode computed using TPD
For rotating PREM with a neutral LC
m=-1, T=5.97230 hr, N=1

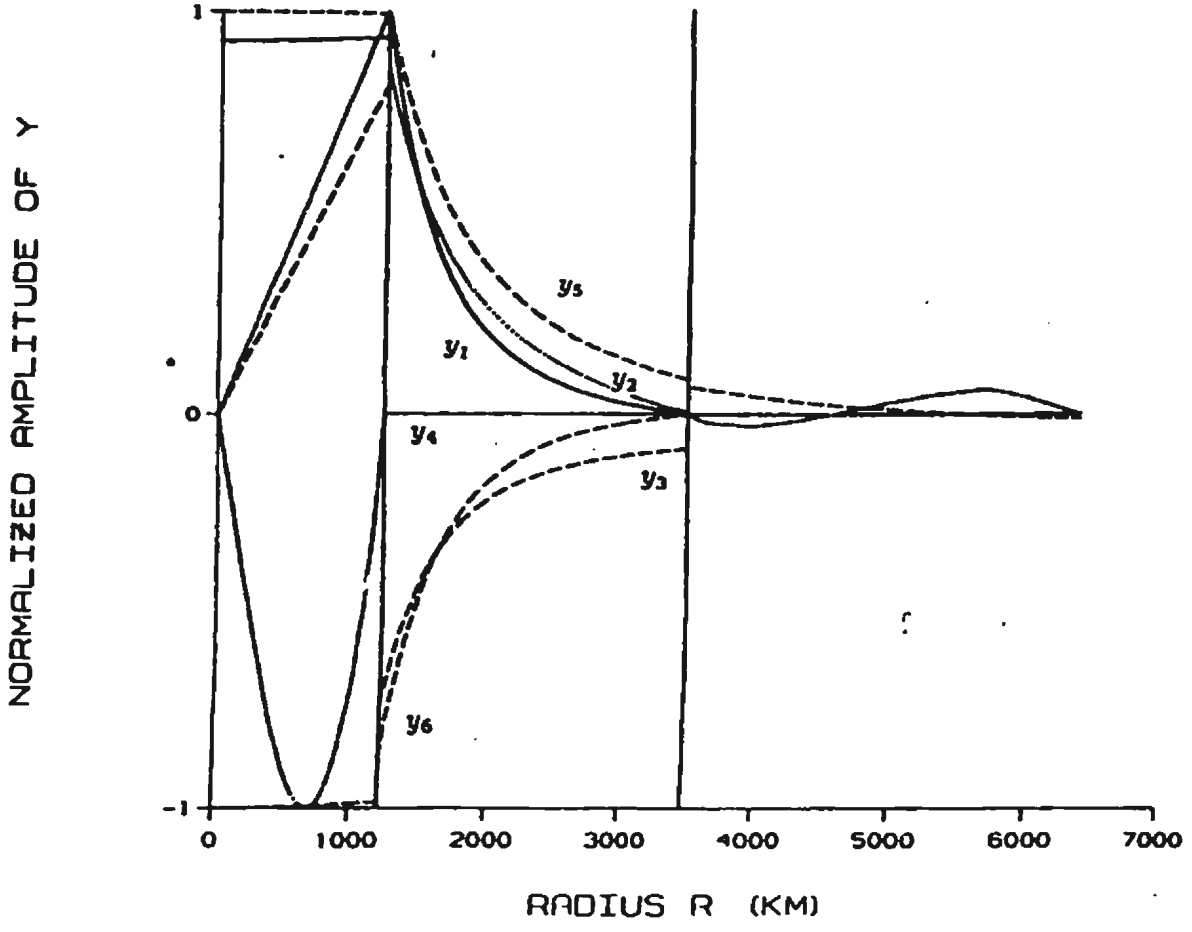

Figure 13: Eigenfunction y_1 of the mantle for the polar mode computed using TPD for a non-rotating PREM with a neutral LC
m=0, T=5.41367 hr, N=1

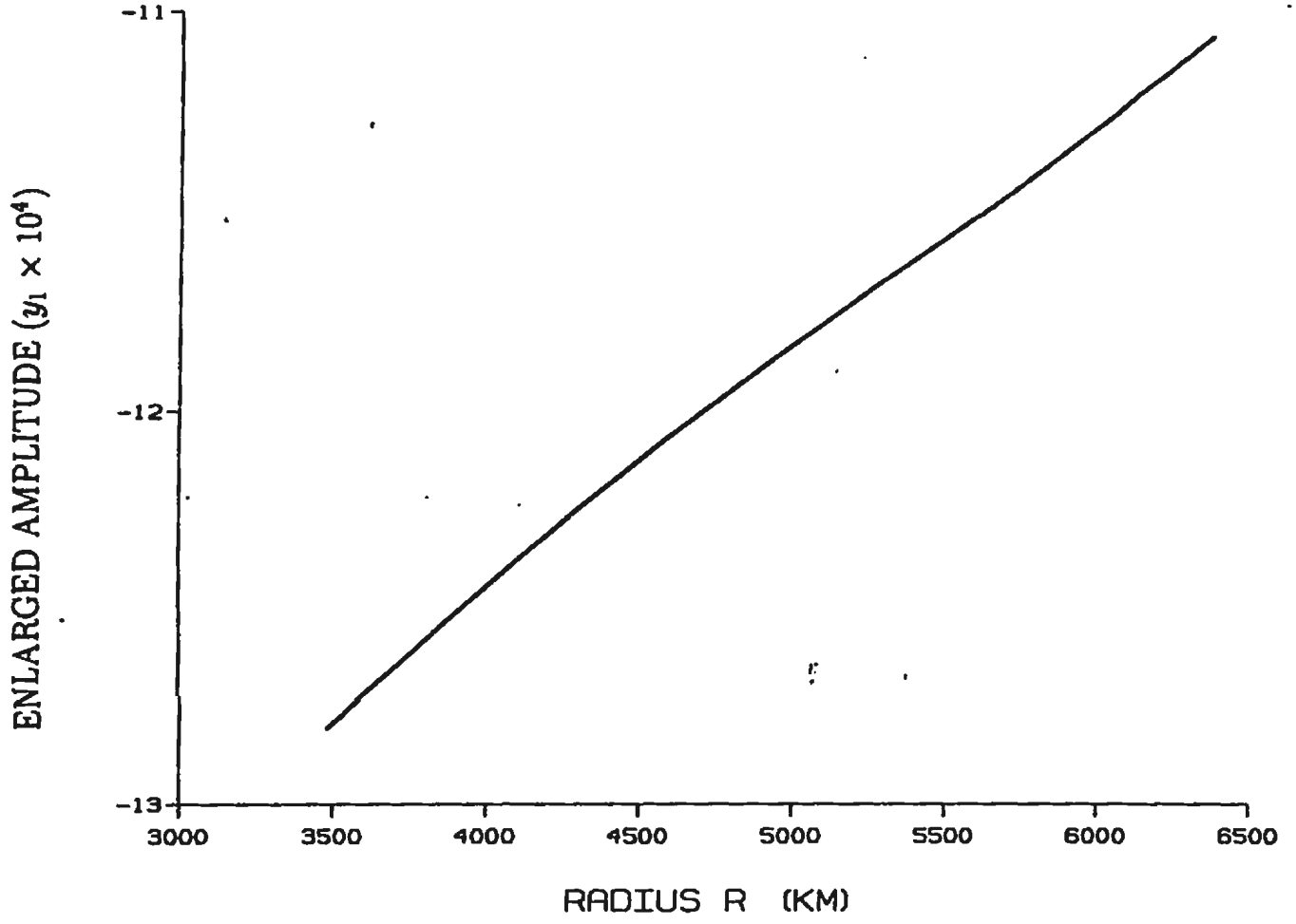

Figure 14: Eigenfunction y_1 of the mantle for the polar mode computed using TPD for a rotating PREM with a neutral LC
m=0, T=5.30334 hr, N=1

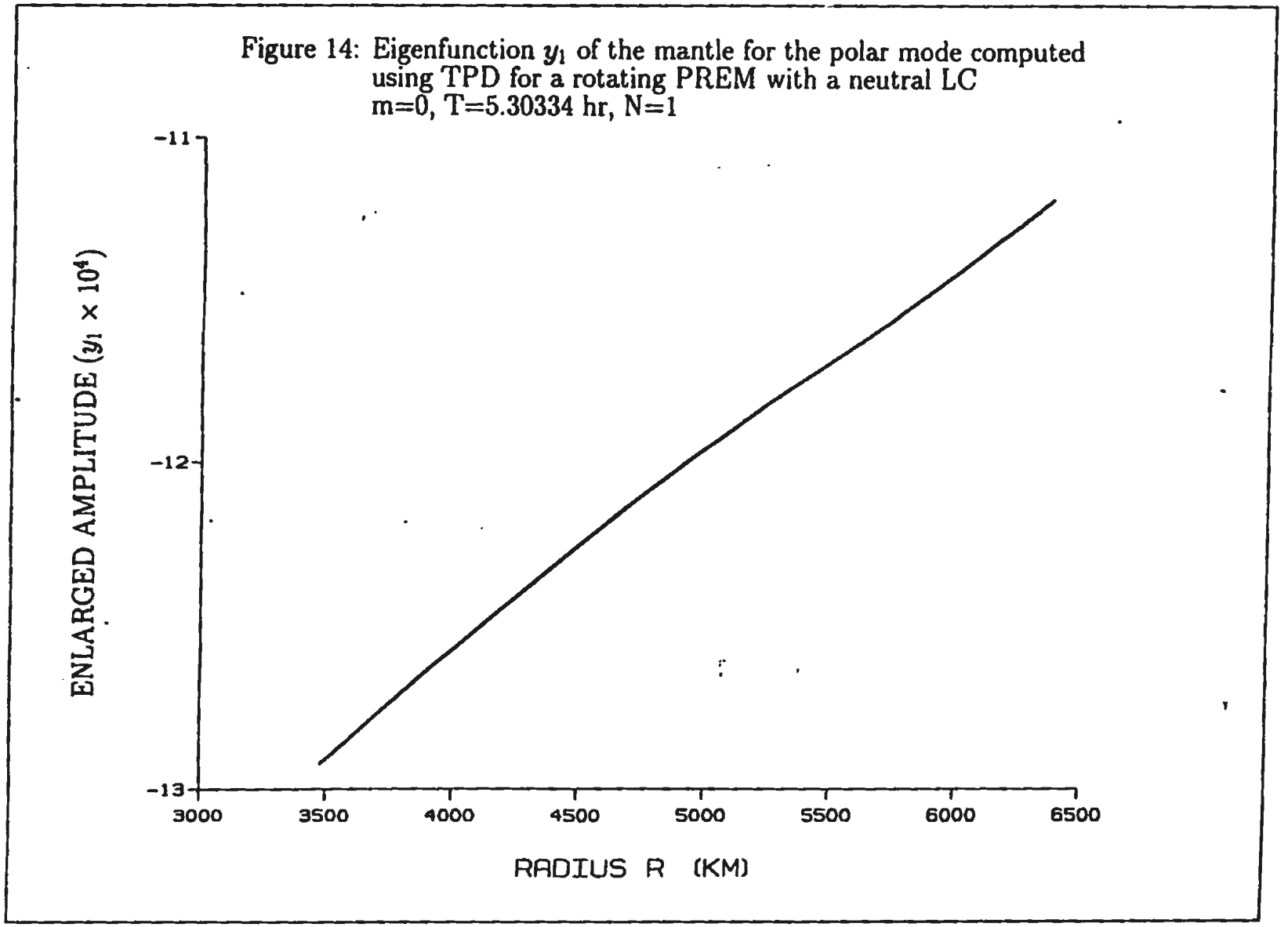

Figure 15: Eigenfunction y_1 of the mantle for the retrograde mode computed using TPD for a rotating PREM with a neutral LC m=1, T=4.75960 hr, N=1

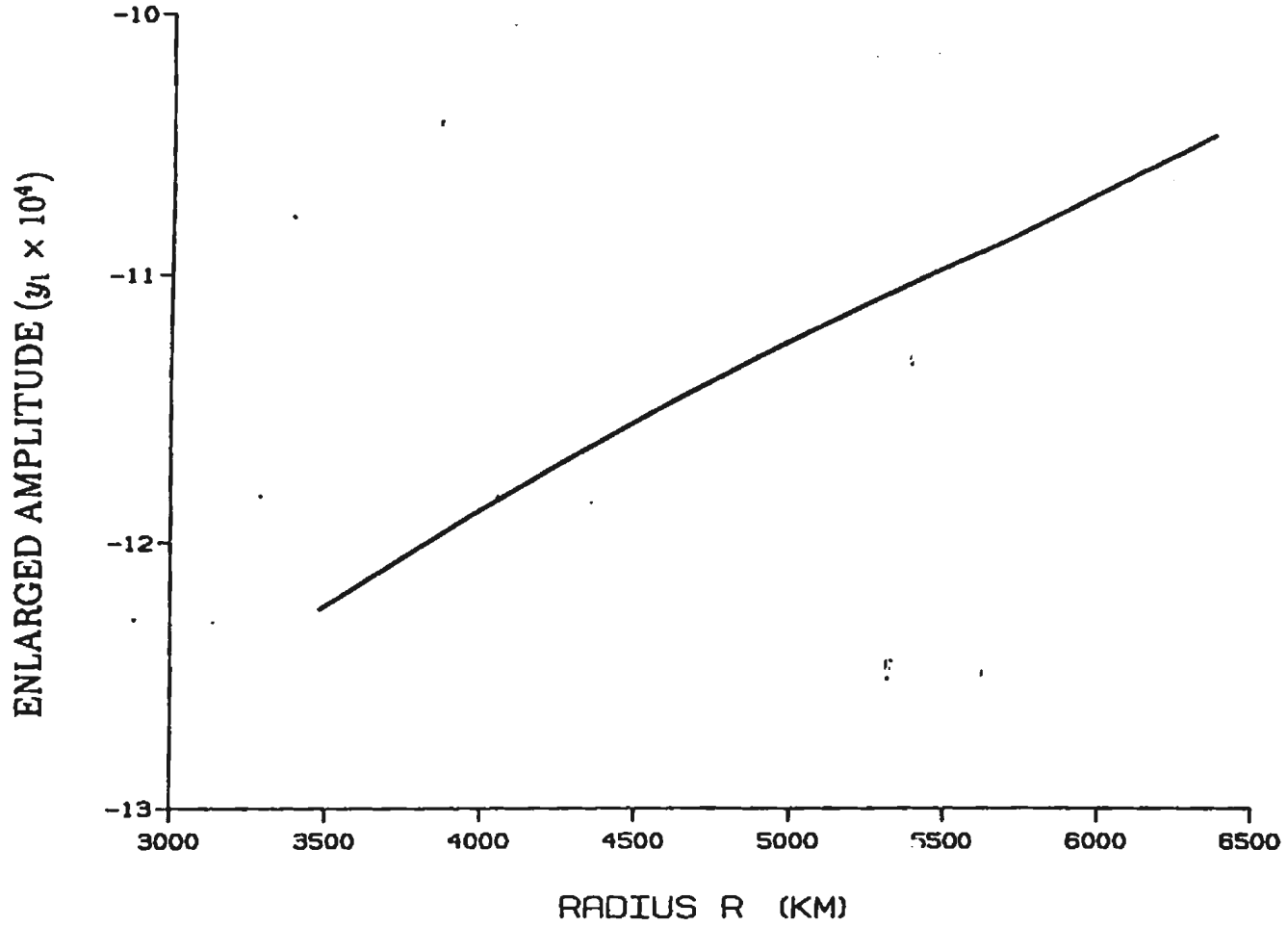

Figure 16: Eigenfunction y_1 of the mantle for the prograde mode computed using TPD for a rotating PREM with a neutral LC m=-1, T=5.97230 hr, N=1

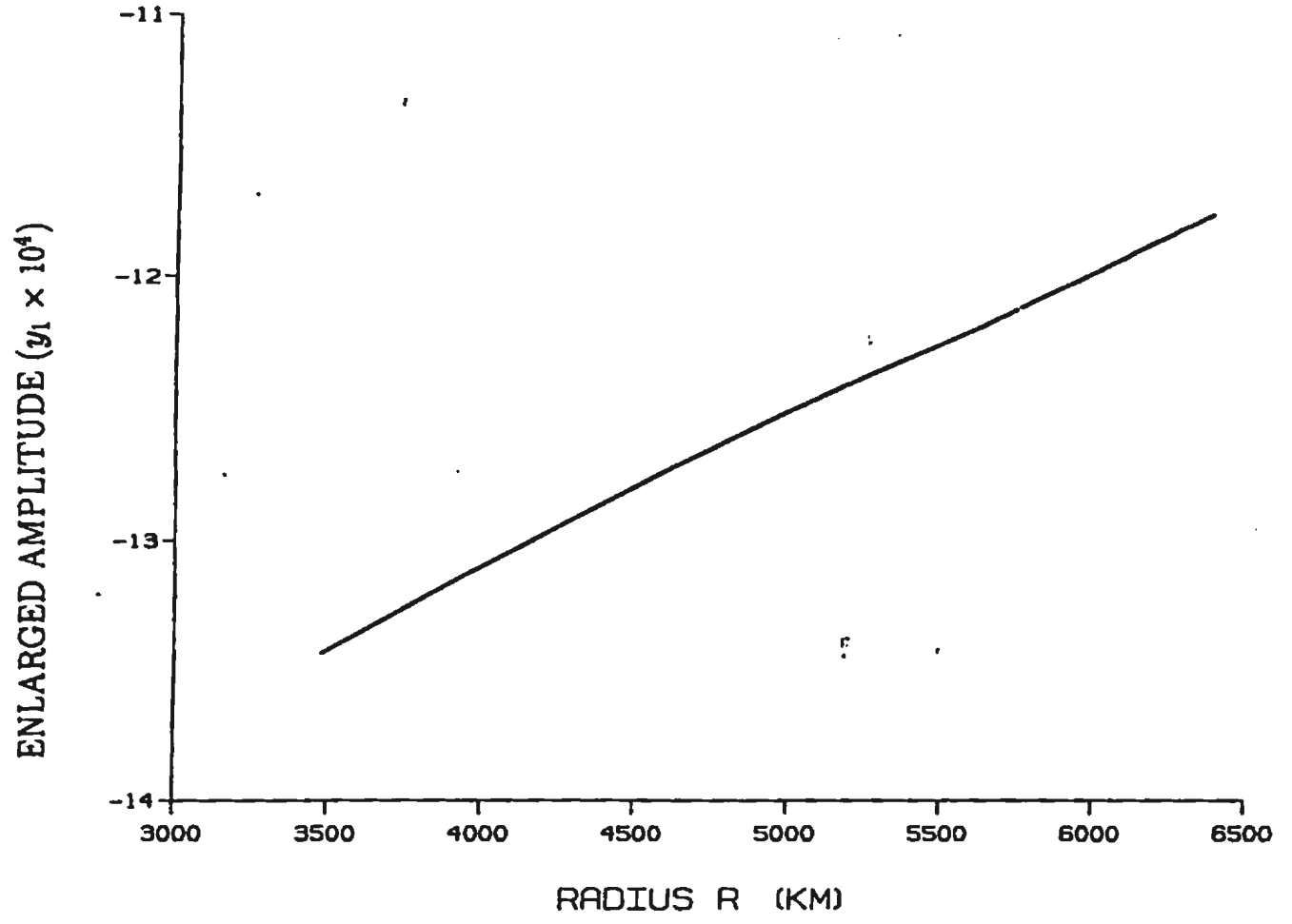

Chapter 7 Effects of Ellipsoidal Stratification and Centrifugal Potential

7.1 Introduction

Although the major effects of the Earth's rotation on the Slichter eigenspectrum have been taken into account by incorporating the Coriolis force into the equation of momentum conservation, there remain two much smaller rotational effects which need to be considered: ellipsoidal stratification and centrifugal potential. Studying these effects requires abandonment of the assumption of a spherically layered Earth where an equilibrium gravity field is purely radial. Now, in the undisturbed Earth which is regarded as in hydrostatic equilibrium in a steadily-rotating reference frame, the surfaces of constant material properties are ellipsoids (to first order in ellipticity) of revolution. Consequently, the equilibrium gravity field is modified by the asphericity of the Earth, as well as the centrifugal potential.

However, the ellipticity of the Earth's strata, defined as the ratio of centrifugal force to gravity, is not a large number. In fact, it never exceeds 1/300 anywhere throughout the Earth. For oscillations which do not significantly redistribute angular momentum within the Earth, such as the Slichter modes, the effects of ellipsoidal stratification and centrifugal potential are therefore expected to be very small. This fact promoted a number of researches, beginning with Backus & Gilbert (1961), to treat these effects as small perturbations to the eigenperiods of normal modes calculated for a non-rotating spherical Earth model. After an error in the original formulation of normal mode perturbation theory was corrected,

Woodhouse & Dahlen (1978) and Dahlen & Sailor (1979) used Rayleigh's variational principle and conventional perturbation theory to obtain the effects of ellipticity to first order and those of Earth's rotation to second order. In addition Dahlen & Sailor (1979) tabulated the splittings, due to ellipticity and rotation, of a large number of normal mode eigenfrequencies computed for a particular spherical Earth model (1066A).

In this thesis, I will explore a different approach to calculating the effects of the ellipsoidal stratification and the centrifugal potential, by incorporating these effects into the governing system of equations in the two-potential description of core dynamics. This will be done in the current chapter (7), and the following two chapters (8 and 9).

In the remaining three sections of this chapter, I will discuss how to adapt the material properties tabulated for the spherical PREM model to an ellipsoidally stratified Earth model, and the methods for implementing governing system of equations in a mean sphere domain (MSD), as well as in an equivalent spherical domain (ESD).

Compared to the properties of the inner and outer cores, those of the mantle play a minor role in determining the Slichter eigenperiods. For this reason and also for saving computational effort, the effects of ellipticity and centrifugal potential are fully retained in the liquid core, retained for degrees $n = 1,\ 3$ in the inner core, and ignored in the mantle. The effects of ellipticity and centrifugal potential on the proper choice of starting solutions at the geocentre for the eigenfunctions are discussed in Chapter 8. A novel feature of this work is the extension of the concept of load Love numbers, hitherto used only at spherical interfaces, to ellipsoidal core boundaries. Chapter 9 will present a Galerkin formulation of the TPD governing equations and the numerical solutions.

7.2 Adapting PREM to Ellipsoidal Stratification

Indeed, inclusion of the effects of the Earth's ellipticity of figure and centrifugal potential to normal mode eigenfrequencies will introduce great complexity into numerical computation. What one wants to do is to calculate free oscillation periods for an ellipsoidal Earth model (with volume V_E) using published material property data, which, however, are tabulated for spherically-layered Earth models. The primary challenge is to bridge this discrepancy in a consistent way. In a rotating ellipsoidally-stratified Earth model in hydrostatic equilibrium, material properties are constant on the equipotential surface W_0=constant. If the mean radius of that surface is r_0, and its ellipticity is $\epsilon(r_0)$, then in a cylindrical polar coordinate system the equation of that surface is given to first order in ellipticity by

$$r = r_0[1 - \frac{2}{3}\epsilon(r_0)P_2(\cos\theta)]. \tag{169}$$

The density at the point located by the position vector $\mathbf{r}$, is given by

$$\rho(\mathbf{r}) = \rho_0(r_0). \tag{170}$$

Then to first order in ellipticity

$$\rho(\mathbf{r}) = \rho_0(r) + h\frac{d\rho_0}{dr}P_2(\cos\theta) \tag{171}$$

where h is defined for convenience in writing

$$h(r) = \frac{2}{3}r\epsilon(r). \tag{172}$$

Thus in equation (169), it could be used to denote

$$h(r_0) = \frac{2}{3}r_0\epsilon(r_0). \tag{173}$$

Equation (171) is the density in the ellipsoidal domain expressed in terms of that in the mean sphere domain. Similar relations hold for rigidity $\mu(\mathbf{r})$ and Lamé parameter $\lambda(\mathbf{r})$.

Smith (1974) developed a method of domain transformation to cope with the elliptical configuration of the Earth. This method has been used to compute free oscillation modes and wobble/nutation modes (Smith 1976, 1977; Wahr 1981). However, as Smith (1974) stated, his method handles the dynamics in the interior of the Earth and that of the boundaries in an inconsistent way. He assigned each external or internal elliptical boundary in ellipsoidal domain a corresponding spherical boundary in an 'equivalent spherical domain' (ESD). In the interior of the volume V_E away from boundaries, he took the location vector $\mathbf{r}$ to be identical to the location vector $\mathbf{r}$ in the ESD. The property quantities ρ, μ and λ expressed in the ESD are transformed to the ellipsoidal domain. The expression (170) for density and similar expressions for other material properties are precisely those used by Smith (1974) in the interior of V_E away from boundaries, i.e. he identifies $\rho_0(r)$, $\mu(r)$ and $\lambda(r)$ with those tabulated as a function of radius r for a spherically-layered Earth model, such as PREM. However, at a point on an equipotential which forms a boundary, he used (169) for radius r and transformed all boundary conditions into the ESD. Treating the interior regions differently from the boundaries involves an error of first order in ellipticity, but only in the vicinity of the boundaries (Smith 1974).

To avoid this inconsistency, one may want to apply Smith's (1974) way of field variable transformations used at boundaries to the interiors too. A consistent way of doing this is to take material properties prescribed in a spherically stratified Earth to be the material properties of the mean sphere corresponding to the ellipsoid of interest, and transform all

field variables in the elliptical domain to the mean sphere domain. The mean radius r_0 of an equipotential is taken to be the location vector in MSD, corresponding to the location vector $\mathbf{r}$ of that equipotential, through the interiors and at the boundaries. This may be particularly necessary for wobble/nutation problems, since the eigenperiods of the latter are critically dependent on ellipticity. The details of this amendment will be discussed in section 7.3.

7.3 Governing Equations in Solid Parts of Ellipsoidal Earth I: Mean Sphere Domain

The original Poisson equation and the equation of momentum conservation in terms of the additional gravitational potential field V_1 and the displacement field $\mathbf{u}$ are

$$\nabla^2 V_1 = 4\pi G \nabla \cdot (\rho_0 \mathbf{u}) \tag{174}$$

$$\begin{aligned}
&(\lambda + 2\mu)[\nabla(\nabla \cdot \mathbf{u})] - \mu \nabla \times (\nabla \times \mathbf{u}) + \nabla(\lambda + \mu)\nabla \cdot \mathbf{u} \\
&+\nabla \times (\mathbf{u} \times \nabla\mu) + \nabla(\mathbf{u} \cdot \nabla\mu) - \mathbf{u}\nabla^2\mu \\
&= -\rho_0\omega^2\mathbf{u} + 2i\rho_0\omega\Omega\dot{\mathbf{k}} \times \mathbf{u} - \rho_0\nabla V_1 + \mathbf{g}_0\nabla \cdot (\rho_0\mathbf{u}) - \nabla(\rho_0\mathbf{u} \cdot \mathbf{g}_0).
\end{aligned} \tag{175}$$

For an amendment to Smith's (1974) theory, i.e. taking a consistent treatment for both the interior and boundaries, the relation (169) for radius r, (170) for the density, and similar relations for other material properties will be used.

First I need to transform mathematical operators defined in the ellipsoidal domain into those in the MSD. The simplicity of this transformation is that the spherical polar coordinate system is retained, and directions of all vector components remain unchanged. Specifically, $\mathbf{r}$ is oriented in the same direction as that of $\mathbf{r}_0$, and their relationship of magnitude is shown in (169). Therefore, r_0 can also be expressed in terms of r as:

$$r_0 = r[1 + \frac{2}{3}\epsilon(r)P_2(\cos\theta)]. \tag{176}$$

The gradient operator expressed in MSD domain is then

$$\begin{aligned}(\nabla)_{\mathbf{r}} &= \hat{\mathbf{r}}\frac{\partial}{\partial r} + \frac{\hat{\theta}}{\mathbf{r}}\frac{\partial}{\partial\theta} + \frac{\hat{\phi}}{\mathbf{r}\sin\theta}\frac{\partial}{\partial\phi} \\ &= \hat{\mathbf{r}}\frac{\partial r_0}{\partial r}\frac{\partial}{\partial r_0} + \frac{\hat{\theta}}{\mathbf{r}}[\frac{\partial r_0}{\partial\theta}\frac{\partial}{\partial r_0} + \frac{\partial}{\partial\theta}] + \frac{\hat{\phi}}{\mathbf{r}\sin\theta}\frac{\partial}{\partial\phi} \\ &= \nabla_0 + \nabla' \end{aligned} \tag{177}$$

where quantities $\partial r_0/\partial r$ and $\partial r_0/\partial\theta$ are derived from (176),

$$\frac{\partial r_0}{\partial r} = 1 + \frac{2}{3}\frac{d(r\epsilon)}{dr}P_2 \tag{178}$$

$$\frac{\partial r_0}{\partial\theta} = \frac{2}{3}r\epsilon\frac{dP_2}{d\theta} \tag{179}$$

and

$$\nabla_0 = \hat{\mathbf{r}}\frac{\partial}{\partial r_0} + \frac{\hat{\theta}}{\mathbf{r_0}}\frac{\partial}{\partial\theta} + \frac{\hat{\phi}}{\mathbf{r_0}\sin\theta}\frac{\partial}{\partial\phi} \tag{180}$$

$$\nabla' = \frac{2}{3}[\epsilon P_2\nabla_0 + r_0\nabla_0(\epsilon P_2)\frac{\partial}{\partial r_0}]. \tag{181}$$

Based on one to one correspondence between an equipotential surface in the ellipsoidal domain and an equipotential surface in the mean sphere domain, it can be assumed that the geopotentials on these two sets of equi-surfaces have an identical value

$$W_0(r_0) = W_0(\mathbf{r}) = V_0(\mathbf{r}) + \frac{1}{3}\Omega^2 r^2[1 - P_2(\cos\theta)] \tag{182}$$

where V_0 is the gravitational potential on an elliptical equipotential surface, P_2 is the Legendre polynomial of second degree, and the last term is the result of the centrifugal potential. The use of equation (169) changes equation (182) to

$$W_0(r_0) - \frac{1}{3}\Omega^2 r_0^2 = V_0(\mathbf{r}) - \frac{1}{3}\Omega^2 r^2 P_2(\cos\theta) - \frac{4}{9}\Omega^2 r_0^2 \epsilon P_2. \tag{183}$$

The LHS of equation (183) is the mean gravitational potential on the equipotential surface 'r_0', and it is a constant on that equipotential. The RHS of (183) remains constant as well. Now, one can write geopotential on r_0 as

$$W_0(r_0) = U_0(r_0) + \frac{1}{3}\Omega^2 r_0^2 \tag{184}$$

where $U_0(r_0)$ is the mean gravitational potential on r_0. Thus, the geopotential on an elliptical equipotential surface, expressed in terms of the gravitational potential on an equilibrium surface of a non-rotating Earth and centrifugal potential, is

$$W_0(\mathbf{r}) = U_0(r) + \frac{2}{3} r\epsilon \frac{dU_0(r)}{dr} P_2 + \frac{1}{3}\Omega^2 r^2 \tag{185}$$

dropping off quantities smaller than the first order in ellipticity. Therefore, the gravity at the point r is

$$\mathbf{g}_0(\mathbf{r}) = \nabla W_0(\mathbf{r}) = \mathbf{g}_0(r) + \mathbf{g}'(r,\theta) \tag{186}$$

where

$$\mathbf{g}_0(r) = -\hat{\mathbf{r}} g_0(r) \tag{187}$$

$$\mathbf{g}'(r,\theta) = -\frac{2}{3}\nabla[\epsilon r g_0(r) P_2] + \frac{2}{3}\Omega^2 \mathbf{r}. \tag{188}$$

Here $g_0(r)$ is the gravitation of spherically layered Earth at point r, and $\mathbf{g}'(r,\theta)$ is the additional gravity caused by the ellipticity of the figure and centrifugal potential.

With a simple transformation using relation (169), gravity in the mean sphere domain will be written as

$$\mathbf{g}_0(\mathbf{r}) = \mathbf{g}_0(r_0) + \mathbf{g}'(r_0, \theta) \tag{189}$$

where

$$\mathbf{g}_0(r_0) = -\hat{\mathbf{r}} g_0(r_0) \tag{190}$$

and

$$\mathbf{g}'(r_0, \theta) = \frac{2}{3}\Omega^2(r_0 - hP_2)\hat{\mathbf{r}} - g_0(r_0)\nabla[h(r_0)P_2(\cos\theta)]. \tag{191}$$

Here $\mathbf{g}_0(r_0)$ is the gravitation of spherically layered Earth, and $\mathbf{g}'(r_0, \theta)$ is the addition to gravity due to the ellipticity and centrifugal potential.

Any field vector or scalar in the ellipsoidal domain can then be transformed into the MSD readily using vector or scalar Taylor expansion, keeping only the first order quantity in ellipticity. For example the displacement field $\mathbf{u}$ and potential field V_1 now are

$$\mathbf{u}(\mathbf{r}) = \mathbf{u}(r_0) - h(r_0)\frac{\partial \mathbf{u}}{\partial r_0}P_2 \tag{192}$$

$$V_1(\mathbf{r}) = V_1(r_0) - h(r_0)\frac{\partial V_1}{\partial r_0}P_2. \tag{193}$$

Substituting (169), (170), similar relations for other material properties, mathematical operator (177), and field variables (192) and (193) into the Poisson equation and equation of momentum conservation, the latter can then be written explicitly as

$$\nabla_0^2 V_1 - hP_2\frac{\partial}{\partial r_0}(\nabla_0^2 V_1) = 4\pi G\{[\nabla_0\rho_0 + \nabla'\rho_0]\cdot[\mathbf{u} - hP_2\frac{\partial \mathbf{u}}{\partial r_0}]$$

$$+\rho_0\nabla\cdot\mathbf{u} - \rho_0 hP_2\frac{\partial \nabla_0\cdot\mathbf{u}}{\partial r_0}\} \tag{194}$$

$$(\lambda+2\mu)[\nabla_0(\nabla_0\cdot\mathbf{u})-hP_2\frac{\partial}{\partial r_0}\nabla_0(\nabla_0\cdot\mathbf{u})]$$

$$-\mu[\nabla_0\times(\nabla_0\times\mathbf{u})-hP_2\frac{\partial}{\partial r_0}\nabla_0\times(\nabla_0\times\mathbf{u})]$$

$$+(\nabla_0+\nabla')(\lambda+\mu)[\nabla_0\cdot\mathbf{u}-hP_2\frac{\partial}{\partial r_0}\nabla_0\cdot\mathbf{u}]$$

$$+(\nabla_0+\nabla')\times[(\mathbf{u}-hP_2\frac{\partial\mathbf{u}}{\partial r_0})\times(\nabla_0\mu+\nabla'\mu)]$$

$$+(\nabla_0+\nabla')[(\mathbf{u}-hP_2\frac{\partial\mathbf{u}}{\partial r_0})\cdot(\nabla_0\mu+\nabla'\mu)]-[\mathbf{u}-hP_2\frac{\partial\mathbf{u}}{\partial r_0}](\nabla_0+\nabla')\cdot[\nabla_0\mu+\nabla'\mu]$$

$$=-\rho_0\omega^2[\mathbf{u}-hP_2\frac{\partial\mathbf{u}}{\partial r_0}]+2i\rho_0\omega\Omega[\hat{\mathbf{k}}\times\mathbf{u}-hP_2\frac{\partial}{\partial r_0}(\hat{\mathbf{k}}\times\mathbf{u})]-\rho_0[\nabla_0V_1-hP_2\frac{\partial\nabla_0V_1}{\partial r_0}]$$

$$+(\mathbf{g}_0+\mathbf{g}')[(\nabla_0+\nabla')\rho_0\cdot(\mathbf{u}-hP_2\frac{\partial\mathbf{u}}{\partial r_0})+\rho_0(\nabla_0\cdot\mathbf{u}-hP_2\frac{\partial\nabla_0\cdot\mathbf{u}}{\partial r_0})]$$

$$-(\nabla_0+\nabla')\rho_0[(\mathbf{u}-hP_2\frac{\partial\mathbf{u}}{\partial r_0})\cdot(\mathbf{g}_0+\mathbf{g}')]$$

$$-\rho_0(\nabla_0+\nabla')[(\mathbf{u}-hP_2\frac{\partial\mathbf{u}}{\partial r_0})\cdot(\mathbf{g}_0+\mathbf{g}')]. \tag{195}$$

Dropping off quantities smaller than first order in ellipticity and rearranging some terms, these two equations become

$$[\text{LHS of (174)}-\text{RHS of (174)}]_{MSD(r_0,\theta,\phi)}=\sum_{i=1}^{4}V_h(i) \tag{196}$$

$$[\text{LHS of (175)}-\text{RHS of (175)}]_{MSD(r_0,\theta,\phi)}=-\sum_{i=1}^{13}\mathbf{m}_h(i)+\sum_{i=1}^{13}\mathbf{f}_h(i) \tag{197}$$

where the notation in subscript on the LHS of these two equations emphasizes that they are to be evaluated at (r_0, θ, ϕ) in the MSD. The quantities in summations on the RHS of these equations are as following

$$V_h(1)=hP_2\frac{\partial}{\partial r_0}(\nabla_0^2V_1) \tag{198}$$

$$V_h(2) = 4\pi G \nabla' \rho_0 \cdot \mathbf{u} \tag{199}$$

$$V_h(3) = -4\pi G h P_2 \nabla_0 \rho_0 \cdot \frac{\partial \mathbf{u}}{\partial r_0} \tag{200}$$

$$V_h(4) = -4\pi G \rho_0 h P_2 \frac{\partial \nabla_0 \cdot \mathbf{u}}{\partial r_0} \tag{201}$$

$$\mathbf{m}_h(1) = (\lambda + 2\mu)[-h P_2 \frac{\partial}{\partial r_0} \nabla_0 (\nabla_0 \cdot \mathbf{u})] \tag{202}$$

$$\mathbf{m}_h(2) = \mu h P_2 \frac{\partial}{\partial r_0} \nabla_0 \times (\nabla_0 \times \mathbf{u}) \tag{203}$$

$$\mathbf{m}_h(3) = \nabla'(\lambda + \mu) \nabla_0 \cdot \mathbf{u} \tag{204}$$

$$\mathbf{m}_h(4) = -\nabla_0 (\lambda + \mu) h P_2 \frac{\partial}{\partial r_0} \nabla_0 \cdot \mathbf{u} \tag{205}$$

$$\mathbf{m}_h(5) = \nabla' \times (\mathbf{u} \times \nabla_0 \mu) \tag{206}$$

$$\mathbf{m}_h(6) = \nabla_0 \times (\mathbf{u} \times \nabla' \mu) \tag{207}$$

$$\mathbf{m}_h(7) = -\nabla_0 \times (h P_2 \frac{\partial \mathbf{u}}{\partial r_0} \times \nabla_0 \mu) \tag{208}$$

$$\mathbf{m}_h(8) = \nabla_0 (\mathbf{u} \cdot \nabla' \mu) \tag{209}$$

$$\mathbf{m}_h(9) = \nabla' (\mathbf{u} \cdot \nabla_0 \mu) \tag{210}$$

$$\mathbf{m}_h(10) = -\nabla_0 (h P_2 \frac{\partial \mathbf{u}}{\partial r_0} \cdot \nabla_0 \mu) \tag{211}$$

$$\mathbf{m}_h(11) = -\mathbf{u} \nabla_0 \cdot \nabla' \mu \tag{212}$$

$$\mathbf{m}_h(12) = -\mathbf{u} \nabla' \cdot \nabla_0 \mu \tag{213}$$

$$\mathbf{m}_h(13) = h P_2 \frac{\partial \mathbf{u}}{\partial r_0} \nabla_0^2 \mu \tag{214}$$

$$\mathbf{f}_h(1) = \rho_0 \omega^2 h P_2 \frac{\partial \mathbf{u}}{\partial r_0} \tag{215}$$

$$\mathbf{f}_h(2) = -2i\rho_0 \omega \Omega h P_2 \frac{\partial}{\partial r_0}(\hat{\mathbf{k}} \times \mathbf{u}) \tag{216}$$

$$\mathbf{f}_h(3) = \rho_0 h P_2 \frac{\partial \nabla_0 V_1}{\partial r_0} \tag{217}$$

$$\mathbf{f}_h(4) = -\mathbf{g}_0 h P_2 \nabla_0 \rho_0 \cdot \frac{\partial \mathbf{u}}{\partial r_0} \tag{218}$$

$$\mathbf{f}_h(5) = -\mathbf{g}_0 \rho_0 h P_2 \frac{\partial \nabla_0 \cdot \mathbf{u}}{\partial r_0} \tag{219}$$

$$\mathbf{f}_h(6) = \mathbf{g}_0 \nabla' \rho_0 \cdot \mathbf{u} \tag{220}$$

$$\mathbf{f}_h(7) = -\nabla_0 \rho_0 \mathbf{u} \cdot \mathbf{g}' \tag{221}$$

$$\mathbf{f}_h(8) = \nabla_0 \rho_0 h P_2 \frac{\partial \mathbf{u}}{\partial r_0} \cdot \mathbf{g}_0 \tag{222}$$

$$\mathbf{f}_h(9) = \mathbf{g}' \nabla_0 \cdot (\rho_0 \mathbf{u}) \tag{223}$$

$$\mathbf{f}_h(10) = -\nabla' \rho_0 \mathbf{u} \cdot \mathbf{g}_0 \tag{224}$$

$$\mathbf{f}_h(11) = \rho_0 \nabla_0 (h P_2 \frac{\partial \mathbf{u}}{\partial r_0} \cdot \mathbf{g}_0) \tag{225}$$

$$\mathbf{f}_h(12) = -\rho_0 \nabla_0 (\mathbf{u} \cdot \mathbf{g}') \tag{226}$$

$$\mathbf{f}_h(13) = -\rho_0 \nabla' (\mathbf{u} \cdot \mathbf{g}_0). \tag{227}$$

Using the orthogonal property of associated Legendre functions and integrating over a surface of a unit sphere, all $\mathbf{m}_h$ and $\mathbf{f}_h$ can be broken down to radial spheroidal, transverse spheroidal and toroidal components respectively. As a result, a set of first order ordinary differential equations in AJP notations can be obtained.

Note that the work done so far on using the MSD shows that the number of additional terms which need to be computed seems considerably larger than when one uses Smith's approach (cf. §7.4). Apparently the reduction in the order of derivatives of material properties involved is offset by the increase in the order of derivatives of field variables. However, a closer examination shows that the terms involving the second derivatives of the field variables are already first order quantities in the ellipticity. Therefore, these second derivatives can be readily substituted by the zero'th order quantities involving only first derivatives of the field variables, and these field variables themselves. Since the ellipticity and centrifugal potential will make only small corrections to the Slichter eigenperiods, both approaches discussed above should yield satisfactory results. Although the MSD formulation could be particularly useful for wobble/nutation modes, in this thesis it does not seem profitable to proceed further with the MSD formulation because the extra computational effort does not seem to be warranted by the small corrections which ellipticity and centrifugal potential will make to the Slichter eigenperiods (see §9.2 below). In this thesis, therefore, I return to the approach pioneered by Smith (1974).

7.4 Governing Equations in Solid Parts of Ellipsoidal Earth II: Smith's Equivalent Spherical Domain

Following Smith's (1974) approach, I adopt the elliptical domain for the interior of the inner core in order to obtain the appropriate form for the system of governing equations. The transformations of the material properties from the spherical domain to the elliptical domain are given by Smith (1974):

$$\rho(\mathbf{r}) = \rho_0(r) + h\rho_0' P_2 \tag{228}$$

$$\mu(\mathbf{r}) = \mu(r) + h\mu' P_2 \tag{229}$$

$$\lambda(\mathbf{r}) = \lambda(r) + h\lambda' P_2 \tag{230}$$

and the gravity $\mathbf{g}_0(\mathbf{r})$ and its additional part $\mathbf{g}'(r,\theta)$ due to the ellipticity and centrifugal potential are given by equations (186) and (188). Note that the prime on ρ_0, μ and λ represents the radial derivative.

Substituting (186), (228) - (230) into the Poisson equation (174) and the equation of momentum conservation (175), and dropping off quantities smaller than the first order in ellipticity, these two equations will be written

$$[\text{LHS of (174)} - \text{RHS of(174)}]_{ESD(r,\theta,\phi)} = \sum_{i=1}^{3} V_h(i) \tag{231}$$

$$[\text{LHS of (175)} - \text{RHS of (175)}]_{ESD(r,\theta,\phi)} = -\sum_{i=1}^{6} \mathbf{m}_h(i) + \sum_{i=1}^{7} \mathbf{f}_h(i) \tag{232}$$

where

$$V_h(1) = 4\pi G P_2 \nabla(h\rho_0') \cdot \mathbf{u} \tag{233}$$

$$V_h(2) = 4\pi G h\rho_0' \nabla P_2 \cdot \mathbf{u} \tag{234}$$

$$V_h(3) = 4\pi G h\rho_0' P_2 \nabla \cdot \mathbf{u} \tag{235}$$

$$\mathbf{m}_h(1) = h(\lambda' + 2\mu') P_2 \nabla(\nabla \cdot \mathbf{u}) \tag{236}$$

$$\mathbf{m}_h(2) = -h\mu' P_2 \nabla \times (\nabla \times \mathbf{u}) \tag{237}$$

$$\mathbf{m}_h(3) = \nabla[h(\lambda' + \mu') P_2] \nabla \cdot \mathbf{u} \tag{238}$$

$$\mathbf{m}_h(4) = \nabla \times [\mathbf{u} \times \nabla(h\mu' P_2)] \tag{239}$$

$$\mathbf{m}_h(5) = \nabla[\mathbf{u} \cdot \nabla(h\mu' P_2)] \tag{240}$$

$$\mathbf{m}_h(6) = -\mathbf{u} \nabla^2(h\mu' P_2) \tag{241}$$

$$\mathbf{f}_h(1) = -\omega^2 h\rho_0' P_2 \mathbf{u} \tag{242}$$

$$\mathbf{f}_h(2) = 2i\omega\Omega h\rho_0' P_2 \hat{\mathbf{k}} \times \mathbf{u} \tag{243}$$

$$\mathbf{f}_h(3) = -h\rho_0' P_2 \nabla V_1 \tag{244}$$

$$\mathbf{f}_h(4) = \mathbf{g}_0' \nabla \cdot (\rho_0 \mathbf{u}) \tag{245}$$

$$\mathbf{f}_h(5) = \mathbf{g}_0 \nabla \cdot (h\rho_0' P_2 \mathbf{u}) \tag{246}$$

$$\mathbf{f}_h(6) = -\nabla(h\rho_0' P_2 \mathbf{u} \cdot \mathbf{g}_0) \tag{247}$$

$$\mathbf{f}_h(7) = -\nabla(\rho_0 \mathbf{u} \cdot \mathbf{g}'). \tag{248}$$

Obviously, there is less work involved here than in the last section, namely one fewer V_h, seven fewer $\mathbf{m}_h$'s and six fewer $\mathbf{f}_h$'s need to be computed, and also there is no second derivative of the displacement field and the additional gravitational potential field involved.

Next, I am going to simplify equations (231) and (232) into a form analogous to those of the AJP equations. Note that I have taken into account the elliptical and Coriolis coupling between degree 1 and degree 3 spheroidal fields in the solid parts of the Earth in deriving equations (231) and (232). Therefore, the degree 2 toroidal field is already included. To do this, I first define a set of extended AJP field variables $y_1, y_2, \cdots, y_{14}$, where degree 1 field variables y_1, y_3, y_5 and y_6 (hence degree 3 field variables y_9, y_{11}, y_{13}, and y_{14}) are defined as in the original AJP notations, but y_2 and y_4 (hence y_{10} and y_{12}) are defined slightly differently. Similarly, for degree 2 field variables, y_7 is defined as in the original AJP notations, and y_8 is defined slightly differently. These modified AJP variables are

$$\delta_{n,1} y_2 + \delta_{n,3} y_{10} = \frac{du_n^m}{dr} + \frac{2u_n^m - n(n+1)v_n^m}{r} \tag{249}$$

$$\delta_{n,1} y_4 + \delta_{n,3} y_{12} = \frac{dv_n^m}{dr} - \frac{v_n^m - u_n^m}{r} \tag{250}$$

$$y_8 = i\frac{dt_n^m}{dr} - \frac{it_n^m}{r}. \tag{251}$$

The changes of these definitions slightly simplify the resulting governing ODE's. It is evident that it is not a disadvantage for some of these field variables to be discontinuous across material interfaces which are no longer spherical.

Next, I substitute these extended AJP variables in the Poisson equation. It results in one ordinary differential equation for degree $n = 1$

$$\frac{dy_6}{dr} = \sum_{i=1}^{14} E_{6,i}\, y_i \tag{252}$$

and another one for degree $n = 3$

$$\frac{dy_{14}}{dr} = \sum_{i=1}^{14} E_{14,i}\, y_i. \tag{253}$$

Following a standard procedure, I will take inner product of the vector momentum conservation equation with vectors $\hat{\mathbf{r}}Y_n^k$, $\nabla Y_n^k r$ and $i\nabla Y_n^k \times \mathbf{r}$; then integrate the resulting expressions on the surface of a unit sphere to obtain the radial spheroidal, transverse spheroidal and toroidal part of the momentum conservation equation respectively. Each of the radial spheroidal and transverse spheroidal parts gives rise to two equations, one for degree $n = 1$ and one for degree $n = 3$. The toroidal part gives rise to one equation for degree $n = 2$. These five resulting ordinary differential equations in extended AJP notations are listed below:

I. Radial spheroidal

$n = 1$

$$\beta_{10}^m \frac{dy_{10}}{dr} = \alpha_{10}^m \frac{dy_2}{dr} + \sum_{i=1}^{14} E_{10,i}\, y_i \tag{254}$$

$n = 3$

$$\beta_2^m \frac{dy_2}{dr} = \alpha_2^m \frac{dy_{10}}{dr} + \sum_{i=1}^{14} E_{2,i}\, y_i \tag{255}$$

where $E_{2,i}$ and $E_{10,i}$ (i=1, 2, $\cdots$, 14) are given in Appendix A, and

$$\beta_{10}^m = -h(\lambda' + 2\mu')A_{n+2}^m \tag{256}$$

$$\alpha_{10}^m = (\lambda + 2\mu) + h(\lambda' + 2\mu')B_n^m \tag{257}$$

$$\beta_2^m = -h(\lambda' + 2\mu')C_{n-2}^m \tag{258}$$

$$\alpha_2^m = (\lambda + 2\mu) + h(\lambda' + 2\mu')B_n^m \tag{259}$$

where A_n^m, B_n^m and C_n^m arise from the representation of $P_2 Y_n^m$ as a linear combination of spherical harmonics:

$$P_2 Y_n^m = A_n^m Y_{n-2}^m + B_n^m Y_n^m + C_n^m Y_{n+2}^m \tag{260}$$

with

$$A_n^m = \frac{3(n+m)(n+m-1)}{2(2n+1)(2n-1)} \tag{261}$$

$$B_n^m = \frac{n(n+1) - 3m^2}{(2n+3)(2n-1)} \tag{262}$$

$$C_n^m = \frac{3(n+2-m)(n+1-m)}{2(n+3)(2n+1)}. \tag{263}$$

Solving equations (254) and (255) together, the ODE's for y_2 and y_{10} follow

$$\frac{dy_2}{dr} = \sum_{i=1}^{14} A_{2,i}\, y_i \tag{264}$$

$$\frac{dy_{10}}{dr} = \sum_{i=1}^{14} A_{10,i}\, y_i \tag{265}$$

where

$$A_{2,i} = -\frac{1}{\alpha_{10}^m}\left[\frac{\beta_{10}^m}{\alpha_2^m} E_{2,i} + E_{10,i}\right] \tag{266}$$

$$A_{10,i} = -\frac{1}{\alpha_2^m}\left[E_{2,i} + \frac{\beta_2^m}{\alpha_{10}^m} E_{10,i}\right]. \tag{267}$$

II. Transverse spheroidal

$n = 1$

$$\beta_{12}^m \frac{dy_{12}}{dr} = \gamma_{12}^m \frac{dy_8}{dr} + \alpha_{12}^m \frac{dy_4}{dr} + \sum_{i=1}^{14} E_{12,i}\, y_i \tag{268}$$

$n = 3$

$$\beta_4^m \frac{dy_4}{dr} = \gamma_4^m \frac{dy_8}{dr} + \alpha_4^m \frac{dy_{12}}{dr} + \sum_{i=1}^{14} E_{4,i}\, y_i \tag{269}$$

where $E_{4,i}$ and $E_{12,i}$ (i=1, 2, $\cdots$, 14) are given in Appendix A, and

$$\beta_{12}^m = -\mu' h \frac{n+3}{n+1} A_{n+2}^m \tag{270}$$

$$\gamma_{12}^m = 3m\mu' h \frac{1}{n(n+1)} J_{n+1}^m \tag{271}$$

$$\alpha_{12}^m = \mu + \mu' h \frac{n(n+1)-3}{n(n+1)} B_n^m \tag{272}$$

$$\beta_4^m = -\mu' h \frac{n-2}{n} C_{n-2}^m \tag{273}$$

$$\gamma_4^m = 3m\mu' h \frac{1}{n(n+1)} H_{n-1}^m \tag{274}$$

$$\alpha_4^m = \mu + \mu' h \frac{n(n+1)-3}{n(n+1)} B_n^m. \tag{275}$$

where J_n^m and H_n^m are defined in (126) and (127).

III. Toroidal

$n = 2$

$$\beta_8^m \frac{dy_8}{dr} = \gamma_8^m \frac{dy_4}{dr} + \alpha_8^m \frac{dy_{12}}{dr} + \sum_{i=1}^{14} E_{8,i}\, y_i \tag{276}$$

where $E_{8,i}$ (i=1, 2, $\cdots$, 14) are given in Appendix A, and

$$\beta_8^m = -\mu - \mu' h \frac{n(n+1)-3}{n(n+1)} B_n^m \tag{277}$$

$$\gamma_8^m = 3m\mu' h \frac{1}{n(n+1)} H_{n-1}^m \tag{278}$$

$$\alpha_8^m = 3m\mu' h \frac{1}{n(n+1)} G_{n+1}^m. \tag{279}$$

Solving equations (268), (269), and (276), the ODE's for y_4, y_8 and y_{12} are obtained

$$\frac{dy_4}{dr} = \sum_{i=1}^{14} A_{4,i}\, y_i \tag{280}$$

$$\frac{dy_8}{dr} = \sum_{i=1}^{14} A_{8,i}\, y_i \tag{281}$$

$$\frac{dy_{12}}{dr} = \sum_{i=1}^{14} A_{12,i}\, y_i \tag{282}$$

where

$$A_{4,i} = -\frac{1}{\bar{\alpha}}[E_{12,i}\beta_8\alpha_4^m + E_{8,i}\gamma_{12}^m\alpha_4^m + E_{4,i}\beta_{12}^m\beta_8^m] \tag{283}$$

$$A_{8,i} = -\frac{1}{\bar{\alpha}}[E_{12,i}\gamma_8^m\alpha_4^m - \alpha_{12}^m(E_{8,i}\alpha_4^m - E_{4,i}\alpha_8^m)] \tag{284}$$

$$A_{12,i} = -\frac{1}{\bar{\alpha}}[E_{12,i}\beta_4^m\beta_8^m + \alpha_{12}^m(E_{8,i}\gamma_4^m + E_{4,i}\beta_8^m)] \tag{285}$$

$$\bar{\alpha} = \alpha_{12}^m\beta_8\alpha_4^m. \tag{286}$$

There are seven ordinary differential equations listed above for y_2, y_4, y_6, y_8, y_{10}, y_{12} and y_{14}. Another seven ordinary differential equations for y_1, y_3, y_5, y_7, y_9, y_{11} and y_{13} are obtained from the definitions of y_2, y_4, y_6, y_8, y_{10}, y_{12} and y_{14}. These fourteen ODE's result form truncating the series for the inner core displacement field and the potential field at degree 3. The basic coefficient matrix $\underline{E}$, from which the final matrix $\underline{A}$ of this equation set is derived, is given in Appendix A.

The basic governing equations for a rotating, ellipsoidal body have been developed in this chapter for both mean sphere domain and equivalent spherical domain. However, only the latter will be used in the numerical calculation of this thesis. This set of fourteen ODE's now has to be integrated from the geocentre to the ICB, to provide the solutions from which the spheroidal load Love numbers at that boundary can be derived. The procedure of doing this and the associated boundary conditions will be discussed in the next chapter.

Chapter 8 Love Numbers at Ellipsoidal Core Boundaries

8.1 Starting Solutions at the Geocentre

From the 14th order ODE's derived in §7.4, there are seven out of fourteen fundamental solutions regular at the geocentre. First, I want to transform y_i's to dimensionless quantities by the following modifications:

$$y_i = a\,\tilde{y}_i\{\delta_{i=1,3,7,9,11} + g_0(a)[\delta_{i=5,13} + \frac{1}{a}\delta_{i=6,14}]\} + \tilde{y}_i\delta_{i=2,4,8,10,12} \tag{287}$$

where $\delta = 1$ only if i takes the indicated integer and $\delta = 0$ otherwise. The y_i's with a tilde $\tilde{}$ are dimensionless quantities. Note that y_2, y_4, y_8, y_{10} and y_{12} defined in §7.4 are already dimensionless. Since I will hereafter work only with dimensionless y_i's, I drop the tilde $\tilde{}$ of these y_i's for convenience in writing. Whenever a dimensioned y_i arises, it will be referred to explicitly.

Near the geocentre, let the solution y_i's and the material property quantities of the inner core be expressed in series expansions:

$$y_i = \sum_{k=0}^{\infty} C_{i,k}\, x^{v+k-1} \tag{288}$$

$$\mu = \mu_0 + \mu_2 x^2 + \cdots \tag{289}$$

$$\lambda = \lambda_0 + \lambda_2 x^2 + \cdots \tag{290}$$

$$\rho_0 = \rho_0(0) + \rho_2 x^2 + \cdots \tag{291}$$

where x is the dimensionless radius defined in (33), and v is an integer. The similar expressions are adopted for gravity g_0 and ellipticity factor h

$$g_0 = \frac{4}{3}\pi G\rho_0(0)Rx + \frac{4}{5}\pi GR\rho_2 x^3 + \cdots \tag{292}$$

$$h = \frac{2}{3}Rx(\epsilon_0 + \epsilon_2 x^2 + \cdots) \tag{293}$$

where μ_0, λ_0, $\rho_0(0)$ and ϵ_0 are values of these quantities at the centre of the Earth, μ_2, λ_2, ρ_2 and ϵ_2 are the coefficients of the terms of power two in the above series expansions, and R is the mean radius of the Earth.

Substituting above defined quantities into the governing differential equations and grouping the coefficients of independent variable x of the same power, starting from the lowest order, I obtain a set of indicial equations which give rise to the dependent coefficients in terms of seven independent coefficients. Then, the solutions of y_i's are found to be

$$y_1 = A + A'x^2 + \cdots \tag{294}$$

$$y_2 = \nu B'x + \cdots \tag{295}$$

$$y_3 = C + C'x^2 + \cdots \tag{296}$$

$$y_4 = \nu D'x + \cdots \tag{297}$$

$$y_5 = Ex + \gamma E'x^3 + \cdots \tag{298}$$

$$y_6 = \nu F + \nu\gamma F'x^2 + \cdots \tag{299}$$

$$y_7 = G'x^2 + \cdots \tag{300}$$

$$y_8 = \nu H' x + \cdots \tag{301}$$

$$y_9 = \bar{A} x^2 + \bar{A}' x^4 + \cdots \tag{302}$$

$$y_{10} = \nu \bar{B}' x^3 + \cdots \tag{303}$$

$$y_{11} = \bar{C} x^2 + \bar{C}' x^4 + \cdots \tag{304}$$

$$y_{12} = \nu \bar{D} x + \nu \bar{D}' x^3 + \cdots \tag{305}$$

$$y_{13} = \bar{E} x^3 + \gamma \bar{E}' x^5 + \cdots \tag{306}$$

$$y_{14} = \nu \bar{F} x^2 + \nu\gamma \bar{F}' x^4 + \cdots \tag{307}$$

where γ, ν are defined in (42), (43). In the above solutions, the independent coefficients are C, E, A', G', $\bar{D}$, $\bar{F}$ and $\bar{D}'$, and the dependent ones are

$$A = C \tag{308}$$

$$F = E - \gamma C \tag{309}$$

$$B' = -\frac{1}{\lambda_0 - \mu_0}[10\mu_0 A' + \frac{1}{\nu} f_1^{\omega} C + R\rho_0(0) g_0(a) F] \tag{310}$$

$$D' = 3(A' - \frac{1}{6} B') \tag{311}$$

$$C' = 2A' - \frac{1}{2} B' \tag{312}$$

$$H' = G' \tag{313}$$

$$F' = -\frac{1}{5} A' - \frac{3}{5} C' + \frac{2}{5} \frac{\rho_2}{\rho_0(0)} \epsilon_0(-3m^2 + 2) A \tag{314}$$

$$E' = \frac{1}{3}A' + \frac{1}{3}F' \tag{315}$$

$$\bar{A} = \frac{3}{4}\bar{D} \tag{316}$$

$$\bar{C} = \frac{1}{4}\bar{D} \tag{317}$$

$$\bar{E} = \frac{1}{3}\gamma\bar{A} + \frac{1}{3}\bar{F} \tag{318}$$

$$\bar{B}' = -\frac{5}{15\lambda_0 + 14\mu_0}\{\frac{36}{5}\mu_0\bar{D}' + \rho_0(0)Rg_0(a)\bar{F} + \rho_0(0)R^2(\omega^2 - 2m\omega\Omega)\bar{A}] \tag{319}$$

$$\bar{A}' = \frac{1}{10}\bar{B}' + \frac{2}{5}\bar{D}' \tag{320}$$

$$\bar{C}' = -\frac{1}{30}\bar{B}' + \frac{1}{5}\bar{D}' \tag{321}$$

$$\bar{E}' = \frac{1}{3}\bar{A}' - \frac{2}{3}\bar{C}' \tag{322}$$

$$\bar{F}' = 5\bar{E}' - \bar{A}' \tag{323}$$

where

$$f_1^{\omega} = \frac{aR\rho_0(0)}{9}\{6\Omega^2 + 8\pi G\rho_0(0)[(3m^2 - 2)\epsilon_0 + 3] + 9(\omega^2 - 2m\omega\Omega)\}. \tag{324}$$

Letting one of the seven independent coefficients be unit at a time, the governing differential equations can be integrated through the inner core to obtain seven sets of fundamental solutions at the inner core boundary. The integrations are started from $x = x_1$, a little distance away from the geocentre (e.g. 1 km). The general solutions are then a superposition of these fundamental solutions:

$$y_i = \sum_{j=1}^{7} c_j y_i^j \tag{325}$$

$i = 1, 2, \ldots, 14$

where $c_1 = C$, $c_2 = E$, $c_3 = A'$, $c_4 = G'$, $c_5 = \tilde{D}$, $c_6 = \tilde{F}$ and $c_7 = \tilde{D}'$. To derive the load Love numbers at the ICB I must next apply the continuity conditions at the ICB to the solutions (325).

8.2 Inner Core Boundary Conditions and Ellipsoidal Love Numbers

In this section I will complete the derivation of the load Love numbers at the ellipsoidal ICB. As discussed in §7.4 that, at the liquid core boundaries, the material properties prescribed for a spherically layered Earth are adopted to be those in the ESD, and all the field variables are transformed from the elliptical domain to the ESD. This is the same treatment as that used in the MSD. Following Smith's (1974) notation, I define the unit normal of equipotentials

$$\hat{\mathbf{n}} = \hat{\mathbf{r}} + h\nabla P_2 \tag{326}$$

and

$$p = r - hP_2 \tag{327}$$

where p is the radius in the elliptical domain (what I have called r in §7.3), and r is the radius in the ESD (what I have called r_0 in the MSD, where r of the ESD = r_0 of the MSD on the outer core boundaries).

Next I want to transform all continuity conditions required at the elliptical liquid core boundaries to the corresponding boundaries in the ESD. Here I only need to write in detail these boundary conditions at the ICB, the same forms apply to the CMB. Due to the presence of ellipticity, the spheroidal and toroidal fields are now coupled together in these boundary conditions. When it is necessary, I shall write expressions for these boundary conditions at the liquid side (a_+) and at the solid side (a_-) of the ICB explicitly. The AJP notations (with modifications to some of them as discussed in §7.4) representing r-functions of the radial spheroidal, transverse spheroidal and toroidal parts of the displacement, as well as that of the additional gravitational potential will be used in these boundary conditions. But first I will keep using notations u_n^m, v_n^m, t_n^m and Φ_n^m for convenience, and will replace them with the AJP's y_i notations when necessary. Again, the dependence of y_i's on order m and degree n will not be indicated explicitly. However, I only list in this section the initial formulations of the relevant boundary conditions. The analytical details will be presented in Appendix B.

(I) Continuity of normal displacement $\hat{\mathbf{n}} \cdot \mathbf{u}$

$$[\hat{\mathbf{n}} \cdot \mathbf{u}]_{a_-} = [\hat{\mathbf{n}} \cdot \mathbf{u}]_{a_+}. \tag{328}$$

(II) Continuity of additional gravitational potential V_1

$$[V_1]_{a_-} = [V_1]_{a_+}. \tag{329}$$

(III) Continuity of gravitational flux $\hat{\mathbf{n}} \cdot [\nabla V_1 - 4\pi G\rho_0 \mathbf{u}]$

$$[\hat{\mathbf{n}} \cdot \nabla V_1]_{a_-} - 4\pi G\rho_0(a_-)[\hat{\mathbf{n}} \cdot \mathbf{u}]_{a_-} = [\hat{\mathbf{n}} \cdot \nabla V_1]_{a_+} - 4\pi G\rho_0(a_+)[\hat{\mathbf{n}} \cdot \mathbf{u}]_{a_+}. \tag{330}$$

(IV) Continuity of normal stress $\hat{\mathbf{n}} \cdot \tau$

Here τ is the additional total stress caused by disturbance. This continuity condition should be assured by the continuity of its radial spheroidal, transverse spheroidal and toroidal parts separately. To find these components, I take the inner product of the normal stress of degree n with $\hat{\mathbf{r}}Y_n^m$, $r\nabla Y_n^m$ and $iY_n^m \times \nabla \mathbf{r}$ of degree l respectively after transforming them onto the ESD, and integrate these over an unit sphere. The resulting expressions can then be simplified using orthogonal relations of the Legendre functions. These three components of the continuous normal stress are

(1) Continuity of radial spheroidal component of $\hat{\mathbf{n}} \cdot \tau$

$$[\hat{\mathbf{n}} \cdot \tau]_{radial}(a_-) = [\hat{\mathbf{n}} \cdot \tau]_{radial}(a_+). \tag{331}$$

(2) Continuity of transverse spheroidal component of $\hat{\mathbf{n}} \cdot \tau$

$$[\hat{\mathbf{n}} \cdot \tau]_{transverse}(a_-) = [\hat{\mathbf{n}} \cdot \tau]_{transverse}(a_+). \tag{332}$$

(3) Continuity of toroidal component of $\hat{\mathbf{n}} \cdot \tau$

$$[\hat{\mathbf{n}} \cdot \tau]_{toroidal}(a_-) = [\hat{\mathbf{n}} \cdot \tau]_{toroidal}(a_+). \tag{333}$$

In Appendix B it is shown that upon use of the boundary conditions (I) and (II), the boundary conditions (III), (IV) and (V) will result in a set of 7 algebraic equations linear in the extended dimensionless AJP variables y_i's (i=1, 2, $\cdots$, 14)

$$\sum_{i=1}^{14} \Lambda_{1,i}^m y_i = \frac{1}{a g_0(a)} \chi_1^m \tag{334}$$

$$\sum_{i=1}^{14} \Lambda_{2,i}^m y_i = \frac{1}{g_0(a)} \left(\frac{dy_5}{dr}\right)_{a_+} \tag{335}$$

$$\sum_{i=1}^{14} \Lambda_{3,i}^m y_i = 0 \tag{336}$$

$$\sum_{i=1}^{14} \Lambda^m_{4,i} y_i = \frac{1}{a g_0(a)} \chi^m_3 \tag{337}$$

$$\sum_{i=1}^{14} \Lambda^m_{5,i} y_i = \frac{1}{g_0(a)} (\frac{dy_{13}}{dr})_{a_+} \tag{338}$$

$$\sum_{i=1}^{14} \Lambda^m_{6,i} y_i = 0 \tag{339}$$

$$\sum_{i=1}^{14} \Lambda^m_{7,i} y_i = 0. \tag{340}$$

Note that all seven continuity conditions at the ICB depend on only four fully dimensioned liquid-side quantities $\chi^m_1(a_+)$, $\chi^m_3(a_+)$, $(dy_5/dr)_{a_+}$ and $(dy_{13}/dr)_{a_+}$.

To construct the general solution for y_1, y_2, $\cdots$ or y_{14} as a linear combination of seven independent solutions regular at the geocentre, seven constants are needed. These seven constants in turn can be determined as linear combinations of the four non-zero quantities on the RHS of the equations (334) - (340). Alternately, I can write each of y_1, y_2, $\cdots$, y_{14} on the solid side of the ICB (except y_4 and y_{12}, which both vanish there) as a linear combination of those four quantities:

$$y_i(a_-) = \frac{1}{a g_0(a)} [H_{i,1} \chi^m_1 + H_{i,2} \chi^m_3 + K_{i,1} (r \frac{dy_5}{dr})_{a_+} + K_{i,2} (r \frac{dy_{13}}{dr})_{a_+}] \tag{341}$$

$i = 1, 2, \cdots, 14$

where $H_{i,1}$, $H_{i,2}$, $K_{i,1}$ and $K_{i,2}$ are internal ellipsoidal load Love numbers at an ellipsoidal ICB. Let one of the four quantities at the RHS of the boundary conditions (334) - (340) be unit at a time (with the others zero), then the load Love numbers will take the corresponding values of y_i's when the equation set of the boundary conditions is solved. Note that if the ellipticity is set to zero, $H_{1,1}$, $H_{2,1}$, $\cdots$, $H_{6,1}$, $K_{1,1}$, $K_{2,1}$, $\cdots$ and $K_{6,1}$ will be reduced to

spherical load Love numbers of degree 1, and $H_{9,2}$, $H_{10,2}$, $\cdots$, $H_{14,2}$, $K_{9,2}$, $K_{10,2}$, $\cdots$ and $K_{14,2}$ will be reduced to spherical load Love numbers of degree 3 respectively. By maintaining the inertial and Coriolis terms in the governing differential equations of the inner core and the starting solutions at the geocentre, the dependence of the ellipsoidal load Love numbers on frequency and azimuthal order number m is fully taken into account.

By now I have derived the spheroidal load Love numbers of the inner core which permit closure of the solution of the governing dynamical equations in the liquid core. Together with the mantle load Love numbers (spherical), they will be used in the surface integrals of the Galerkin equations for representing the effects of the inner core and mantle on the liquid core dynamics. This is the subject of Chapter 9.

Chapter 9 Galerkin Solution of the Two-Potential Description in Ellipsoidally-stratified Outer Core

9.1 Formulating the Galerkin Equations

In an elliptical liquid core, the Galerkin formulations based on the TPD take equivalent forms to the equations (161) and (162) of §6.2, with unit normal $\hat{\mathbf{N}}$ of the inner and outer boundaries of the liquid core defined in the elliptical configuration (note that I have previously used $\hat{\mathbf{n}}$ as the unit normal of the liquid core boundaries for spherical Earth models). Now let $\hat{\mathbf{n}}$ be the unit normal of the equipotentials, then $\hat{\mathbf{n}} = -\hat{\mathbf{N}}$ at the ICB, and $\hat{\mathbf{n}} = \hat{\mathbf{N}}$ at the CMB. For convenience, I shall carry out the calculations of the surface integrals of the Galerkin equations in the transformed ESD, and the volume integrals in the elliptical domain. The gravity $\mathbf{g}_0(\mathbf{r})$ and the material properties $\rho(\mathbf{r})$ and $\lambda(\mathbf{r})$ shall be modified accordingly. I now discuss in detail the handling of these two kinds of integrals.

9.1.1 Surface integrals on the surfaces of the equivalent spherical domain

In the ESD, I simply take material properties prescribed in a spherically stratified Earth to be the material properties in the ESD, and transform all field variables [the position vector $\mathbf{p}$, the gravity $\mathbf{g}_0(\mathbf{p})$ and the additional gravitational potential $V_1(\mathbf{p})$] and trial functions from

the elliptical domain to the ESD:

$$p = r - hP_2 \tag{342}$$

$$\mathbf{g}_0(\mathbf{p}) = \hat{\mathbf{r}}[-g_0(r) + \frac{2}{3}\Omega^2(r - hP_2) - g_0\frac{dh}{dr}P_2] - g_0(r)h\nabla P_2 \tag{343}$$

$$V_1(\mathbf{p}) = V_1(r) - h\frac{dV_1}{dr}P_2 \tag{344}$$

$$\chi_l^m(\mathbf{p}) = \chi_l^m(r) - h\frac{\partial\chi_l^m}{\partial r}P_2. \tag{345}$$

The stability parameter $\beta(\mathbf{p})$ must also be a constant on an equipotential, thus

$$\beta(\mathbf{p}) = \beta(r). \tag{346}$$

Therefore

$$\beta(\mathbf{p})B = \omega^2(1-\mu^2)\alpha^2 + \beta g_0^2(\mathbf{p}) - \mu\beta[\hat{\mathbf{k}}\cdot\mathbf{g}_0(\mathbf{p})]^2. \tag{347}$$

The other quantities involved in the surface integrals of equations (161) and (162) are as follows:

$$g_0^2(\mathbf{p}) = (-g_0 + \frac{2}{3}\Omega^2 r)^2 - 2(-g_0 + \frac{2}{3}\Omega^2 r)(\frac{2}{3}\Omega^2 hP_2 + g_0\frac{dh}{dr}P_2) \tag{348}$$

$$\hat{\mathbf{k}}\cdot\mathbf{g}_0(\mathbf{p}) = x[-g_0 + \frac{2}{3}\Omega^2(r - hP_2) - g_0\frac{dh}{dr}P_2] - 3g_0\frac{h}{r}x(1-x^2) \tag{349}$$

$$x = \cos\theta \tag{350}$$

$$\hat{\mathbf{n}}\cdot\mathbf{u} = [u_n^m P_n^m + \frac{h}{r}P_2'(-\sin\theta v_n^m\frac{dP_n^m}{d\theta} + m\frac{it_n^m}{\sin\theta}P_n^m) - h\frac{du_n^m}{dr}P_2P_n^m]e^{im\phi} \tag{351}$$

$$dS = a^2(1 - \frac{4}{3}\epsilon(a)P_2)\sin\theta d\theta d\phi \qquad \text{on the ICB} \tag{352}$$

$$dS = b^2(1 - \frac{4}{3}\epsilon(b)P_2)\sin\theta d\theta d\phi \qquad \text{on the CMB} \tag{353}$$

where a and b are radii of the ICB and CMB respectively, and ϵ is the ellipticity.

At the ICB, $u_1^m = y_1$, $u_3^m = y_9$, $\Phi_1^m = y_5$ and $\Phi_3^m = y_{13}$ are calculated using the internal ellipsoidal load Love numbers of degree 1 developed in §8.2, and the others (either of higher degree or zero'th order) are calculated using the spherical internal load Love numbers developed in §3.2. At the CMB, all these quantities are calculated using spherical internal load Love numbers of the mantle.

9.1.2 Volume integrals in the elliptical domain

Transformation of the material properties ρ_0, λ and the gravity $\mathbf{g}_0$ prescribed on a spherically layered Earth to the elliptical domain is given by equations (228), (230) and (186). The same transformation applies to the stability parameter β:

$$\beta(\mathbf{r}) = \beta(r) + h\frac{d\beta}{dr}P_2. \tag{354}$$

Another related quantity is

$$\beta(\mathbf{r})B = \omega^2(1-\mu^2)\alpha^2 + \beta g_0^2(\mathbf{r}) - \mu\beta(\mathbf{r})[\hat{\mathbf{k}}\cdot\mathbf{g}_0(\mathbf{r})]^2 \tag{355}$$

where

$$\alpha^2(\mathbf{r}) = \alpha^2(r) + h\frac{d\alpha^2}{dr}P_2 \tag{356}$$

$$g_0^2(\mathbf{r}) = (-g_0 + \frac{2}{3}\Omega^2 r)^2 - 2(-g_0 + \frac{2}{3}\Omega^2 r)(h\frac{dg_0}{dr} + g_0\frac{dh}{dr})P_2 \tag{357}$$

$$\hat{\mathbf{k}}\cdot\mathbf{g}_0(\mathbf{p}) = x[-g_0 + \frac{2}{3}\Omega^2 r - (h\frac{dg_0}{dr} + g_0\frac{dh}{dr})P_2] - 3g_0\frac{h}{r}x(1-x^2) \tag{358}$$

and x is defined by (350) in §9.1.1.

All resulting volume integrals can be reduced to double integrals, reflecting the dependence of radius r on θ (azimuth dependence can always be integrated out in advance when the Earth is modelled as cylindrically symmetric). The integrations with respect to r are from $a(x) = a[1 - \frac{2}{3}\epsilon_0(a)P_2(x)]$ to $b(x) = b[1 - \frac{2}{3}\epsilon_0(b)P_2(x)]$, where a and b are mean radius of the ICB and CMB respectively. In principle, after the above transformations, each integrand can be written as a product of a function of r with a function of x, then integration by parts can be performed to reduce a double integration to a single integration. For example, let an integrand $T(r,x)r^2 = f(r)g(x)$, then

$$
\begin{aligned}
I &= \int_{LC} T(r,x)r^2 dr dx d\phi \\
&= 2\pi \int_{-1}^{1} \int_{a(x)}^{b(x)} f(r)g(x) dr dx \\
&= 2\pi \int_{-1}^{1} [F(r)]_{a-h(a)P_2(x)}^{b-h(b)P_2(x)} g(x) dx \\
&= 2\pi \int_{-1}^{1} \{F[b - h(b)P_2] - F[a - h(a)P_2]\} g(x) dx
\end{aligned}
\tag{359}
$$

where $f(r) = dF(r)/dr$. Expanding F of the above expression in Taylor series and only keeping quantities of first order in ellipticity, then equation (359) becomes

$$
I = 2\pi \{ \int_a^b f(r) dr \int_{-1}^{1} g(x) dx - [h(b)f(b) - h(a)f(a)] \int_{-1}^{1} g(x) P_2(x) dx \}. \tag{360}
$$

However, if the liquid core is non-neutrally stratified, some of the terms in the final integrals will be so complicated that changing from double to single integrations will involve very heavy algebra. Therefore, in this thesis, some double integrations will still be present in the final computations, at the expense of a prolonged computational time.

9.2 Eigenperiods: Numerical Results for the Ellipsoidal Earth Model

Dahlen and Sailor (1979) derived a convenient formula for calculating the rotational and elliptical splitting of normal modes. Their tabulated splitting parameters are for the Earth model 1066A. For the Slichter eigenperiods, they predict the combined effects of the ellipticity and centrifugal potential to be as follows: a decrease of 0.090% for the polar mode ($m = 0$) and increases of 0.080% and 0.097% for the retrograde and prograde modes ($m = +1$ and $m = -1$) respectively.

By extending Dahlen & Sailor's (1979) calculations to PREM, Wu & Rochester (1994) have estimated the fractional effects of ellipticity and centrifugal potential on the Slichter eigenperiods for that Earth model, with Coriolis coupling fully taken into account. They found that these effects increase the eigenperiods of the retrograde mode ($m = 1$) and the prograde mode ($m = -1$) by 0.080% and 0.097% respectively, and decrease that of the polar mode ($m = 0$) by 0.088%.

The results of my calculations, listed in Table 9 (for PREM with the outer core modified to be strictly neutral) and Table 10 (for PREM), are of the same sign but slightly different in magnitude from the effects predicted by the perturbation theory. For the modified PREM model, I obtained a decrease of 0.094% for the polar mode ($m = 0$) and increases of 0.063% and 0.101% for the retrograde and prograde modes ($m = +1$ and $m = -1$) respectively.

Table 9: Rotational and elliptical splitting of the Slichter modes for PREM Earth model (with a neutral liquid core).
L=7 (the number of the radial trial function)
N=5 (the degree of the associated Legendre functions)
Eigenperiods are in hr.

		rotating	
	m=0	m=1	m=-1
$\epsilon = 0$	5.303	4.760	5.972
$\epsilon \neq 0$	5.298	4.763	5.978
Increment	-0.094%	+0.063%	+0.101%

Table 10: Rotational and elliptical splitting of the Slichter modes for the original PREM Earth model.
L=4 (the number of the radial trial function)
N=3 (the degree of the associated Legendre functions)
Eigenperiods are in hr.

		rotating	
	m=0	m=1	m=-1
$\epsilon = 0$	5.307	4.763	5.972
$\epsilon \neq 0$	5.304	4.767	5.980
Increment	-0.056%	+0.084%	+0.134%

To assure a convergent eigenperiod, the highest number of the radial function and the degree of the associated Legendre function in the trial function are $L = 6$ and $N = 5$ respectively for a spherically stratified Earth. Here the number L specifies that a $2(L-1)$-term polynomial will be used for the radial part of the trial function, with the lowest power of $-L$ and the highest power of $L-1$ respectively (omitting $\nu = 0$ and 1, as in the construction of expression (99)). The accuracy of the convergence is up to 1×10^{-5} hour. However, when the ellipticity of the inner and outer core are taken into account, the convergence with such a radial number and degree can only reach 1×10^{-3} hour. A close examination shows that while the eigenperiod converges very well with the associated Legendre functions (one only needs to retain it up to degree 5), it starts to oscillate once the number of the radial trial function exceeds 7 (Table 11). Although there will always be a danger in approximating a function with a polynomial of order greater than 5 (Hornbeck 1975), the problem here may well be related to a more complicated formulation of the Galerkin equations. If a different type of trial function, such as Legendre function which has an orthogonal property (Wu, 1993), is chosen, it might have some advantage. For the case of a neutrally stratified liquid core, all the integrations with respect to polar angle θ are carried out analytically, and those with respect to radius r are carried out numerically. In this latter case, the round-off error may easily accumulate if a great deal of numerical integrations are involved. If L is increased above 6, it seems to add only numerical 'noise' to the results. It might be helpful to use double-double precision in computations so as to avoid the accumulation of numerical noise.

Table 11: Display of the convergence of the eigenperiods (hr) of the Slichter modes for an ellipsoidal Earth model. The radial trial function is approximated with a polynomial.
I: PREM Earth model with a neutral liquid core
II: PREM Earth model with a non-neutral liquid core.

I

L	N	m=0	m=1	m=-1
2	1	5.29231	4.76426	5.97734
2	3	5.29662	4.76697	5.98123
3	3	5.29952	4.76232	5.98093
4	3	5.29893	4.76292	5.98000
4	5	5.29894	4.76293	5.98001
4	7	5.29894	4.76293	5.98001
4	9	5.29894	4.76293	5.98001
5	5	5.29873	4.76289	5.97949
6	5	5.29844	4.76284	5.97874
7	5	5.29817	4.76277	5.97799
8	5	5.30205	4.95154	5.98947
9	5	5.29572	4.76052	5.98868

II

2	1	5.29504	4.76542	5.97817
2	3	5.29811	4.76728	5.97986
3	3	5.30412	4.76733	5.98445
4	3	5.30385	4.76815	5.98747

As I mentioned in the last section, if the assumption of a neutral stratification of the liquid core is dropped, it will result in a great increase in CPU time for the eigenperiods computation, in which several terms of double integrations need to be evaluated. From computational practice, I found that it is very difficult to obtain a convergent approximation for these terms, especially when the number L and degree N are larger than 3. In fact when L and N increase, the integrands of these terms become nearly singular. To handle these singularities successfully, an extraordinarily long CPU time is needed. Because of limited capacity of the present computing facilities, I will list in this thesis only the results for the PREM model at a lower number $L(=3)$ and degree $N(=3)$: a decrease of 0.06% for the polar mode ($m = 0$) and increases of 0.08% and 0.15% for the azimuthal modes ($m = +1$ and $m = -1$) respectively. In order to avoid using extremely long CPU time, the best way to improve calculations is to transfer all the double integrations into single ones, even if a great amount of algebra is required. This transformation may also remove singular points in these integrands. On the other hand, using a different type of trial function in formulations and using double-double precision in computations would improve the convergence.

The work I presented in Chapters 7, 8 and 9 is an advance on the calculations by Smith (1976). First, Smith did not take the Coriolis effect into account in the outer core as completely as I have. His calculations were equivalent to truncating the liquid fields at $N=1$, whereas my calculations retained the field of at least $N=3$. Second, Smith did not explicitly distinguish the numerical effects of Coriolis coupling and those of the ellipticity and centrifugal potential, whereas I did. Due to the smallness of the ellipticity, and the gravitational nature of the restoring force, the influence of the ellipticity and centrifugal potential on the

Slichter modes is relatively small, compared to that of the Coriolis effects. The work reported in Chapter 7, 8 and 9 also improves on the calculations permitted by the work of Dahlen & Sailor (1979) because the Coriolis effects are more fully taken into account in the liquid core in my calculations. Indeed, it provides a direct test of the validity of the perturbation theory for computing the effects of the ellipticity and centrifugal potential.

Chapter 10 Effect of a Mushy Inner Core Boundary

10.1 Replacing the Inner Core Boundary by a Thin Mushy Transition Zone

The density contrast at the ICB is inferred mostly from the amplitude ratio $PKiKP$ / PcP. The poor determination of this contrast is due to insufficient detection of the $PKiKP$ wave and also the strongly scattered nature of a PcP wave. While the uncertainties in interpreting PcP observations are introduced by possible complex structure at the CMB (Buchbinder *et al.*, 1973; Souriau & Souriau, 1989), the weakness of the signals reflected from the ICB may indicate uncertainty in the ICB itself: it may not be a sharp discontinuity, instead it may be a transition zone with low rigidity. The thickness of the possible transition zone is also poorly determined. In a recent study based on synthetic seismograms using $PKiKP$ and $PKJKP$ data, Cummins & Johnson (1988) proposed that the thickness of the transition zone must be 5 km or less, which broadly agrees with the result of Phinney (1970). The latter author obtained a thickness of 1.5 km or less using a different approach which retains a special form of the transition zone where analytic solutions exist. For the purpose of investigating its influence to the Slichter mode, it may be useful to look at a variation of the thickness, for example, from 1 km to 5 km, upper bounded at the PREM inner core boundary (1221.5 km). Also, for the sake of simplicity, the Earth is taken to be spherical in order to examine how a mushy zone at the ICB affects the Slichter eigenperiods.

First I turn to Loper & Fearn (1983) for guidance in constructing a model of the transition zone at the ICB. Currently, the Earth models deduced from seismology all place a sharp ICB immediately beneath the liquid outer core. Studies of the anelasticity and P wave speed of the inner core also indicate a non-homogeneous region several hundred kilometres thick immediately below the ICB. Therefore, from a seismological point of view, the transition zone at the ICB is most likely of a form in which the outer core contains no solid but the inner core may contain liquid in a dendrite mushy zone (Loper & Fearn, 1983). This mushy zone should have a significant mass fraction of solid which forms a mechanically rigid matrix capable of sustaining shear waves. The model also should allow for liquid inclusion to occur in the interstices of the solid matrix. If the shear modulus of the inner core is μ_s, the shear modulus μ_t of the transition zone can be estimated using Loper & Fearn's (1983) formula (64)

$$\mu_t = (1 - f)^{\phi}\mu_s \tag{361}$$

where f is the fluid fraction parameter defined as

$$f = V_L/V. \tag{362}$$

V_L is the volume of the fluid in the transition zone, and V is the total volume of the transition zone, and $\phi \geq 1$.

In principle, I could require that the density (ρ_0) and the elastic parameters (λ and μ) change smoothly through the transition zone and continue across its upper and lower boundaries. While the requirement for continuity of the Lamé parameter λ and the density ρ_0 can be implemented easily, such a requirement for the shear modulus μ will pose some

difficulty. When $\mu = 0$, two of the six ordinary differential equations of the transition zone become improper, so a special treatment is needed at this point. To avoid this difficulty, I allow for a little discontinuity in shear modulus at the upper boundary of the transition zone (PREM's ICB). For example, I take $\mu_s = 0$ just outside of the ICB, at $a + h/20$ or so, where a is the radius of the ICB and h the thickness of the transition zone. A fitted polynomial using this point just above the ICB and another point at the lower boundary of the transition zone will give a small non-zero μ_s just below the ICB.

The procedure for modifying the PREM inner core model to have a mushy transition zone of thickness h can be outlined as follows: (1) Find values of the density, rigidity and Lamé parameter at the lower boundary of the transition zone $a - h$, using the profiles of these properties of the inner core; (2) Find values of the density and Lamé's parameter just above the upper boundary of the transition zone (PREM's ICB) using the profiles of these properties of the liquid core (rigidity vanishes at this point); (3) Use a cubic spline technique to determine polynomials for these properties in the transition zone (note that to obtain a small non-zero μ_s at the upper boundary of the transition zone, I choose the second point for interpolating μ_s to be $a + h/20$); (4) With μ_s computed at any point in the transition zone by the corresponding fitted polynomial, equation (361) can then be used to obtain the value of μ_f at that point for any chosen f and ϕ.

Table 12 lists the values of the density and Lamé parameter at the lower and upper boundaries of the transition zone, as well as at its middle point. Since the density and Lamé parameter are functions of radius r (hence h) only, I table them separately from the rigidity. The latter is not only a function of r, but also a function of f and ϕ. The thickness h varies from 1 - 5 km and $\phi = 1$. Table 13 displays the values of μ_f as f varies from 0.0 - 0.5, h varies from 1 - 5 km and $\phi = 1$. It is obvious that due to the intrusion of fluid in the transition zone, the rigidity of the zone is reduced. Softening of the transition zone then in turn reduces the effective elastic restoring force at the inner core boundary; hence the Slichter eigenperiods are slightly lengthened.

In programming, I integrate the inner core governing differential equations of the PREM model from the centre of the Earth to the lower boundary of the transition zone, then continue across the transition zone to reach the upper boundary - the ICB. In the transition zone, the density, rigidity and Lamé parameter of the inner core are replaced by the above modified ones. At the lower boundary of the transition zone, I need not do any extra work since this is a boundary where the density and elastic parameters change smoothly. Finally, a set of internal load Love numbers can be found at the upper boundary, where the general solid/liquid continuity conditions apply.

Although the density of the transition zone has been slightly altered from that of the PREM inner core, it seems safe to assume that the effect of the change in mass of the inner core is negligible.

Table 12: Density ρ_0 (10^3 kg m^{-3}) and Lamé parameter λ (10^{11} kg m^{-1}s^{-2}) of the transitions zone. h: 1 - 5 km (for any chosen f and ϕ).
r_1=a-h, the lower boundary of the transition zone;
r_2=a-h/2, the middle point of the transition zone;
r_3=a, the upper boundary of the transition zone, where a=1221.5 km (the radius of the PREM's ICB).

	$r\backslash h$ (km)	1	2	3	4	5
	r_1	12.7642	12.7647	12.7652	12.7657	12.7663
ρ_0	r_2	12.4635	12.4637	12.4640	12.4643	12.4645
	r_3	12.1628	12.1628	12.1628	12.1628	12.1682
	r_1	1.23898	1.23909	1.23920	1.23931	1.23942
λ	r_2	1.27159	1.27165	1.27170	1.27176	1.27181
	r_3	1.30420	1.30420	1.30420	1.30420	1.30420

Table 13: Rigidity μ_f (10^{10} kg m^{-1}s^{-2}) of the transition zone. h: 1 - 5 km; f: 0.0 - 0.5; ϕ=1. r_1=a-h, the lower boundary of the transition zone; r_2=a-h/2, the middle point in the transition zone; r_3=a, the upper boundary of the transition zone. (a=1221.5 km, the radius of the ICB).

			f=0.0		
$r\backslash h$ (km)	1	2	3	4	5
r_1	1.56770	1.56801	1.56831	1.56862	1.56892
r_2	1.53066	1.53081	1.53096	1.53111	1.53127
r_3	1.49361	1.49361	1.49361	1.49361	1.49361
			f=0.1		
$r\backslash h$ (km)	1	2	3	4	5
r_1	1.41093	1.41121	1.41148	1.41175	1.41203
r_2	1.37759	1.37773	1.37787	1.37800	1.37814
r_3	1.34425	1.34425	1.34425	1.34425	1.34425
			f=0.2		
$r\backslash h$ (km)	1	2	3	4	5
r_1	1.25416	1.25441	1.25465	1.25489	1.25514
r_2	1.22453	1.22465	1.22477	1.22489	1.22501
r_3	1.19489	1.19489	1.19489	1.19489	1.19489
			f=0.3		
$r\backslash h$ (km)	1	2	3	4	5
r_1	1.09739	1.09761	1.09782	1.09803	1.09824
r_2	1.07146	1.07157	1.07167	1.07178	1.07189
r_3	1.04553	1.04553	1.04553	1.04553	1.04553
			f=0.4		
$r\backslash h$ (km)	1	2	3	4	5
r_1	0.94062	0.94080	0.94099	0.94117	0.94135
r_2	0.91839	0.91849	0.91858	0.91867	0.91876
r_3	0.89617	0.89617	0.89617	0.89617	0.89617
			f=0.5		
$r\backslash h$ (km)	1	2	3	4	5
r_1	0.78385	0.78400	0.78416	0.78431	0.78446
r_2	0.76533	0.76541	0.76548	0.76556	0.76563
r_3	0.74681	0.74681	0.74681	0.74681	0.74681

10.2 Eigenperiods: Numerical Results for the Mushy Inner Core Boundary

The Slichter eigenperiods for a suite of transition zone models are listed in Table 14. To obtain these results, I have set the parameter ϕ of equation (361) to be 1. I also examined the cases where ϕ equals 2 and 3, and the results show that the eigenperiods are affected very little, only about 0.003% changes from eigenperiods in Table 14. In other words, the Slichter modes seem to be insensitive to this parameter.

The effect of adding the mushy transition zone at the ICB is to lengthen the eigenperiods of the Slichter modes, as would be expected, since the effective density jump is slightly reduced and the rigidity of the ICB is also reduced. The results displayed in Table 14 show that, with the thickness of the mushy zone up to 5 km and the fluid content up to 50%, the eigenperiods of the Slichter modes are altered only slightly, with 0.604%, 0.577%, 0.467% and 0.647% increments for non-rotating, rotating-axial, prograde and retrograde modes respectively. This outcome reflects the nature of the Slichter modes with their main restoring force being gravitation (the elasticity of the inner core plays only a minor role in sustaining the oscillation). On the other hand, the smallness of the eigenperiod increment is also due to the limited thickness of the transition layer. It is evident from Table 14 that the eigenperiod change with respect to the change of the thickness of the mushy zone is much larger than that with respect to the change of the fluid fraction of it.

Table 14: Eigenperiods (hr) of the Slichter modes for the PREM model with a mushy ICB. f: the fluid fraction; h: the thickness of the transition zone. L=5, N=5, and ϕ=1.

non-rotating (PREM: 5.42047)

$f\backslash h$ (km)	1	2	3	4	5
0.0	5.42694	5.43342	5.43992	5.44643	5.45296
0.1	5.42695	5.43344	5.43994	5.44647	5.45301
0.2	5.42696	5.43346	5.43997	5.44650	5.45305
0.3	5.42697	5.43347	5.44000	5.44654	5.45310
0.4	5.42698	5.43349	5.44003	5.44658	5.45315
0.5	5.42698	5.43351	5.44006	5.44662	5.45319

rotating, m=0 (PREM: 5.30868)

$f\backslash h$ (km)	1	2	3	4	5
0.0	5.31475	5.32081	5.32688	5.33297	5.33907
0.1	5.31475	5.32082	5.32691	5.33301	5.33912
0.2	5.31476	5.32084	5.32693	5.33304	5.33916
0.3	5.31477	5.32086	5.32696	5.33307	5.33920
0.4	5.31478	5.32088	5.32698	5.33311	5.33925
0.5	5.31479	5.32089	5.32701	5.33314	5.33929

rotating, m=1 (PREM: 4.76424)

$f\backslash h$ (km)	1	2	3	4	5
0.0	4.76915	4.77405	4.77897	4.78391	4.78885
0.1	4.76915	4.77407	4.77900	4.78393	4.78888
0.2	4.76916	4.77408	4.77902	4.78396	4.78891
0.3	4.76917	4.77410	4.77904	4.78399	4.78895
0.4	4.76918	4.77411	4.77906	4.78402	4.78899
0.5	4.76918	4.77413	4.77908	4.78405	4.78902

rotating, m=-1 (PREM: 5.97827)

$f\backslash h$ (km)	1	2	3	4	5
0.0	5.98594	5.99359	6.00126	6.00895	6.01666
0.1	5.98595	5.99361	6.00129	6.00900	6.01672
0.2	5.98596	5.99363	6.00133	6.00904	6.01677
0.3	5.98598	5.99366	6.00136	6.00908	6.01683
0.4	5.98598	5.99368	6.00139	6.00913	6.01688
0.5	5.98600	5.99370	6.00143	6.00917	6.01694

Chapter 11 Summary

This thesis is a systematic study of the Slichter modes for a realistic Earth model which takes into account basic properties of the Earth, such as elasticity of the solid inner core and mantle, radial stratification of the liquid core (neutral and non-neutral), ellipticity of the inner core and liquid core, and possible mushy state of the inner core boundary. I have employed both recent theories and traditional mathematical methods such as the subseismic approximation, the two potential description of core dynamics, variational principle and Galerkin method. The study confirms that, for a realistic Earth model such as PREM, the periods of the Slichter triplet are 4.76, 5.30 and 5.98 hours.

In the past few years, a great deal of effort has been expended to detect evidence of core undertones and the Slichter oscillations. For the latter, there has been a major increase in observational possibility due to development of superconducting gravimeter, formation of a globally distributed network, and advance of more sophisticated data analysis techniques. Together with previous research (Slichter 1961, Busse 1974, Crossley 1975, Smith 1976, Dahlen & Sailor 1979, Crossley *et al* 1992 and Rochester & Peng 1990, 1993), this study provides a theoretical reference for the anticipated observations and possible identification of the modes. In turn, the data observed will put strong constraints on the internal structure of the Earth's core, and help to gain a better understanding of the planet's evolution.

The main achievements of this study can be summarized as:

(1) I correctly take into account the frequency-dependent nature of the internal load Love numbers at the ICB and CMB. This is done by keeping both the inertial and Coriolis self-coupling terms in the equation of the momentum conservation of the solid inner core

and mantle, as well as in the derivation of the starting solutions at the geocentre. Therefore, the load Love numbers developed in this thesis are dependent on the frequency of vibration and the azimuthal order number m, as well as the degree n of a particular member of the coupling chain of the displacement field. The idea of introducing the internal load Love numbers is to represent the effects of the solid inner core and mantle on the liquid core dynamics in an economic way. Because these load Love numbers (especially at the ICB) exhibit strong resonance at periods long enough to be comparable with the Slichter eigenperiods, it is absolutely essential to use dynamic load Love numbers in modelling these long-period normal modes.

(2) I apply the SSA and a variational principle to estimate the Slichter eigenperiods for a rotating Earth model with a neutrally stratified liquid core. The assumption of neutral stratification of the liquid core enables the deformable ICB and CMB be fully taken into account in conjunction with the SSA and the variational method. The main advantage for applying the SSA in a neutral liquid core is that the SSWE, one of the resulting governing partial differential equations, can be solved independently for the potential field χ. The Poisson equation can then be solved independently for the other potential field V_1.

To fully take advantage of the SSA and the variational principle, I introduced the novel effective load Love numbers, which are also strongly frequency-dependent. The application of these effective load Love numbers made it possible to avoid a requirement in the associated boundary conditions that the Poisson equation has to be solved simultaneously with the SSWE for V_1. Of course the effective load Love numbers are only useful when the SSA is invoked, and when the liquid core is treated as neutrally-stratified.

The application of the SSA and a variational principle is limited due to the nature of its approximation and the stringent requirement of fixed outer core boundaries or deformable boundaries with a strictly neutrally stratified liquid core. However, it can be used effectively to obtain a close reference value of the eigenperiod for a realistic but relatively simple Earth model. While the eigenperiods of the Slichter modes are obtained correctly using the SSA (with an expected small error), the eigenfunctions so calculated in the mantle exhibit some kind of distortion. The displacement field **u** in the mantle has the wrong sign when SSA is used in the core. This strongly suggests a failure of the SSA to properly conserve linear momentum. In a neutral liquid core, the SSA removes the sources of V_1 to the core boundaries by reducing the Poisson equation to a Laplace equation. This distortion of V_1 in the outer core may be responsible for starting y_5 off with the wrong value at the bottom of the mantle. Therefore, one should totally avoid using this approximation if the computation of eigenfunctions are involved, even for a simple Earth model. The alternative is to use the two potential description of core dynamics, extended perturbation theory, or extended direct integration method.

(3) I applied the exact TPD of core dynamics and a Galerkin method to calculate the eigenperiods of the Slichter modes for a realistic Earth model, with both spherical and ellipsoidal stratification.

The results for the neutrally stratified liquid core provide a test of how accurate the predictions using the SSA are. The calculations have proved that the SSA only brings minor errors (0.043%, 0.031%, 0.006%) to the eigenperiods of the Slichter modes. It is clear that the situation for a non-neutrally stratified liquid core can be handled equally easily by the TPD.

The assumption of neutral stratification of the liquid core leads to small changes (0.102%, 0.101%, 0.097%) in the eigenperiods of the Slichter modes for PREM. The use of the Galerkin method avoids the constraint in a variational principle that the linear operators in both the SSA and TPD must be Hermitean. Therefore, the Galerkin method is an effective tool to be used in core dynamics, as far as the computational economy is concerned.

In the applications of the variational principle and the Galerkin method, I have taken advantage of the natural character of the boundary conditions, namely the trial functions of an eigenvalue problem are not required to satisfy these boundary conditions exactly. Instead they satisfy these boundary conditions only in an average sense. This is achieved by adding the proper boundary conditions into the functionals of the variational principle or the resulting Galerkin equations. The use of the natural boundary conditions also conveniently reduces the need of calculating the derivatives of the liquid core field variables from second order to first order. However, the approximate nature of such a treatment causes some discontinuities of some eigenfunctions (y_1, y_2, y_5 and y_6) across the outer boundaries. These discontinuities are not present when the direct integration method is used or when the trial functions satisfy the boundary conditions exactly. This is the price which has to be paid for the convenience of using the natural property of the boundary conditions.

(4) I have taken the Coriolis coupling chain of the displacement field of the liquid core longer than previously undertaken for the Slichter modes. Due to the absence of rigidity in the liquid core, one has to retain enough terms in the coupling chain of the displacement field to ensure a convergent eigenperiod. For a long period free oscillation, such as the Slichter mode, when one cannot be confident that a perturbation treatment, or a heavily truncated

coupling chain (Crossley, 1975; Smith, 1976), would yield satisfactory results, an alternative treatment has to be sought. The approaches used in this thesis, such as the SSA and the TPD, or the extended direct integration method used by Crossley (1992) are all capable of retaining a longer coupling chain in the numerical computations. For a spherical Earth model, it is shown that truncating the coupling chain at degree 3 will be enough to have a convergent eigenperiod for PREM. However, in the latter case, I only take into account the self-coupling of the spheroidal displacement field in the solid parts of the Earth, whereas Smith (1976) kept coupling up to the toroidal field of degree 2. The practice of ignoring toroidal field in the solid parts of the Earth has been justified by calculation (Rochester & Peng, 1993). For the ellipsoidal Earth model, I have retained the toroidal coupling of degree 2 to degree 1 and 3 in the inner core.

For a given Earth model, the minimum truncation level of the coupling chain required for obtaining a convergent eigenperiod is also dependent on the complexity of the problem. It seems that the more complicated the formulation is, the longer a coupling chain needs to be retained. In this thesis, this number is 3 for a spherical stratification, and 5 for an ellipsoidal stratification, of the PREM. The latter is seen to have a more complicated formulation than the former. On the other hand, the convergence of the eigenperiods is also dependent on construction of radial trial functions. The calculations of taking into account the ellipticity of the inner and outer cores and the centrifugal potential demonstrate that when the truncation number of the radial trial functions of polynomial-type exceeds 7, the eigenperiods start to fluctuate rather than further converge. This may suggest that a different type of radial trial function, such as Legendre polynomials which have a property of orthogonality, should be

used in the latter case. To prevent adding more numerical noise, it might also be helpful to eliminate all double integrations resulting from the complicated formulations which arise from taking into consideration the ellipticity and centrifugal potential.

(5) The Slichter modes are indeed dominated by degree 1 displacement field of the inner core. The results of this thesis show that the effects of higher degree displacement field of the solid inner core and mantle are relatively small. They result in a correction of only 0.1% to the eigenperiods of the modes.

(6) This is the first time that ellipsoidal load Love numbers have been used to estimate the effects of the ellipticity and centrifugal force on the Slichter eigenperiods. This approach provides an alternative to the perturbation calculation of Dahlen & Sailor (1979), or the direct integration by Smith (1976). For the purpose of developing the ellipsoidal load Love numbers, I have discussed in detail the formulations of the governing differential equations in a way which treats both the interior and boundaries of an ellipsoidal body consistently. I have also given the formulation using Smith's (1974) approach, in more detail than he did, and have emphasized that his approach involves a small discrepancy in the vicinity of the boundaries. To save computational effort, in the final calculation of the eigenperiods, I chose to use Smith's (1974) approach for taking into account the ellipticity of the inner and outer cores. This is based on the fact that the main restoring force for the Slichter oscillation acts at the ICB and is gravitational in nature. The effects of the ellipticity and centrifugal force are small corrections to the eigenperiods of the modes calculated for a spherical Earth model. Therefore, the small discrepancy between the method of treating the interior and the method of treating the boundaries should cause only negligible errors in the eigenperiods

of the Slichter triplet. Again, the frequency-dependent nature of these ellipsoidal load Love numbers is correctly retained in this thesis.

(7) This is the first time that the effect of a mushy inner core boundary on the Slichter modes has been investigated. I have modelled the transition zone with different thicknesses (1 - 5 km) and different liquid contents (0 - 50%), which may include most possible states of the zone. With the presence of the mushy zone, the rigidity of the inner core boundary and the density jump across it are reduced. These effects in turn reduce the effective gravitational restoring force, which results in an increase in the vibration periods. The results obtained in this thesis suggest that the influence of the mushy inner core boundary on the Slichter triplet is relatively small. The increments in eigenperiods are about 0.577%, 0.467%, and 0.647% for a realistic Earth model such as PREM, with a mushy zone of 5 km in thickness and 50% in fluid content. However, though small, the effects of the mushy inner core boundary on the Slichter modes are comparable to, or larger than, some effects discussed in this thesis. Therefore, the possibility of a mushy inner core boundary could significantly influence mode identification. It seems reasonable to say that the central period of 5.3 hours is the lower bound of the Slichter modes for PREM, insofar as a softer inner core boundary is a sound and practical theory.

(8) Some ideas discussed in this thesis may be useful to other theoretical modellings. For example, ellipsoidal Love numbers may be conveniently applied in wobble/nutation problems. Since the existence of the latter depends totally on the ellipticity and centrifugal potential, the consistent way of formulating the governing equations in the interior of a body and on its boundaries, as discussed in §7.3, should be used. Since the accompanying displacement

fields are of the form given by (6), with $m = \pm 1$, this will result in a set of new ellipsoidal Love numbers other than those developed in this thesis.

The use of Love numbers also makes the estimate of the effects of the transition zone at the ICB convenient. If present, such a mushy layer will affect the modelling of other phenomena, such as free inner core nutation, anelasticity of the inner core, effects of the inner core on inertial/gravity modes, etc.

Clearly there are still more things to be studied about the Slichter oscillation. For example, it may be worthwhile to look further into the damping of the oscillation due to liquid core viscosity, and estimate the time scale of damping by this mechanism. It may also be worthwhile to carry out an independent calculation (e.g. with an alternate approach) to confirm the apparently negligible effect of thermal damping studied by Rochester (unpublished).

Certainly more effort is needed to further study the excitation of the Slichter oscillation, and to develop more sophisticated data processing techniques to extract useful signals from existing observational data, such as that from superconducting gravimeter observations. To separate a surface gravity signal as weak as 0.5 nanogal (Crossley, 1992) from various noises in the observational data is indeed a challenge. After all, any prediction of the eigenperiods of the Slichter modes has to be tested by observations!

References

Alterman, Z., Jarosch, H. and Pekeris, C.L., 1959. Oscillation of the Earth, Proc. Roy. Soc. London, A, **252**, 80-95

Anderson, O.L. & Young, D.A., 1988. Crystallization of the Earth's inner core, in Structure and Dynamics of Earth's Deep Interior, eds. D.E. Smylie and R. Hide, AGU, 83-90

Backus, G. & Gilbert, F., 1961. The rotational splitting of the free oscillations of the Earth, Proc. natn. Acad. Sci., **47**, 362 - 371

Braginskii, S.I., 1963. Structure of the F layer and reasons for convection in the Earth's core, Dokl. Akad. Nauk. SSSR., Engl. Transl., **149**, 8-10

Buchbinder, G.G.R., Wright, C. and Poupinet, G., 1973. Observations of $PKiKP$ at distances less than 110 deg, Bulletin of the Seismological Society of America, **65**, 1699-1707

Buffett, B. A. & Goertz, D., 1995. Magnetic damping of the translational oscillation of the inner core, Geophys. J. Int., **120**, 103-110

Bullen, K.E. & B.A. Bolt, 1985. An Introduction to the Theory of Seismology, 4th edition, Cambridge University Press. 499 pp.

Busse, F.H., 1974. On the free oscillation of the Earth's inner core, J. Geophys. Res., **79**, 753-757

Crossley, D.J., 1975. The free oscillation equations at the centre of the Earth, Geophys. J. R. Astr. Soc., **41**, 153-163

Crossley, D.J., 1975. Core undertones with rotation, Geophys. J. R. Astr. Soc., **42**, 477-488

Crossley, D.J., 1984. Oscillatory flow in the liquid core, Phys. Earth Planet. Int., **36**, 1-16

Crossley, D.J., 1988. The excitation of core modes by earthquakes, in Structure and Dynamics of Earth's Deep Interior, eds. D.E. Smylie and R.Hide, AGU, 41-50

Crossley, D.J., 1992. Eigensolutions and seismic excitation of the Slichter mode triplet for a fully rotating Earth model (abstract), Eos, Trans. Am. Geophys. Un, **73**. 60

Crossley, D.J., 1993. The gravity effect of core modes for a rotating Earth, J. Geomagn. Geoelectr., **45**, 1371-1381

Crossley, D.J., Hinderer, J. and Legros, H., 1991. On the excitation, detection and damping of core modes, Phys. Earth Planet. Int., **68**, 97 - 116

Crossley, D.J. & Rochester, M.G., 1980. Simple core undertones, Geophys. J. R. Astr. Soc., **60**, 129-161

Crossley, D.J. & Rochester, M.G., 1992. The subseismic approximation in core dynamics, Geophys. J. Int., **108**, 502 - 506

Crossley, D.J., Rochester, M.G. and Peng, Z.R., 1992. Slichter modes and Love numbers, Geophys. Research Letters, **19**, 1679-1682

Cummins, P. & Johnson, L., 1988. Synthetic seismograms for an inner core transition of finite thickness, Geophys. J. R. Astr. Soc., **94**, 21-34

Dahlen, F.A. & Sailor, R.V., 1979. Rotational and elliptical splitting of the free oscillation of the Earth, Geophys. J. R. Astr. Soc., **58**, 609-623

de Boeck, I., Van Hoolst, T. & Smeyers, P., 1992. The subseismic approximation for low-frequency modes of the Earth applied to low-degree, low-frequency g-modes of non-rotating stars, Astronomy and Astrophysics, **259**, 167-174

Dehant, V., 1988. Nutation and inelasticity of the Earth, in Proceedings of the 128th Symposium of IAU/IAG on Earth rotation and reference Frame, 1987, Washington, eds Babcock, A. & Wilkins, G. A., Reidel, Dordrecht, 323-329.

Dziewonski, A.M. & Anderson, D.L., 1981. Preliminary reference Earth model, Phys. Earth Planet. Int., **25**, 297-356

Fearn, D.R. & Loper, D.E., 1981. Compositional convection and stratification of Earth's core Nature, **289**, 393-394

Friedlander, S., 1987. Internal waves in a rotating stratified spherical shell: asymptotic solutions, Geophys. J. R. Astr. Soc., **89**, 637-655

Friedlander, S., 1988. Stability and waves in the Earth's fluid core, in Proc. U.S.-Italy Conference on Energy Stability and Convection,Capri, May 1986, Longman Scientific Press Pitman Research Notes in Mathematics, ed. Straughan, B., Longman, London, **168**, 325-345

Gilbert, F. & Dziewonski, A.M., 1975. An introduction of normal mode theory to the retrieval of structural parameters and source mechanism from seismic spectra, Philos. Trans. R. Soc. London Ser. A, **278**, 187-269

Gubbins, D., 1977. Energetics of the earth's core, J. Geophys., **43**, 453-464

Gubbins, D., Thomson, C.J. and Whaler, K.A., 1982. Stable regions in the Earth's liquid core, Geophys. J. R. Astr. Soc., **68**, 241-251

Haardeng-Pedersen, G.P., 1975. Studies on the dynamics of the rotating Earth, Ph. D. thesis, Memorial University of Newfoundland, 225 pp.

Haardeng-Pedersen, G.P. & Bodri, B., 1980. On the upper limit of undertone periods, Geophys. J. R. astr. Soc., **62**, 367-377

Haddon, R.A.M. & Bullen, K.E., 1969. An Earth model incorporating free oscillation data, Phys. Earth Planet. Int., **2**, 37-49

Higgins, G. & Kennedy, G.C., 1971. The adiabatic gradient and the melting point gradient of the core of the Earth, J. Geophys. Res., **76**, 1870-1878

Hinderer, J., Crossley, D.J., Jensen, O.G. & Xu, H., 1992. Gravity noise levels and periodic signals observed from a common 2 year analysis of the French and Canadian superconducting gravimeters (abstract), Eos, Trans. Am. Geophys. Un, **73**. 60

Hornbeck, R.W., 1975. Numerical Methods, Quantum Publishers,Inc., 310 pp.

Jackson, B.V. & Slichter, L.B., 1974. The residual daily Earth tides at the south pole, J. Geophys. Res., **79**, 1711-1715

Jensen, O., Crossley, D.J., & Hinderer, J., 1992. Simple data decomposition reveals a surprisingly rich harmonic spectrum in superconducting gravimeter data (abstract), Eos, Trans. Am. Geophys. Un, **73**. 60

Johnson, I. & Smylie, D.E., 1977. A variational approach to whole- Earth dynamics, Geophys. J. Roy. Astr. Soc., **50**, 35-54

Kennedy, G.C. & Higgins, G.H., 1973. The core paradox, J. Geophys. Res., **78**, 900-904

Lamb, H., 1882. Proc. Lond. Math. Soc. **13**, 189 - 212

Loper, D.E., 1984. The dynamical structure of D" and deep plums in a

non-Newtonian mantle, Phys. Earth Planet. Interiors, **34**, 57-67

Loper, D.E. & Fearn, D.R., 1983. A seismic model of a partial molten inner core, J. Geophys. Res., **88**, 1235-1242

Masters, G., 1979. Observational constraints on the chemical and thermal structure of the Earth's deep interior, Geophys. J. R. Astr. Soc., **57**, 507-534

McElhinny, M.W. & Senanayake, W.E., 1980. Paleomagnetic evidence for existence of the geomagnetic field 3.5 Ga ago, J. Geophys. Res., **85**, 3523-3528

Pekeris, C.L., 1966. The internal constitution of the Earth, Geophys. J. R. Astr. Soc., **11**, 85-132

Pekeris, C.L. & Accad, Y., 1972. Dynamics of the liquid core of the Earth, Philosophical Transactions of Royal Society of London, Series A, **273**, 237-260

Peng, Z.R., 1990. Subseismic description of the Slichter modes in a rotating Earth, M.Sc. thesis, Memorial University of Newfoundland, 81 pp.

Phinney, R.A., 1970. Reflection of acoustic waves from a continuously varying interfacial region, Rev. Geophys. Space Phys., **8**, 517-532

Rieutord, M., 1991. Linear theory of rotating fluids using spherical harmonics, II. Time-periodic flows, Geophys. Astrophys. Fluid Dynamics, **59**, 185-208

Rochester, M.G., 1989. Normal modes of rotating self-gravitating compressible stratified fluid bodies: the subseismic wave equation, in Continuum mechanics and its applications, eds. G.A.C. Graham & S.K. Malik, Hemisphere Publishing Corporation, New York, 797-823

Rochester, M.G., Jacobs, J.A., Smylie, D.E. & Chong, K.F., 1975. Can precession power

the geomagnetic dynamo? Geophys. J. R. Astr. Soc., **43**, 661-678

Rochester, M.G. & Peng, Z.R., 1990. The Slichter mode revisited: a test of the subseismic approximation, Eos, Trans. Am. Geophys. Un, **71**, 1479

Rochester, M.G. & Peng, Z.R., 1993. The Slichter modes of the rotating Earth: a test of the subseismic approximation, Geophys. J. Int., **113**, 575-585

Rydelek, P.A. & Knopoff, L., 1984. Spectral analysis of gapped data: search for mode ${}_1S_1$ at the South Pole, J. Geophys. Res., **89**, 1899-1902

Seyed-Mahmoud, B., 1994. Wobble/nutation of a rotating ellipsoidal Earth with liquid outer core: implementation of a new set of equations describing dynamics of rotating fluid, M.Sc. thesis, Memorial University of Newfoundland, 79 pp.

Shearer, P. & Masters, G., 1990. The density and shear velocity contrast at the inner core boundary, Geophys. J. Int., **102**, 491-498

Shen, P.Y., 1983. On oscillations of the Earth's fluid core, Geophys. J. R. Astr. Soc., **75**, 737-757

Slichter, L.B., 1961. The fundamental free mode of the Earth's inner core, Proc. Nat. Acad. Sci., U.S.A., **47**, 186-190

Smith, M., 1974. The scalar equations of infinitesimal elastic-gravitational motion for a rotating, slightly elliptical Earth, Geophys. J. R. Astr. Soc., **37**, 491-526

Smith, M., 1976. Translational inner core oscillation of a rotating, slightly elliptical Earth, J. Geophys. Res., **81**, 3055-3065

Smith, M., 1977. Wobble and nutation of the Earth, Geophys. J. R. Astr. Soc., **50**,

103-140

Smylie, D.E., 1974. Dynamics of the outer core, Veroff. Zentralinst. Phys. Erde, Akad. Wiss. D. D. R., **30**, 91-104

Smylie, D.E., 1988. Variational calculation of core modes in realistic Earth models, in Structure and Dynamics of Earth's Deep Interior, eds. Smylie, D.E. & Hide, R., AGU, Washington, D.C., 23-28

Smylie, D.E., 1992. The inner core translational triplet and the density near Earth's center, Science, **255**, 1678-1682

Smylie, D.E., Jiang, X.H., Brennan, B.J. and Sato, K., 1992. Numerical calculation of modes of oscillation of the Earth's core, Geophys. J. Int., **108**, 465-490

Smylie, D.E. & Qin, Y., 1992. The effects of viscosity and rotation on the translational oscillations of the inner core (abstract), Eos, Trans. Am. Geophys. Un., **73**, 60

Smylie, D.E. & Rochester, M.G., 1981. Compressibility, core dynamics and the subseismic wave equation, Physics of the Earth and Planetary Interiors, **24**, 308-319

Smylie, D.E. & Rochester, M.G., 1986a. Long period core dynamics, in Earth Rotation: Solved and Unsolved Problems, Proc. NATO Advanced Study Workshop, eds. Cazenave, A. & Reidel, D., 297-324,

Smylie, D.E. & Rochester, M.G., 1986b. A variational principle for the subseismic wave equation, Geophys. J. R. Astr. Soc., **86**, 553-561

Smylie, D.E., Szeto, A.M.K. and Rochester, M. G., 1984. The dynamics of the Earth's inner and outer core, Rep. Prog. Phys., **47**, 855-906

Smylie, D.E., Szeto, A.M.K. and Sato, K., 1990. Elastic boundary conditions in long-

period core oscillations, Geophys. J. Int., **100**, 183-192

Souriau, A. & Souriau, M., 1989. Ellipticity and density at the inner core boundary from subcritical $PKiKP$ and PcP data, Geophys. J. Int., **98**, 39-54

Takeuchi, H. & Saito, M., 1971. Seismic surface waves, Methods comput. Phys., **11**, 217-295

Verhoogen, J., 1961. Heat balance of the Earth's core, Geophys. J., **4**, 276-281

Wahr, J. M. 1981. Body tides on an elliptical, rotating, elastic and oceanless Earth, Geophys. J. R. Astr. Soc., **64**, 677-703

Webb, S., 1992. Axisymmetric inertial gravity oscillations of compressible stratified fluid in a rigid sphere: an approximation to the Earth's outer core, M.Sc. thesis, Memorial University of Newfoundland, 164 pp.

Widmer, R., Masters, G. & Gilbert, F., 1988. The spherical Earth revisited (abstract), Eos, Trans. Am. Geophys. Un., **69**, 1310

Woodhouse, J.H. & Dahlen, F.A., 1978. The effect of a general aspherical perturbation on the free oscillations of the Earth, Geophys. J. R. Astr. Soc., **53**, 335-354

Wu, W.J., 1993. A new subseismic governing system of equations and its extensions. Phys. Earth Planet. Inter., **75**, 289-315

Wu, W.J. & Rochester, M.G., 1988. A new variational principle for core dynamics (abstract), Eos, Trans. Am. Geophys. Un., **69**, 1310

Wu, W.J. & Rochester, M.G., 1990. Core dynamics: the two-potential description and a new variational principle, Geophys. J. Int., **103**, 697-706

Wu, W.J. & Rochester, M.G., 1993. Computing core oscillation eigenperiods: a test of the

subseismic approximation, Phys. Earth Planet. Interiors, **78**, 33-50

Wu, W.J. & Rochester, M.G., 1994. Gravity and Slichter modes of the rotating Earth, Phys. Earth Planet. Interiors, **87**, 137-154

Zienkiewicz, O.C. & Morgan, K., 1982. Finite Elements and Approximation, John Wiley & Sons, 328 pp.

Appendix A Coefficients of 14th Order System of Ordinary Differential Equations in the Ellipsoidally-Stratified Rotating Inner Core

In §7.4 the system of ordinary differential equations governing the Slichter oscillation field variables of degree $n = 1$ and $n = 3$, coupled by the Coriolis effect, ellipticity and centrifugal potential, is put into the form

$$\frac{dy_i}{dr} = \sum_{j=1}^{14} A_{i,j} y_j \qquad i = 1,\ 2,\ \cdots,\ 14$$

where $A_{i,j} = E_{i,j}$ for i =1, 3, 5, 7, 9, 11, and 13, and $A_{i,j}$ are expressed in terms of $E_{i,j}$ for i=2, 4, 6, 8, 10, 12 and 14. I list in this appendix the matrix $\underline{E}$. Note that some of my field variables differ from those used by Alterman *et al* (1959), as explained by equations (249) - (251) of §7.4. The non-zero coefficients $E_{i,j}$ are:

$$E_{1,1} = -\frac{2}{r}$$

$$E_{1,2} = 1$$

$$E_{1,3} = \frac{l(l+1)}{r}$$

$$E_{2,1} = -2l(l+1)\mu' \frac{h}{r_2} C_l^m - 4\frac{1}{r}\frac{d}{dr}(h\mu') C_l^m + \omega^2 \rho_0' h C_l^m$$

$$+4\pi G \rho_0 \rho_0' h C_l^m + \frac{2}{r}\frac{d}{dr}(\rho_0 g_0 h) C_l^m - \rho_0 \frac{d^2}{dr^2}(h g_0) C_l^m - 2l\rho_0 g_0 \frac{h}{r^2} C_l^m$$

$$+\rho_0' \frac{dg_0}{dr} h C_l^m - \frac{2}{3}\Omega^2 \rho_0' h C_l^m$$

$$E_{2,2} = \frac{d}{dr}(h\lambda')C_l^m + 2\frac{d}{dr}(h\mu')C_l^m$$

$$E_{2,3} = 2l(l+1)\mu'\frac{h}{r_2}C_l^m + \frac{2l(l+1)}{r}\frac{d}{dr}(h\mu')C_l^m - 2m\omega\Omega\rho_0' hC_l^m$$

$$-\frac{l(l+1)}{r}\frac{d}{dr}(\rho_0 g_0 h)C_l^m + 2l\rho_0\frac{d}{dr}(\frac{hg_0}{r})C_l^m + 2l\rho_0 g_0\frac{h}{r^2}C_l^m + \frac{2l(l+3)}{3}\Omega^2\rho_0' hC_l^m$$

$$E_{2,4} = l(l-1)\mu'\frac{h}{r}C_l^m + 2l\rho_0 g_0\frac{h}{r}C_l^m$$

$$E_{2,6} = \rho_0' hC_l^m$$

$$E_{2,7} = -2(l+1)\omega\Omega\rho_0 H_{l+1}^m + 2\omega\Omega\rho_0' h[(l+2)G_{l+1}^m C_l^m - (l+1)H_{l+1}^m B_{l+2}^m]$$

$$+3m\rho_0\frac{d}{dr}(\frac{hg_0}{r})H_{l+1}^m + 3m\rho_0 g_0\frac{h}{r^2}H_{l+1}^m + 2m\Omega^2\rho_0' hH_l^m$$

$$E_{2,8} = -3m\mu'\frac{h}{r}H_{l+1}^m + 3m\rho_0 g_0\frac{h}{r}H_{l+1}^m$$

$$E_{2,9} = -2(l+2)(l+3)\frac{\mu}{r_2} - 4\frac{\mu'}{r} - 2(l+2)(l+3)\mu'\frac{h}{r_2}B_{l+2}^m - 4\frac{1}{r}\frac{d}{dr}(h\mu')B_{l+2}^m + \rho_0\omega^2$$

$$-\rho_0\frac{dg_0}{dr} + \frac{2\rho_0 g_0}{r} + 4\pi G\rho_0^2 + \omega^2\rho_0' hB_{l+2}^m + 4\pi G\rho_0\rho_0' hB_{l+2}^m$$

$$+\frac{2}{r}\frac{d}{dr}(\rho_0 g_0 h)B_{l+2}^m - \frac{2}{3}\Omega^2\rho_0 - \rho_0\frac{d^2}{dr^2}(hg_0)B_{l+2}^m$$

$$+3\rho_0 g_0\frac{h}{r^2}B_{l+2}^m - \rho_0' h\frac{dg_0}{dr}B_{l+2}^m - \frac{2}{3}\Omega^2\rho_0' hB_{l+2}^m$$

$$E_{2,10} = \lambda' + 2\mu' + \frac{d}{dr}(h\lambda')B_{l+2}^m + 2\frac{d}{dr}(h\mu')B_{l+2}^m$$

$$E_{2,11} = 2(l+2)(l+3)\frac{\mu}{r_2} + 2(l+2)(l+3)\frac{\mu'}{r} + 2(l+2)(l+3)\mu'\frac{h}{r_2}B_{l+2}^m$$

$$+\frac{2(l+2)(l+3)}{r}\frac{d}{dr}(h\mu')B_{l+2}^m - 2m\rho_0\omega\Omega - (l+2)(l+3)\frac{\rho_0 g_0}{r}$$

$$-2m\omega\Omega\rho_0' hB_{l+2}^m - \frac{(l+2)(l+3)}{r}\frac{d}{dr}(\rho_0 g_0 h)B_{l+2}^m + \frac{2}{3}(l+2)(l+3)\Omega^2\rho_0$$

$$-3\rho_0\frac{d}{dr}(\frac{hy_0}{r})B^m_{l+2} - 3\rho_0 g_0\frac{h}{r^2}B^m_{l+2} + \frac{2(l+2)(l+3)}{3}\Omega^2\rho_0' h B^m_{l+2}$$

$$E_{2,12} = (l+2)(l+3)\frac{\mu}{r} + (l^2+5l+9)\mu'\frac{h}{r}B^m_{l+2} - 3\rho_0 g_0\frac{h}{r}B^m_{l+2}$$

$$E_{2,14} = \rho_0 + \rho_0' h B^m_{l+2}$$

$$E_{3,1} = -\frac{1}{r}$$

$$E_{3,3} = \frac{1}{r}$$

$$E_{3,4} = 1$$

$$E_{4,1} = 2\mu'\frac{h}{r^2}C^m_l - \frac{2m\omega\Omega}{(l+2)(l+3)}\rho_0' h C^m_l - \frac{l}{l+2}\rho_0' g_0\frac{h}{r}C^m_l$$

$$-\frac{\rho_0}{r}\frac{d}{dr}(hg_0)C^m_l + \frac{2}{3}\Omega^2\rho_0' h C^m_l$$

$$E_{4,2} = \lambda'\frac{h}{r}C^m_l + \frac{2}{l+2}\rho_0 g_0\frac{h}{r}C^m_l$$

$$E_{4,3} = -\frac{2l}{l+2}(l^2+3l-1)\mu'\frac{h}{r^2}C^m_l + \frac{l}{l+2}\omega^2\rho_0' h C^m_l$$

$$-\frac{6m}{(l+2)(l+3)}\omega\Omega\rho_0' h C^m_l + 2l\rho_0 g_0\frac{h}{r^2}C^m_l$$

$$E_{4,4} = \frac{3l}{l+2}\mu'\frac{h}{r}C^m_l + \frac{l}{l+2}\frac{d}{dr}(h\mu')C^m_l$$

$$E_{4,5} = \frac{l}{l+2}\rho_0'\frac{h}{r}C^m_l$$

$$E_{4,7} = -\frac{6ml(l+4)}{(l+2)(l+3)}\mu'\frac{h}{r^2}H^m_{l+1} - \frac{2(l+1)}{l+2}\rho_0\omega\Omega H^m_{l+1} + \frac{3m}{(l+2)(l+3)}\omega^2\rho_0' h H^m_{l+1}$$

$$-\frac{2}{(l+2)(l+3)}\omega\Omega\rho_0' h\{l(l+3)G^m_{l+1}C^m_l + [(l+2)(l+3)-3]H^m_{l+1}B^m_{l+2}$$

$$-(l+3)B_{l+1}H^m_{l+1} + (l+2)C_{l+1}G^m_{l+3}\} + 3m\rho_0 g_0\frac{h}{r^2}H^m_{l+1}$$

$$E_{4,8} = \frac{9m}{(l+2)(l+3)}\mu'\frac{h}{r}H^m_{l+1} + \frac{3m}{(l+2)(l+3)}\frac{d}{dr}(h\mu')H^m_{l+1}$$

$$E_{4,9} = \frac{2\mu}{r^2} + 2\mu'\frac{h}{r^2}B^m_{l+2} - \frac{2m}{(l+2)(l+3)}\omega\Omega\rho_0 - \frac{\rho_0 g_0}{r} - \frac{2m}{(l+2)(l+3)}\omega\Omega\rho_0' h B^m_{l+2}$$

$$+\frac{2}{3}\Omega^2\rho_0 - \frac{\rho_0}{r}\frac{d}{dr}(hg_0)B^m_{l+2} - \frac{(l+2)(l+3)-3}{(l+2)(l+3)}\rho_0' g_0\frac{h}{r}B^m_{l+2} + \frac{2}{3}\Omega^2\rho_0' h B^m_{l+2}$$

$$E_{4,10} = \frac{\lambda}{r} + \lambda'\frac{h}{r}B^m_{l+2} + \frac{3}{(l+2)(l+3)}\rho_0 g_0\frac{h}{r}B^m_{l+2}$$

$$E_{4,11} = -2[(l+2)(l+3)-1]\frac{\mu}{r^2} - 2\frac{[(l+2)(l+3)-3][(l+2)(l+3)-4]}{(l+2)(l+3)}\mu'\frac{h}{r^2}B^m_{l+2}$$

$$+\rho_0\omega^2 - \frac{2m}{(l+2)(l+3)}\omega\Omega\rho_0 + \frac{(l+2)(l+3)-3}{(l+2)(l+3)}\omega^2\rho_0' h B^m_{l+2}$$

$$-\frac{6m}{(l+2)(l+3)}\omega\Omega\rho_0' h B^m_{l+2} - \frac{2m}{(l+2)(l+3)}\omega\Omega\rho_0' h - 3\frac{\rho_0 g_0 h}{r^2}B^m_{l+2}$$

$$E_{4,12} = \frac{3\mu}{r} + \mu' + 3\frac{(l+2)(l+3)-3}{(l+2)(l+3)}\mu'\frac{h}{r}B^m_{l+2} + \frac{(l+2)(l+3)-3}{(l+2)(l+3)}\frac{d}{dr}(h\mu')B^m_{l+2}$$

$$E_{4,13} = \frac{\rho_0}{r} + \frac{(l+2)(l+3)-3}{(l+2)(l+3)}\rho_0'\frac{h}{r}B^m_{l+2}$$

$$E_{5,1} = 4\pi G\rho_0$$

$$E_{5,6} = 1$$

$$E_{6,1} = 4\pi G\frac{d}{dr}(h\rho_0')B^m_l$$

$$E_{6,2} = 4\pi G h\rho_0' B^m_l$$

$$E_{6,3} = -4\pi G\rho_0\frac{l(l+1)}{r} + 12\pi G\rho_0'\frac{h}{r}B^m_l$$

$$E_{6,5} = \frac{l(l+1)}{r^2}$$

$$E_{6,6} = -\frac{2}{r}$$

$$E_{6,7} = -12m\pi G\rho_0'\frac{h}{r}G_{l+1}^m$$

$$E_{6,9} = 4\pi G\frac{d}{dr}(h\rho_0')A_{l+2}^m$$

$$E_{6,10} = 4\pi Gh\rho_0'A_{l+2}^m$$

$$E_{6,11} = 8(l+3)\pi G\rho_0'\frac{h}{r}A_{l+2}^m$$

$$E_{7,1} = \frac{1}{r}$$

$$E_{7,8} = 1$$

$$E_{8,1} = \frac{2}{l+1}\omega\Omega\rho_0 H_l^m - \frac{3m}{(l+1)(l+2)}\rho_0' g_0\frac{h}{r}H_l^m$$

$$+\frac{2}{(l+1)(l+2)}\omega\Omega\rho_0' h[(l+2)B_l^m H_l^m - (l+1)C_l^m G_{l+2}^m]$$

$$E_{8,2} = -\frac{3m}{(l+1)(l+2)}\rho_0 g_0\frac{h}{r}H_l^m$$

$$E_{8,3} = -6m\frac{(l-1)(l+3)}{(l+1)(l+2)}\mu'\frac{h}{r^2}H_l^m - \frac{2l}{l+1}\rho_0\omega\Omega H_l^m + \frac{3m}{(l+1)(l+2)}\omega^2\rho_0' h H_l^m$$

$$-\frac{2}{(l+1)(l+2)}\omega\Omega\rho_0' h\{(l-1)(l+2)G_l^m C_{l-1}^m + [(l+1)(l+2)-3]H_l^m B_{l+1}^m$$

$$-(l+2)B_l^m H_l^m + (l+1)C_l^m G_{l+2}^m\}$$

$$E_{8,4} = \frac{9m}{(l+1)(l+2)}\mu'\frac{h}{r}H_l^m + \frac{3m}{(l+1)(l+2)}\frac{d}{dr}(h\mu')H_l^m$$

$$E_{8,5} = \frac{3m}{(l+1)(l+2)}\rho_0'\frac{h}{r}H_l^m$$

$$E_{8,7} = -[(l+1)(l+2)-2]\frac{\mu}{r^2} - \frac{[(l+1)(l+2)-2][(l+1)(l+2)-3]}{(l+1)(l+2)}\mu'\frac{h}{r^2}B_{l+1}^m$$

$$+3\mu'\frac{h}{r^2}B_{l+1}^m + \rho_0\omega^2 - \frac{2m}{(l+1)(l+2)}\omega\Omega\rho_0 + \frac{(l+1)(l+2)-3}{(l+1)(l+2)}\omega^2\rho_0' h B_{l+1}^m$$

$$-\frac{6m}{(l+1)(l+2)}\omega\Omega\rho_0' h B_{l+1}^m - \frac{2m}{(l+1)(l+2)}\omega\Omega\rho_0' h$$

$$E_{8,8} = \frac{3\mu}{r} + \mu' + 3\frac{(l+1)(l+2)-3}{(l+1)(l+2)}\mu'\frac{h}{r}B_{l+1}^m + \frac{(l+1)(l+2)-3}{(l+1)(l+2)}\frac{d}{dr}(h\mu')B_{l+1}^m$$

$$E_{8,9} = -\frac{2}{l+2}\rho_0\omega\Omega G_{l+2}^m - \frac{3m}{(l+1)(l+2)}\rho_0' g_0\frac{h}{r}G_{l+2}^m$$

$$+\frac{2}{(l+1)(l+2)}\omega\Omega\rho_0' h[(l+2)A_{l+2}^m H_l^m - (l+1)B_{l+2}^m G_{l+2}^m]$$

$$E_{8,10} = -\frac{3m}{(l+1)(l+2)}\rho_0 g_0\frac{h}{r}G_{l+2}^m$$

$$E_{8,11} = -\frac{6ml(l+4)}{(l+1)(l+2)}\mu'\frac{h}{r^2}G_{l+2}^m - \frac{2(l+3)}{l+2}\omega\Omega\rho_0 G_{l+2}^m + \frac{3m}{(l+1)(l+2)}\omega^2\rho_0' h G_{l+2}^m$$

$$-\frac{2}{(l+1)(l+2)}\omega\Omega\rho_0' h\{[(l+1)(l+2)-3]G_{l+2}^m B_{l+1}^m + (l+1)(l+4)H_{l+2}^m A_{l+3}^m$$

$$-(l+2)A_{l+2}^m H_l^m + (l+1)B_{l+2}^m G_{l+2}^m\}$$

$$E_{8,12} = \frac{9m}{(l+1)(l+2)}\mu'\frac{h}{r}G_{l+2}^m + \frac{3m}{(l+1)(l+2)}\frac{d}{dr}(h\mu')G_{l+2}^m$$

$$E_{8,13} = \frac{3m}{(l+1)(l+2)}\rho_0'\frac{h}{r}G_{l+3}^m$$

$$E_{9,9} = -\frac{2}{r}$$

$$E_{9,10} = 1$$

$$E_{9,11} = \frac{(l+2)(l+3)}{r}$$

$$E_{10,1} = -2l(l+1)\frac{\mu}{r^2} - 4\frac{\mu'}{r} - 2l(l+1)\mu'\frac{h}{r^2}B_l^m - 4\frac{1}{r}\frac{d}{dr}(h\mu')B_l^m + \rho_0\omega^2 - \rho_0\frac{dg_0}{dr}$$

$$+\frac{2\rho_0 g_0}{r} + 4\pi G\rho_0^2 + \omega^2\rho_0' h B_l^m + 4\pi G\rho_0\rho_0' h B_l^m + \frac{2}{r}\frac{d}{dr}(\rho_0 g_0 h)B_l^m$$

$$-\frac{2}{3}\Omega^2\rho_0 - \rho_0\frac{d^2}{dr^2}(hg_0)B_l^m + 3\rho_0 g_0\frac{h}{r^2}B_l^m - \rho_0' h\frac{dg_0}{dr}B_l^m - \frac{2}{3}\Omega^2\rho_0' h B_l^m$$

$$E_{10,2} = \lambda' + 2\mu' + \frac{d}{dr}(h\lambda')B_l^m + 2\frac{d}{dr}(h\mu')B_l^m$$

$$E_{10,3} = 2l(l+1)\frac{\mu}{r^2} + 2l(l+1)\frac{\mu'}{r} + 2l(l+1)\mu'\frac{h}{r^2}B_l^m + \frac{2l(l+1)}{r}\frac{d}{dr}(h\mu')B_l^m$$

$$-2m\rho_0\omega\Omega - l(l+1)\frac{\rho_0 g_0}{r} - 2m\omega\Omega\rho_0' h B_l^m - \frac{l(l+1)}{r}\frac{d}{dr}(\rho_0 g_0 h)B_l^m$$

$$+\frac{2}{3}l(l+1)\Omega^2\rho_0 - 3\rho_0\frac{d}{dr}(\frac{hg_0}{r})B_l^m - 3\rho_0 g_0\frac{h}{r^2}B_l^m + \frac{2[l(l+3)-3]}{3}\Omega^2\rho_0' h B_l^m$$

$$E_{10,4} = l(l+1)\frac{\mu}{r} + (l^2+l+3)\mu'\frac{h}{r}B_l^m - 3\rho_0 g_0\frac{h}{r}B_l^m$$

$$E_{10,6} = \rho_0 + \rho_0' h B_l^m$$

$$E_{10,7} = 2(l+2)\omega\Omega\rho_0 G_{l+1}^m + 2\omega\Omega\rho_0' h[(l+2)G_{l+1}^m B_l^m - (l+1)H_{l+1}^m A_{l+2}^m]$$

$$+3m\rho_0\frac{d}{dr}(\frac{hg_0}{r})G_{l+1}^m + 3m\rho_0 g_0\frac{h}{r^2}G_{l+1}^m + 2m\Omega^2\rho_0' h G_{l+1}^m$$

$$E_{10,8} = -3m\mu'\frac{h}{r}G_{l+1}^m + 3m\rho_0 g_0\frac{h}{r}G_{l+1}^m$$

$$E_{10,9} = -2(l+2)(l+3)\mu'\frac{h}{r_2}A_{l+2}^m - \frac{4}{r}\frac{d}{dr}(h\mu')A_{l+2}^m + \omega^2\rho_0' h A_{l+2}^m + 4\pi G\rho_0\rho_0' h A_{l+2}^m$$

$$+\frac{2}{r}\frac{d}{dr}(\rho_0 g_0 h)A_{l+2}^m - \rho_0\frac{d^2}{dr^2}(hg_0)A_{l+2}^m + 2(l+3)\rho_0 g_0\frac{h}{r^2}A_{l+2}^m - \rho_0' h\frac{dg_0}{dr}A_{l+2}^m$$

$$-\frac{2}{3}\Omega^2\rho_0' h A_{l+2}^m$$

$$E_{10,10} = \frac{d}{dr}(h\lambda')A_{l+2}^m + 2\frac{d}{dr}(h\mu')A_{l+2}^m$$

$$E_{10,11} = 2(l+2)(l+3)\mu'\frac{h}{r_2}A_{l+2}^m + \frac{2(l+2)(l+3)}{r}\frac{d}{dr}(h\mu')A_{l+2}^m - 2m\omega\Omega\rho_0' h A_{l+2}^m$$

$$-\frac{(l+2)(l+3)}{r}\frac{d}{dr}(\rho_0 g_0 h)A_{l+2}^m - 2(l+3)\rho_0\frac{d}{dr}(\frac{hg_0}{r})A_{l+2}^m$$

$$-2(l+3)\rho_0 g_0\frac{h}{r^2}A_{l+2}^m + \frac{2l(l+3)}{3}\Omega^2\rho_0' h A_{l+2}^m$$

$$E_{10,12} = (l+3)(l+4)\mu'\frac{h}{r}A^m_{l+2} - 2(l+3)\rho_0 g_0 \frac{h}{r}A^m_{l+2}$$

$$E_{10,14} = \rho_0' h A^m_{l+2}$$

$$E_{11,9} = -\frac{1}{r}$$

$$E_{11,11} = \frac{1}{r}$$

$$E_{11,12} = 1$$

$$E_{12,1} = \frac{2\mu}{r^2} + 2\mu'\frac{h}{r^2}B^m_l - \frac{2m}{l(l+1)}\omega\Omega\rho_0 - \frac{\rho_0 g_0}{r} - \frac{2m}{l(l+1)}\omega\Omega\rho_0' h B^m_l$$
$$+\frac{2}{3}\Omega^2\rho_0 - \frac{l(l+1)-3}{l(l+1)}\rho_0' g_0 \frac{h}{r}B^m_l - \frac{\rho_0}{r}\frac{d}{dr}(hg_0)B^m_l + \frac{2}{3}\Omega^2\rho_0' h B^m_l$$

$$E_{12,2} = \frac{\lambda}{r} + \lambda'\frac{h}{r} + \frac{3}{l(l+1)}\rho_0 g_0 \frac{h}{r}B^m_l$$

$$E_{12,3} = -2[l(l+1)-1]\frac{\mu}{r^2} - 2\frac{[l(l+1)-3][l(l+1)-4]}{l(l+1)}\mu'\frac{h}{r^2}B^m_l + \rho_0\omega^2$$
$$-\frac{2m}{l(l+1)}\omega\Omega\rho_0 + \frac{l(l+1)-3}{l(l+1)}\omega^2\rho_0' h B^m_l - \frac{6m}{l(l+1)}\omega\Omega\rho_0' h B^m_l$$
$$-\frac{2m}{l(l+1)}\omega\Omega\rho_0' h - 3\frac{\rho_0 g_0 h}{r^2}B^m_l$$

$$E_{12,4} = \frac{3\mu}{r} + \mu' + 3\frac{l(l+1)-3}{l(l+1)}\mu'\frac{h}{r}B^m_l + \frac{l(l+1)-3}{l(l+1)}\frac{d}{dr}(h\mu')B^m_l$$

$$E_{12,5} = \frac{\rho_0}{r} + \frac{l(l+1)-3}{l(l+1)}\rho_0'\frac{h}{r}B^m_l$$

$$E_{12,7} = -6m\frac{(l-1)(l+3)}{l(l+1)}\mu'\frac{h}{r^2}G^m_{l+1} - 2\frac{l(l+2)}{l(l+1)}\rho_0\omega\Omega G^m_{l+1} + \frac{3m}{l(l+1)}\omega^2\rho_0' h G^m_{l+1}$$
$$-\frac{2}{l(l+1)}\omega\Omega\rho_0' h\{l(l+3)H^m_{l+1}A^m_{l+2} + [l(l+1)-3]G^m_{l+1}B^m_l - (l+1)A^m_{l+1}H^m_{l-1}$$
$$+lB^m_{l+1}G^m_{l+1}\} + 3m\frac{\rho_0 g_0 h}{r^2}G^m_{l+1}$$

$$E_{12,8} = \frac{9m}{l(l+1)}\mu'\frac{h}{r}G^m_{l+1} + \frac{3m}{l(l+1)}\frac{d}{dr}(h\mu')G^m_{l+1}$$

$$E_{12,9} = 2\mu'\frac{h}{r^2}A^m_{l+2} - \frac{2m\omega\Omega}{l(l+1)}\rho_0' h A^m_{l+2} - \frac{l+3}{l+1}\rho_0' g_0 \frac{h}{r}A^m_{l+2} - \frac{\rho_0}{r}\frac{d}{dr}(hg_0)A^m_{l+2}$$
$$+\frac{2}{3}\Omega^2\rho_0' h A^m_{l+2}$$

$$E_{12,10} = \lambda'\frac{h}{r}A^m_{l+2} - \frac{2}{l+1}\rho_0 g_0 \frac{h}{r}A^m_{l+2}$$

$$E_{12,11} = -\frac{2(l+3)}{l+1}(l^2+3l-1)\mu'\frac{h}{r^2}A^m_{l+2} + \frac{l+3}{l+1}\omega^2\rho_0' h A^m_{l+2}$$
$$-\frac{6m}{l(l+1)}\omega\Omega\rho_0' h A^m_{l+2} - 2(l+3)\rho_0 g_0 \frac{h}{r^2}A^m_{l+2}$$

$$E_{12,12} = \frac{3(l+3)}{l+1}\mu'\frac{h}{r}A^m_{l+2} + \frac{l+3}{l+1}\frac{d}{dr}(h\mu')A^m_{l+2}$$

$$E_{12,13} = \frac{l+3}{l+1}\rho_0'\frac{h}{r}A^m_{l+2}$$

$$E_{13,9} = 4\pi G\rho_0$$

$$E_{13,14} = 1$$

$$E_{14,1} = 4\pi G\frac{d}{dr}(h\rho_0')C^m_l$$

$$E_{14,2} = 4\pi G h\rho_0' C^m_l$$

$$E_{14,3} = -8l\pi G\rho_0'\frac{h}{r}C^m_l$$

$$E_{14,7} = -12m\pi G\rho_0'\frac{h}{r}H^m_{l+1}$$

$$E_{14,9} = 4\pi G\frac{d}{dr}(h\rho_0')B^m_{l+2}$$

$$E_{14,10} = 4\pi G h\rho_0' B^m_{l+2}$$

$$E_{14,11} = -4\pi G\rho_0\frac{(l+2)(l+3)}{r} + 12\pi G\rho_0'\frac{h}{r}B^m_{l+2}$$

$$E_{14,13} = \frac{(l+2)(l+3)}{r^2}$$

$$E_{14,14} = -\frac{2}{r}$$

Appendix B Continuity Conditions at Ellipsoidal Core Boundaries

Results of the first section (**B.1**) of this appendix will be used in the second section (**B.2**) of this appendix.

B.1 Coefficients of the 4th Order System of Ordinary Differential Equations in the Spherically-Stratified Rotating Liquid Core

In a spherically stratified liquid core, there are 4 governing differential equations of degree n linear in modified AJP variables y_1, y_2, y_5 and y_6 (cf. §7.4)

$$\frac{dy_i}{dr} = a_{i,1}y_1 + a_{i,2}y_2 + a_{i,3}y_3 + a_{i,5}y_5 + a_{i,6}y_6 \tag{B.1}$$

$$i = 1, 2, 5, 6$$

and one algebraic equation for y_3

$$y_3 = -\frac{1}{a_{4,3}}[a_{4,1}y_1 + a_{4,2}y_2 + a_{4,5}y_5] \tag{B.2}$$

where the non-zero $a_{i,j}$ are

$$a_{1,1} = -\frac{2}{r}$$

$$a_{1,2} = 1$$

$$a_{1,3} = \frac{n(n+1)}{r}$$

$$a_{2,1} = -\frac{1}{\lambda}[\omega^2\rho_0 + \frac{4\rho_0 g_0}{r}]$$

$$a_{2,2} = -\frac{1}{\lambda}\frac{d\lambda}{dr}$$

$$a_{2,3} = -\frac{1}{\lambda}[-2m\omega\Omega\rho_0 - n(n+1)\frac{\rho_0 g_0}{r}]$$

$$a_{2,6} = -\frac{1}{\lambda}\rho_0$$

$$a_{4,1} = -\frac{2m\omega\Omega}{n(n+1)}\rho_0 - \frac{\rho_0 g_0}{r}$$

$$a_{4,2} = \frac{\lambda}{r}$$

$$a_{4,3} = \omega^2\rho_0 - \frac{2m\omega\Omega}{n(n+1)}\rho_0$$

$$a_{4,5} = \frac{\rho_0}{r}$$

$$a_{5,1} = 4\pi G\rho_0$$

$$a_{5,6} = 1$$

$$a_{6,3} = -4\pi G\rho_0\frac{n(n+1)}{r}$$

$$a_{6,5} = \frac{n(n+1)}{r^2}$$

$$a_{6,6} = -\frac{2}{r}.$$

For deriving some quantities which will be used in the ellipsoidal boundary conditions of §8.2, I will modify these governing equations of the spherical liquid core, with the field variable y_2 replaced by χ_1^m and y_6 replaced by $(dy_5/dr)_{a_+}$. Recall that y_2 is defined slightly differently in §7.4 from the original definition of AJP. By comparing with (62) and (63) of §3.2, it can be written for $n = 1$

$$y_2 = -\frac{1}{\alpha^2}[\chi_1^m + y_5 - g_0 y_1] \tag{B.3}$$

therefore,

$$\chi_1^m = -\alpha^2 y_2 + g_0 y_1 - y_5. \tag{B.4}$$

Substituting (B.3) into (B.2); substituting the resulting expression and (B.3) into dy_2/dr of (B.1), the latter can then be expressed in terms of the variables y_1, χ_1^m, y_5 and y_6, i.e. y_2 is replaced by χ_1^m

$$\frac{dy_2}{dr} = T_{2,1} y_1 + T_{2,2}\chi_1^m + T_{2,3} y_5 + T_{2,4} y_6 \tag{B.5}$$

where

$$T_{2,1} = a_{2,1} + \frac{g_0}{\alpha^2}[a_{2,2} - \frac{a_{2,3}a_{4,2}}{a_{4,3}}] - \frac{a_{2,3}a_{4,1}}{a_{4,3}}$$

$$T_{2,2} = -\frac{1}{\alpha^2}[a_{2,2} - \frac{a_{2,3}a_{4,2}}{a_{4,3}}]$$

$$T_{2,3} = -\frac{a_{2,3}a_{4,5}}{a_{4,3}} - \frac{1}{\alpha^2}[a_{2,2} - \frac{a_{2,3}a_{4,2}}{a_{4,3}}]$$

$$T_{2,4} = a_{2,6}$$

Next, taking the first derivative of equation (B.4) to get $d\chi_1^m/dr$, substituting (B.5) into the resulting expression, and making the necessary substitutions for y_2 and y_3 in dy_5/dr, as well as in dy_6/dr of (B.1), the governing equations of degree 1 can be expressed in terms of variables y_1, χ_1^m, y_5 and y_6

$$\frac{dy_1}{dr} = e_{1,1} y_1 + e_{1,2}\chi_1^m + e_{1,3} y_5 \tag{B.6}$$

$$\frac{dx_1^m}{dr} = e_{2,1}y_1 + e_{2,2}x_1^m + e_{2,3}y_5 + e_{2,4}y_6 \tag{B.7}$$

$$\frac{dy_5}{dr} = e_{3,1}y_1 + e_{3,4}y_6 \tag{B.8}$$

$$\frac{dy_6}{dr} = e_{4,1}y_1 + e_{4,2}x_1^m + e_{4,3}y_5 + e_{4,4}y_6 \tag{B.9}$$

where

$$e_{1,1} = a_{1,1} + (a_{1,2} - \frac{a_{1,3}a_{4,2}}{a_{4,3}})\frac{g_0}{\alpha^2} - \frac{a_{1,3}a_{4,1}}{a_{4,3}}$$

$$e_{1,2} = -\frac{1}{\alpha^2}(a_{1,2} - \frac{a_{1,3}a_{4,2}}{a_{4,3}}g_0)$$

$$e_{1,3} = -\frac{1}{\alpha^2}(a_{1,2} + \frac{a_{1,3}a_{4,2}}{a_{4,3}}) - \frac{a_{4,5}a_{1,3}}{a_{4,3}}$$

$$e_{2,1} = -\frac{2g_0}{\alpha}\frac{d\alpha}{dr} - \alpha^2 T_{2,1} + \frac{dg_0}{dr} + g_0 e_{1,1} - a_{5,1}$$

$$e_{2,2} = -\frac{2}{\alpha}\frac{d\alpha}{dr} - \alpha^2 T_{2,2} + g_0 e_{1,2}$$

$$e_{2,3} = -\frac{2}{\alpha}\frac{d\alpha}{dr} - \alpha^2 T_{2,3} + g_0 e_{1,3}$$

$$e_{2,4} = -\alpha^2 T_{2,4} - a_{5,6}$$

$$e_{3,1} = a_{5,1}$$

$$e_{3,4} = a_{5,6}$$

$$e_{4,1} = -\frac{a_{6,3}}{a_{4,3}}[a_{4,1} + \frac{g_0}{\alpha^2}a_{4,2}]$$

$$e_{4,2} = \frac{1}{\alpha^2}\frac{a_{4,2}c_{6,3}}{a_{4,3}}$$

$$e_{4,3} = -\frac{a_{6,3}}{a_{4,3}}(-\frac{a_{4,2}}{\alpha^2} + a_{4,5}) + a_{6,5}$$

$$e_{4,4} = a_{6,6}.$$

With above equations and definitions, the second derivative of y_5, which is needed in the boundary conditions at the ICB, can be obtained readily

$$(\frac{d^2y_5}{dr^2})_{a_+} = F_{3,1}y_1 + F_{3,2}\chi_1^m + F_{3,3}y_5 + F_{3,4}y_6. \tag{B.10}$$

However,

$$y_6 = -a_{5,1}y_1 + \frac{dy_5}{dr} \tag{B.11}$$

therefore,

$$(\frac{d^2y_5}{dr^2})_{a_+} = (F_{3,1} - a_{5,1}F_{3,4})y_1(a_+) + F_{3,2}\chi_1^m(a_+) + F_{3,3}y_5(a_+)$$

$$+F_{3,4}(\frac{dy_5}{dr})_{a_+} \tag{B.12}$$

where

$$F_{3,1} = \frac{da_{5,1}}{dr} + a_{5,1}e_{1,1} + e_{4,1}$$

$$F_{3,2} = a_{5,1}e_{1,2} + e_{4,2}$$

$$F_{3,3} = a_{5,1}e_{1,3} + e_{4,3}$$

$$F_{3,4} = e_{4,4}.$$

Substituting (B.11) into (B.7), the expression for $d\chi_1^m/dr$ is obtained

$$\frac{d\chi_1^m}{dr} = (e_{2,1} - a_{5,1}e_{2,4})y_1(a_-) + e_{2,2}\chi_1^m(a_+) + e_{2,3}y_5(a_+) + e_{2,4}(\frac{dy_5}{dr})_{a_+}. \tag{B.13}$$

The corresponding degree 3 quantities can be obtained in a similar manner. Therefore, for $n = 3$

$$y_{10} = -\rho_0[\chi_3^m + y_{13} - g_0 y_9] \tag{B.14}$$

$$\chi_3^m = -\frac{1}{\rho_{11}} y_{10} + g_0 y_9 - y_{13} \tag{B.15}$$

and

$$(\frac{d^2 y_{13}}{dr^2})_{a_+} = (F_{7,5} - F_{7,8} a_{13,9}) y_9(a_+) + F_{7,8} \chi_3^m(a_+)$$

$$+ F_{7,7} y_{13}(a_+) + F_{7,8}(\frac{dy_{13}}{dr})_{a_+} \tag{B.16}$$

$$\frac{d\chi_3^m}{dr} = (e_{8,5} - a_{13,9} e_{8,8}) y_9(a_+) + e_{8,8} \chi_3^m(a_+) + e_{8,7} y_{13}(a_+)$$

$$+ e_{8,8}(\frac{dy_{13}}{dr})_{a_+} \tag{B.17}$$

where

$$F_{7,5} = \frac{da_{13,9}}{dr} + a_{13,9} e_{5,5} + e_{8,5}$$

$$F_{7,8} = a_{13,9} e_{5,8} + e_{8,2}$$

$$F_{7,7} = a_{13,9} e_{5,7} + e_{8,7}$$

$$F_{7,8} = e_{8,8}$$

$$e_{5,5} = a_{9,9} + (a_{9,10} - \frac{a_{9,11} a_{12,10}}{a_{12,11}}) \frac{g_0}{\alpha^2} - \frac{a_{9,11} a_{12,9}}{a_{12,11}}$$

$$e_{5,8} = -\frac{1}{\alpha^2}(a_{9,10} - \frac{a_{9,11} a_{12,10}}{a_{12,11}} g_0)$$

$$e_{5,7} = -\frac{1}{\alpha^2}(a_{9,10} + \frac{a_{9,11}a_{12,10}}{a_{12,11}}) - \frac{a_{12,13}a_{9,11}}{a_{12,11}}$$

$$e_{6,5} = -\frac{2g_0}{\alpha}\frac{d\alpha}{dr} - \alpha^2 T_{6,5} + \frac{dg_0}{dr} + g_0 e_{5,5} - a_{12,9}$$

$$e_{6,6} = -\frac{2}{\alpha}\frac{d\alpha}{dr} - \alpha^2 T_{6,6} + g_0 e_{5,6}$$

$$e_{6,7} = -\frac{2}{\alpha}\frac{d\alpha}{dr} - \alpha^2 T_{6,7} + g_0 e_{5,7}$$

$$e_{6,8} = -\alpha^2 T_{6,8} - a_{13,14}$$

$$e_{7,5} = a_{13,9}$$

$$e_{7,8} = a_{13,14}$$

$$e_{8,5} = -\frac{a_{14,11}}{a_{12,11}}[a_{12,9} + \frac{g_0}{\alpha^2}a_{12,10}]$$

$$e_{8,6} = \frac{1}{\alpha^2}\frac{a_{12,10}a_{14,11}}{a_{12,11}}$$

$$e_{8,7} = -\frac{a_{14,11}}{a_{12,11}}(-\frac{a_{12,10}}{\alpha^2} + a_{12,13}) + a_{14,13}$$

$$e_{8,8} = a_{14,14}$$

$$T_{6,5} = a_{10,9} + \frac{g_0}{\alpha^2}[a_{10,10} - \frac{a_{10,11}a_{12,10}}{a_{12,11}}] - \frac{a_{10,11}a_{12,9}}{a_{12,11}}$$

$$T_{6,6} = -\frac{1}{\alpha^2}[a_{10,10} - \frac{a_{10,11}a_{12,10}}{a_{12,11}}]$$

$$T_{6,7} = -\frac{a_{10,11}a_{12,13}}{a_{12,11}} - \frac{1}{\alpha^2}[a_{10,10} - \frac{a_{10,11}a_{12,10}}{a_{12,11}}]$$

$$T_{6,8} = a_{10,14}.$$

B.2 Analysis of Continuity Conditions Across an Ellipsoidal Inner Core Boundary

I have listed in §8.2 the initial formulations of the boundary conditions at the ellipsoidal ICB. They are equations (328), (329), (330), (331), (332) and (333).

Now, substituting (326) and (327) in the LHS of (328), expanding the resulting expression in Taylor series (dropping quantities smaller than the first order in the ellipticity), and using the linear independence of, and recurrence relations among, the associated Legendre functions of different degree, the normal displacement on the solid side of the ICB can then be written as:

$$[\hat{\mathbf{n}} \cdot \mathbf{u}]_{a-} = \sum_{n=1}^{\infty} [\hat{\mathbf{n}} \cdot \mathbf{u}]_{a-}^{m,n} e^{im\phi} \tag{B.18}$$

where

$$[\hat{\mathbf{n}} \cdot \mathbf{u}]_{a-}^{m,n} = u_n^m P_n^m + \frac{h}{a} v_n^m [2(n+1) A_n^m P_{n-2}^m + 3 B_n^m P_n^m - 2n C_n^m P_{n+2}^m]$$

$$-3m\frac{h}{a} i t_n^m [J_n^m P_{n-1}^m + H_n^m P_{n+1}^m] - h \frac{du_n^m}{dr} [A_n^m P_{n-2}^m + B_n^m P_n^m + C_n^m P_{n+2}^m] \tag{B.19}$$

where A_n^m, B_n^m, C_n^m are defined in (261), (262) and (263), and J_n^m and H_n^m are defined in (126) and (127) respectively. For $n = 1$ and $n = 3$, (B.18) gives rise to two equations linear in y_i's

$$[\hat{\mathbf{n}} \cdot \mathbf{u}]_{a-}^{m,1} = \sum_{i=1}^{7} Q_{2,i} y_i \tag{B.20}$$

$$[\hat{\mathbf{n}} \cdot \mathbf{u}]_{a-}^{m,3} = \sum_{i=7}^{11} Q_{5,i} y_i \tag{B.21}$$

where the non-zero $Q_{i,j}$ are

$$Q_{2,1} = P_1^m - hE_{1,1}(B_1^m P_1^m + C_1^m P_3^m),$$

$$Q_{2,2} = -hE_{1,2}(B_1^m P_1^m + C_1^m P_3^m)$$

$$Q_{2,3} = \frac{h}{a}(3B_1^m P_1^m - 2C_1^m P_3^m) - hE_{1,3}(B_1^m P_1^m + C_1^m P_3^m)$$

$$Q_{2,7} = -3m\frac{h}{a}H_1^m P_2^m$$

$$Q_{5,7} = -3m\frac{h}{a}J_3^m P_2^m$$

$$Q_{5,9} = P_3^m - hE_{9,9}(A_3^m P_1^m + B_3^m P_3^m)$$

$$Q_{5,10} = -hE_{9,10}(A_3^m P_1^m + B_3^m P_3^m)$$

$$Q_{5,11} = \frac{h}{a}(8A_3^m P_1^m + 3B_3^m P_3^m) - hE_{9,11}(A_3^m P_1^m + B_3^m P_3^m)$$

where $E_{i,j}$'s are from Appendix A. Note that the above procedure will be applied to all the boundary conditions.

Similarly, LHS or RHS of (329) will be defined as

$$[V_1]_a = \sum_{n=1}^{\infty}[V_1]_a^{m,n}e^{im\phi} \tag{B.22}$$

where

$$[V_1]_a^{m,n} = \Phi_n^m P_n^m - h\frac{d\Phi_n^m}{dr}[A_n^m P_{n-2}^m + B_n^m P_n^m + C_n^m P_{n+2}^m] \tag{B.23}$$

Then, the following relations will be found from (329) for $n = 1$ and $n = 3$:

$$\Phi_1^m(a_+) = h(A_3^m\frac{d\Phi_1^m}{dr} + B_1^m\frac{d\Phi_1^m}{dr})_{a_+} + \Phi_1^m(a_-) - h(A_3^m\frac{d\Phi_1^m}{dr} + B_1^m\frac{d\Phi_1^m}{dr})_{a_-} \tag{B.24}$$

$$\Phi_3^m(a_+) = h(B_3^m \frac{d\Phi_3^m}{dr} + C_1^m \frac{d\Phi_1^m}{dr})_{a_-} + \Phi_3^m(a_-) - h(B_3^m \frac{d\Phi_3^m}{dr} + C_1^m \frac{d\Phi_1^m}{dr})_{a_-} \tag{B.25}$$

using the linear independence of the associated Legendre functions.

Using the boundary conditions (328) and (B.23), the equation (330) (boundary conditions (III)) can be written

$$[\hat{\mathbf{n}} \cdot \nabla V_1]_{a_-} - [\hat{\mathbf{n}} \cdot \nabla V_1]_{a_+} = -4\pi G \, \Delta\rho_0 \, [\hat{\mathbf{n}} \cdot \mathbf{u}]_{a_-} \tag{B.26}$$

where

$$\Delta\rho_0 = \rho_0(a_+) - \rho_0(a_-) \tag{B.27}$$

The expression (B.26) will be expanded explicitly, using the linear independence of, and recurrence relations among, the associated Legendre functions, as:

$$[\frac{d\Phi_n^m(a_-)}{dr} - \frac{d\Phi_n^m(a_+)}{dr}]P_n^m + \frac{h}{r^2}[\Phi_n^m(a_-) - \Phi_n^m(a_+)][2(n+1)A_n^m P_{n-2}^m + 3B_n^m P_n^m$$

$$-2nC_n^m P_{n+2}^m] - h[\frac{d^2\Phi_n^m(a_-)}{dr^2} - \frac{d^2\Phi_n^m(a_+)}{dr^2}](A_n^m P_{n-2}^m + B_n^m P_n^m + C_n^m P_{n+2}^m)$$

$$= -4\pi G \, \Delta\rho_0 \, [\hat{\mathbf{n}} \cdot \mathbf{u}]_{a_-}^{m,n}. \tag{B.28}$$

Since $\Phi_n^m(a_-) - \Phi_n^m(a_+) = 0$ to first order in the ellipticity, the second term on the LHS of equation (B.28) is of second order, and thus can be ignored. In the third term on the LHS of equation (B.28), the quantities $(d^2\Phi_n^m/dr^2)_{a_-}$ and $(d^2\Phi_n^m/dr^2)_{a_+}$ are needed only to zero'th order in the ellipticity. Therefore, they are equivalent to d^2y_5/dr^2 and d^2y_{13}/dr^2 of (B.12) and (B.16) in Section **B.1** of this appendix. Since y_1, y_9, y_5 and y_{13} in equations (B.12) and (B.16) all are zero'th order quantities, they are continuous across the ICB and can be replaced by those of the solid inner core.

It is desirable at this point to write down some spherical solid inner core quantities which will be used in the derivations of the boundary conditions at the ICB, in terms of the modified dimensionless AJP variables:

$$\frac{dy_1}{dr} = aE_{1,1}y_1 + y_2 + aE_{1,3}y_3 \tag{B.29}$$

$$\frac{dy_9}{dr} = aE_{9,9}y_9 + y_{10} + aE_{9,11}y_{11} \tag{B.30}$$

$$\frac{dy_2}{dr} = \sum_{i=1}^{14} A^0_{2,i}y_i \tag{B.31}$$

$$\frac{dy_{10}}{dr} = \sum_{i=1}^{14} A^0_{10,i}y_i \tag{B.32}$$

where $A^0_{i,j}$ are the coefficients of the modified governing differential equations for a spherical inner core. Therefore, $A^0_{i,j} = A_{i,j}(\epsilon = 0)$, and the latter are derived in §7.4. By using (B.31), (B.32), and the expression for dy_3/dr and dy_{11}/dr (cf. §7.4 and **B.1** of this appendix), the second derivative of y_1 and y_9 can be obtained

$$\frac{d^2y_1}{dr^2} = \sum_{i=1}^{14} \xi_{1,i}y_i \tag{B.33}$$

$$\frac{d^2y_9}{dr^2} = \sum_{i=1}^{14} \xi_{4,i}y_i \tag{B.34}$$

where

$$\xi_{1,i} = a(\frac{dE_{1,1}}{dr} + E^2_{1,1} + E_{1,3}E_{3,1})\delta_{i,1} + E_{1,1}\delta_{i,2} + a(\frac{dE_{1,3}}{dr} + E_{1,1}E_{1,3} + E_{1,3}E_{3,3})\delta_{i,3}$$

$$+E_{1,3}\delta_{i,4} + w(i)A^0_{1,i}$$

$$\xi_{4,i} = a(\frac{dE_{9,9}}{dr} + E^2_{9,9} + E_{9,11}E_{11,9})\delta_{i,9} + E_{9,9}\delta_{i,10}$$

$$+a(\frac{dE_{9,11}}{dr} + E_{9,9}E_{9,11} + E_{9,11}E_{11,11})\delta_{i,11} + E_{9,11}\delta_{i,12} + w(i)A^0_{10,i}$$

where $w(i)$'s are factors arising from changing the y_i's from the dimensioned quantities to the dimensionless ones according to the relation (287) of §8.1, e.g. $w(1) = a$, $w(5) = ag_0(a)$, etc. Similarly

$$\frac{dy_5}{dr} = aE_{5,1}y_1 + g_0(a)y_6 \tag{B.35}$$

$$\frac{dy_{13}}{dr} = aE_{13,9}y_9 + g_0(a)y_{14} \tag{B.36}$$

$$(\frac{d^2y_5}{dr^2})_{a_-} = \sum_{i=1}^{6} \xi_{2,i}y_i \tag{B.37}$$

$$(\frac{d^2y_{13}}{dr^2})_{a_-} = \sum_{i=9}^{14} \xi_{5,i}y_i \tag{B.38}$$

where

$$\xi_{2,i} = a(\frac{dE_{5,1}}{dr} + E_{1,1}E_{5,5})\delta_{i,1} + E_{1,2}E_{5,1}\delta_{i,2} + a(E_{1,3}E_{5,1} + E_{6,3})\delta_{i,3}$$

$$+ag_0(a)E_{6,5}\delta_{i,5} + g_0(a)E_{6,6}\delta_{i,6}$$

$$\xi_{5,i} = a(\frac{dE_{13,9}}{dr} + E_{9,9}E_{13,13})\delta_{i,9} + E_{9,10}E_{13,9}\delta_{i,10} + a(E_{9,11}E_{13,9} + E_{14,11})\delta_{i,11}$$

$$+ag_0(a)E_{14,13}\delta_{i,13} + g_0(a)E_{14,14}\delta_{i,14}.$$

Substituting (B.12), (B.16), (B.20), (B.21), (B.35), (B.36), (B.37) and (B.38) into equation (B.28), moving all the terms involving solid inner core quantities to the LHS, moving all the terms involving liquid core quantities to the RHS of (B.28), and using the dimensionless AJP variables in the inner core, equation (B.28) can then be written for $n = 1$ and $n = 3$ as

$$\sum_{i=1}^{14} \Pi_{2,i}^m y_i(a_-) = \frac{1}{g_0(a)}[g_{2,1}\chi_1^m + g_{2,2}\chi_3^m + g_{2,3}(\frac{dy_5}{dr})_{a_+} + g_{2,4}(\frac{dy_{13}}{dr})_{a_+}] \tag{B.39}$$

$$\sum_{i=1}^{14} \Pi_{5,i}^m y_i(a_-) = \frac{1}{g_0(a)}[g_{5,1}\chi_1^m + g_{5,2}\chi_3^m + g_{5,3}(\frac{dy_5}{dr})_{a_+} + g_{5,4}(\frac{dy_{13}}{dr})_{a_+}] \tag{B.40}$$

where

$$\Pi^m_{2,i} = \frac{4\pi G}{g_0(a)}\Delta\rho_0 Q_{2,i} + \frac{a}{g_0(a)}E_{5,1}\delta_{i,5} + \delta_{i,8} - \frac{h}{g_0(a)}(A^m_3\xi_{5,i} + B^m_1\xi_{2,i})$$

$$+\frac{ha}{g_0(a)}\{B^m_1[(F_{3,1} - F_{3,4}a_{5,1})\delta_{i,1} + F_{3,3}g_0(a)\delta_{i,5}]$$

$$+A^m_3[(F_{7,5} - F_{7,8}a_{13,9})\delta_{i,9} + F_{7,7}g_0(a)\delta_{i,13}]\}$$

$$\Pi^m_{5,i} = \frac{4\pi G}{g_0(a)}\Delta\rho_0 Q_{5,i} + \frac{a}{g_0(a)}E_{13,9}\delta_{i,9} + \delta_{i,14} - \frac{h}{g_0(a)}(B^m_3\xi_{5,i} + C^m_1\xi_{2,i})$$

$$+\frac{ha}{g_0(a)}\{C^m_1[(F_{3,1} - F_{3,4}a_{5,1})\delta_{i,1} + F_{3,3}g_0(a)\delta_{i,5}]$$

$$+B^m_3[(F_{7,5} - F_{7,8}a_{13,9})\delta_{i,9} + F_{7,7}g_0(a)\delta_{i,13}]\}$$

$$g_{2,1} = -hB^m_1F_{3,2}$$

$$g_{2,2} = -hA^m_3F_{7,6}$$

$$g_{2,3} = 1 - hB^m_1F_{3,4}$$

$$g_{2,4} = -hA^m_3F_{7,8}$$

$$g_{5,1} = -hC^m_1F_{3,2}$$

$$g_{5,2} = -hB^m_3F_{7,6}$$

$$g_{5,3} = -hC^m_1F_{3,4}$$

$$g_{5,4} = 1 - hB^m_3F_{7,8}.$$

Similarly as in (I) for the normal displacement, I define the radial spheroidal, transverse spheroidal and toroidal components of the normal stress as:

$$[\hat{\mathbf{n}} \cdot \tau]_{radial} = \sum_{n=1}^{\infty} [\hat{\mathbf{n}} \cdot \tau]^{m,n}_{radial} e^{im\phi} \tag{B.41}$$

$$[\hat{\mathbf{n}} \cdot \tau]_{transverse} = \sum_{n=1}^{\infty} [\hat{\mathbf{n}} \cdot \tau]^{m,n}_{transverse} e^{im\phi} \tag{B.42}$$

$$[\hat{\mathbf{n}} \cdot \tau]_{toroidal} = \sum_{n=1}^{\infty} [\hat{\mathbf{n}} \cdot \tau]^{m,n}_{toroidal} e^{im\phi} \tag{B.43}$$

At the solid side of the ICB, the above three components are found from taking inner product of the normal stress of degree n with $\hat{\mathbf{r}} Y_l^m$, $r \nabla Y_l^m$ and $i Y_l^m \times \nabla \mathbf{r}$ of degree l and integrating the resulting expressions over unit sphere. These expressions are then simplified by using the orthogonality properties of the associated Legendre functions. For $n = 1$, $n = 3$ and $n = 2$, these components at the solid side of the ICB are represented by the following:

$$[\hat{\mathbf{n}} \cdot \tau]^{m,1}_{radial}(a_-) = \sum_{i=1}^{14} Q_{1,i} y_i \tag{B.44}$$

$$[\hat{\mathbf{n}} \cdot \tau]^{m,3}_{radial}(a_-) = \sum_{i=1}^{14} Q_{4,i} y_i \tag{B.45}$$

$$[\hat{\mathbf{n}} \cdot \tau]^{m,1}_{transverse}(a_-) = \sum_{i=1}^{14} Q_{3,i} y_i \tag{B.46}$$

$$[\hat{\mathbf{n}} \cdot \tau]^{m,3}_{transverse}(a_-) = \sum_{i=1}^{14} Q_{6,i} y_i \tag{B.47}$$

$$i[\hat{\mathbf{n}} \cdot \tau]^{m,2}_{toroidal}(a_-) = \sum_{i=1}^{14} Q_{7,i} y_i \tag{B.48}$$

where

$$Q_{1,i} = 2\mu a(E_{1,1}\delta_{i,1} + E_{1,3}\delta_{i,3}) + \lambda\delta_{i,2}$$

$$-h[\lambda(A_3^m A_{10,i}^0 + B_1^m A_{2,i}^0) + 2\mu(A_3^m \xi_{4,i} + B_1^m \xi_{1,i})]$$

$$+\frac{h\mu}{a}(8A_3^m \delta_{i,12} + B_1^m \delta_{i,4} - 3mJ_2^m \delta_{i,8})$$

$$Q_{3,i} = 2\mu\delta_{i,4} - \mu h(4A_3^m A_{12,i}^0 - B_1^m A_{4,i}^0) - 3m\mu h J_2^m A_{8,i}^0 + \frac{\lambda}{a}h(-2A_3^m\delta_{i,10} + B_1^m\delta_{i,2})$$

$$+\frac{2\mu}{r^2}h(-2A_3^m\delta_{i,9} + B_1^m\delta_{i,1}) + \frac{2\mu}{r^2}h(32A_3^m\delta_{i,11} - 3B_1^m\delta_{i,3}) + 6m\frac{2\mu}{r^2}hJ_2^m\delta_{i,7}$$

$$Q_{4,i} = 2\mu a(E_{9,9}\delta_{i,9} + E_{9,11}\delta_{i,11}) + \lambda\delta_{i,10} - h[\lambda(B_3^m A_{10,i}^0 + C_1^m A_{2,i}^0)$$

$$+2\mu(B_3^m\xi_{4,i} + C_1^m\xi_{1,i})] + \frac{h\mu}{a}(3B_3^m\delta_{i,12} - 2C_1^m\delta_{i,4} - 3mH_2^m\delta_{i,8})$$

$$Q_{6,i} = 2\mu\delta_{i,12} - \mu h(9B_3^m A_{12,i}^0 - 4B_1^m A_{4,i}^0) - 3m\mu h H_2^m A_{8,i}^0 + \frac{\lambda}{a}h(3B_3^m\delta_{i,10} + 8C_1^m\delta_{i,2})$$

$$+\frac{2\mu}{r^2}h(3B_3^m\delta_{i,9} + 8C_1^m\delta_{i,1}) + \frac{2\mu}{r^2}h(27B_3^m\delta_{i,11} - 8C_1^m\delta_{i,3}) - 9m\frac{2\mu}{r^2}hH_2^m\delta_{i,7}$$

$$Q_{7,i} = 6\mu\delta_{i,8} - 3m\mu h(J_3^m A_{12,i}^0 + H_1^m A_{4,i}^0) - 3\mu h B_2^m A_{8,i}^0 - 3m\frac{\lambda}{a}h(J_3^m\delta_{i,10} + H_1^m\delta_{i,2})$$

$$-3m\frac{2\mu}{a^2}h(J_3^m\delta_{i,9} + H_1^m\delta_{i,1}) + 3m\frac{2\mu}{a^2}h(6J_3^m\delta_{i,11} + H_1^m\delta_{i,3}) + 36\frac{\mu}{a^2}hB_2^m\delta i, 7.$$

At the liquid side of the ICB, the normal stress in terms of the reduced pressure χ and additional gravitational potential V_1 is

$$[\hat{\mathbf{n}}\cdot\tau](a_+) = -\rho(a_+)[\chi + V_1 + \mathbf{u}\cdot\mathbf{g}_0]_{p=r-hP_2}\,\hat{\mathbf{n}} \tag{B.49}$$

where

$$\mathbf{u}\cdot\mathbf{g}_0 = -|\mathbf{g}|_{p=r-hp_2}[\hat{\mathbf{n}}\cdot\mathbf{u}]_{a_+} = -|\mathbf{g}|_{p=r-hp_2}[\hat{\mathbf{n}}\cdot\mathbf{u}]_{a_-} \tag{B.50}$$

using the boundary condition (I), and

$$-|\mathbf{g}|_{p=r-hp_2} = -g_0(r) + \tfrac{2}{3}\Omega^2 r + \tfrac{2}{3}\Omega^2 hP_2 - \tfrac{dh}{dr}g_0 P_2. \tag{B.51}$$

Substituting (B.50) into (B.49), the radial spheroidal part of the normal stress in the ESD at the liquid side of the ICB is then expressed in terms of quantities on both the liquid and solid sides of the ICB

$$[\hat{\mathbf{n}}\cdot\tau]^{m,n}_{radial}(a_+) = -\rho_0(a_+)\{(\chi_l^m + \Phi_l^m)[J0]_l^n - h(\frac{d\chi_l^m}{dr} + \frac{d\Phi_l^m}{dr})[J2]_l^n\}_{r=a_+}$$

$$+\rho_0(a_+)[g_0(a) - \frac{2}{3}\Omega^2 a]\{u_l^m[J0]_l^n + \frac{h}{a}v_l^m[J1]_l^n + m\frac{h}{a}it_l^m[J3]_l^n$$

$$-h\frac{du_l^m}{dr}[J2]_l^n\}_{r=a_-} + \rho_0(a_+)[\frac{dh}{dr}g_0(a) - \tfrac{2}{3}\Omega^2 h]u_l^m(a_-)[J2]_l^n \qquad \text{(B.52)}$$

where

$$[J0]_l^n = \delta_{l,n}\frac{4\pi(-1)^m}{2n+1}$$

$$[J1]_l^n = [2(n+3)A_l^m\delta_{l,n+2} + 3B_l^m\delta_{l,n} - 2(n-2)C_l^m\delta_{l,n-2}]\frac{4\pi(-1)^m}{2n+1}$$

$$[J2]_l^n = [A_l^m\delta_{l,n+2} + B_l^m\delta_{l,n} + C_l^m\delta_{l,n-2}]\frac{4\pi(-1)^m}{2n+1}$$

$$[J3]_l^n = [-3(J_l^m\delta_{l,n+1} + H_l^m\delta_{l,n-1})]\frac{4\pi(-1)^m}{2n+1}.$$

Note that the integer l arises from the independent set of the associated Legendre functions of degree l which are multiplied to the boundary condition (IV) to obtain its three components. Therefore, l will be determined by the choice of degree n.

Since $[\hat{\mathbf{n}}\cdot\tau]_{radial}(a_+) = [\hat{\mathbf{n}}\cdot\tau]_{radial}(a_-)$ at the ICB, the final expressions of this condition for $n = 1$ and $n = 3$ can be reached by making the following substitutions: Φ_1^m and Φ_3^m from (B.24) and (B.25), $d\chi_1^m/dr$ and $a\chi_3^m$ from (B.13) and (B.17), and dy_1/dr and dy_9/dr from (B.29) and (B.30); replacing all the zero'th order quantities, which are continuous across the ICB on the liquid side of the ICB, by those on the solid side of the ICB, and moving all quantities of the solid inner core to the LHS

$$\sum_{i=1}^{14} \Pi_{1,i}^m y_i(a_-) = \frac{1}{ag_0(a)}[g_{1,1}\chi_1^m + g_{1,2}\chi_3^m + g_{1,3}(\frac{dy_3}{dr})_{a_+} + g_{1,4}(\frac{dy_{12}}{dr})_{a_+}] \tag{B.53}$$

$$\sum_{i=1}^{14} \Pi_{4,i}^m y_i(a_-) = \frac{1}{ag_0(a)}[g_{4,1}\chi_1^m + g_{4,2}\chi_3^m + g_{4,3}(\frac{dy_3}{dr})_{a_+} + g_{4,4}(\frac{dy_{12}}{dr})_{a_+}] \tag{B.54}$$

where

$$\Pi_{1,i}^m = -\frac{1}{a\rho_0(a_+)g_0(a)}Q_{1,i} + \frac{1}{ag_0(a)}[g_0(a) - \frac{2}{3}\Omega^2 a]Q_{2,i}$$

$$+\frac{1}{g_0(a)}[(\frac{dh}{dr})_{a_-}g_0(a) - \frac{2}{3}\Omega^2 h](A_3^m\delta_{i,9} + B_1^m\delta_{i,1}) - \delta_{i,5}$$

$$+\frac{h}{R}[A_3^m(\frac{1}{g_0(a)}E_{13,9}\delta_{i,13} + \frac{1}{a}\delta_{i,14}) + B_1^m(\frac{1}{g_0(a)}E_{5,1}\delta_{i,5} + \frac{1}{a}\delta_{i,6})]$$

$$+\frac{h}{g_0(a)}\{A_3^m[(e_{6,5} - e_{6,6}a_{13,9})\delta_{i,9} + e_{6,7}g_0(a)\delta_{i,13}]$$

$$+B_1^m[(e_{2,1} - e_{2,4}a_{5,1})\delta_{i,1} + e_{2,3}g_0(a)\delta_{i,5}]\}$$

$$\Pi_{4,i}^m = -\frac{1}{a\rho_0(a_+)g_0(a)}Q_{4,i} + \frac{1}{ag_0(a)}[g_0(a) - \frac{2}{3}\Omega^2 a]Q_{5,i}$$

$$+\frac{1}{g_0(a)}[(\frac{dh}{dr})_{a_-}g_0(a) - \frac{2}{3}\Omega^2 h](B_3^m\delta_{i,9} + C_1^m\delta_{i,1}) - \delta_{i,13}$$

$$+\frac{h}{R}[B_3^m(\frac{1}{g_0(a)}E_{13,9}\delta_{i,13} + \frac{1}{a}\delta_{i,14}) + C_1^m(\frac{1}{g_0(a)}E_{5,1}\delta_{i,5} + \frac{1}{a}\delta_{i,6})]$$

$$+\frac{h}{g_0(a)}\{B_3^m[(e_{6,5} - e_{6,6}a_{13,9})\delta_{i,9} + e_{6,7}g_0(a)\delta_{i,13}]$$

$$+C_1^m[(e_{2,1} - e_{2,4}a_{5,1})\delta_{i,1} + e_{2,3}g_0(a)\delta_{i,5}]\}$$

$$g_{1,1} = 1 - hB_1^m e_{2,2}$$

$$g_{1,2} = -hA_3^m e_{6,6}$$

$$g_{1,3} = -hB_1^m e_{2,4}$$

$$g_{1,4} = -hA_3^m e_{6,8}$$

$$g_{4,1} = -hC_1^m e_{2,2}$$

$$g_{4,2} = 1 - hB_3^m e_{6,6}$$

$$g_{4,3} = -hC_1^m e_{2,4}$$

$$g_{4,4} = -hB_3^m e_{6,8}$$

Similarly, continuity of the transverse spheroidal and toroidal components of the normal stress leads to three more boundary conditions, $n = 1$ and $n = 3$ for the spheroidal and $n = 2$ for the toroidal:

$$\sum_{i=1}^{14} \Pi_{3,i}^m y_i(a_-) = g_{3,1}\chi_1^m + g_{3,2}\chi_3^m \tag{B.55}$$

$$\sum_{i=1}^{14} \Pi_{6,i}^m y_i(a_-) = g_{6,1}\chi_1^m + g_{6,2}\chi_3^m \tag{B.56}$$

$$\sum_{i=1}^{14} \Pi_{7,i}^m y_i(a_-) = g_{7,1}\chi_1^m + g_{7,2}\chi_3^m \tag{B.57}$$

where

$$\Pi_{3,i}^m = -\frac{1}{2\rho_0(a_+)ag_0(a)}Q_{3,i} - \frac{h}{2ag_0(a)}[g_0(a) - \frac{2}{3}\Omega^2 a]$$

$$(-2A_3^m\delta_{i,9} + 3B_1^m\delta_{i,1}) - \frac{h}{2a}(-2A_3^m\delta_{i,13} + 3B_1^m\delta_{i,5})$$

$$\Pi_{6,i}^m = -\frac{1}{12\rho_0(a_+)ag_0(a)}Q_{6,i}$$

$$-\frac{h}{12ag_0(a)}[g_0(a) - \frac{2}{3}\Omega^2 a](3B_3^m\delta_{i,9} + 8C_1^m\delta_{i,1}) - \frac{h}{12a}(3B_3^m\delta_{i,13} + 8C_1^m\delta_{i,5})$$

$$\Pi_{7,i}^m = \frac{1}{6\rho_0(a_+)ag_0(a)}Q_{7,i} + \frac{3mh}{6ag_0(a)}[g_0(a) - \frac{2}{3}\Omega^2 a](G_3^m\delta_{i,9} + H_1^m\delta_{i,1})$$

$$-\frac{3mh}{6a}(G_3^m\delta_{i,13}+H_1^m\delta_{i,5})$$

$$g_{3,1}=\frac{3}{2}\frac{hB_1^m}{a^2g_0(a)}$$

$$g_{3,2}=-\frac{hA_3^m}{a^2g_0(a)}$$

$$g_{6,1}=\frac{2}{3}\frac{hC_1^m}{a^2g_0(a)}$$

$$g_{6,2}=\frac{1}{4}\frac{hB_3^m}{a^2g_0(a)}$$

$$g_{7,1}=\frac{m}{2}\frac{hH_1^m}{a^2g_0(a)}$$

$$g_{7,2}=\frac{m}{2}\frac{hJ_3^m}{a^2g_0(a)}$$

The above 7 continuity conditions (B.53), (B.39), (B.55), (B.54), (B.40), (B.56) and (B.57) at the ICB depend on only 4 quantities from the liquid side of the ICB χ_1^m, χ_3^m, $(dy_5/dr)_{a_-}$ and $(dy_{13}/dr)_{a_-}$. Because this set of equations is linear in these 4 variables, they can be further simplified into the final forms listed in §8.3

$$\sum_{i=1}^{14}\Lambda_{1,i}^m y_i=\frac{1}{ag_0(a)}\chi_1^m \tag{B.58}$$

$$\sum_{i=1}^{14}\Lambda_{2,i}^m y_i=\frac{1}{g_0(a)}\left(\frac{dy_5}{dr}\right)_{a_+} \tag{B.59}$$

$$\sum_{i=1}^{14}\Lambda_{3,i}^m y_i=0 \tag{B.60}$$

$$\sum_{i=1}^{14}\Lambda_{4,i}^m y_i=\frac{1}{ag_0(a)}\chi_3^m \tag{B.61}$$

$$\sum_{i=1}^{14}\Lambda_{5,i}^m y_i=\frac{1}{g_0(a)}\left(\frac{dy_{13}}{dr}\right)_{a_+} \tag{B.62}$$

$$\sum_{i=1}^{14}\Lambda_{6,i}^m y_i=0 \tag{B.63}$$

$$\sum_{i=1}^{14} \Lambda_{7,i}^m y_i = 0 \qquad \text{(B.6-1)}$$

where

$$\Lambda_{1,i}^m = [1 + hB_1^m(F_{3,4} + e_{2,2})](g_{2,3}\Pi_{1,i}^m - \frac{g_{1,3}}{a}\Pi_{2,i}^m) - g_{1,2}\Lambda_{4,i}^m - g_{1,4}\Lambda_{5,i}^m$$

$$\Lambda_{2,i}^m = \frac{1}{g_{2,3}}[\Pi_{2,i}^m - ag_{2,1}(g_{2,3}\Pi_{1,i}^m - \frac{g_{1,3}}{a}\Pi_{2,i}^m)] - ag_{2,2}\Lambda_{4,i}^m - g_{2,4}\Lambda_{5,i}^m$$

$$\Lambda_{3,i}^m = \Pi_{3,i}^m - ag_0(a)(g_{3,1}\Lambda_{1,i}^m + g_{3,2}\Lambda_{4,i}^m)$$

$$\Lambda_{4,i}^m = \frac{1}{g_{4,2}}[\Pi_{4,i}^m - g_{4,1}(g_{2,3}\Pi_{1,i}^m - \frac{g_{1,3}}{a}\Pi_{2,i}^m) - \frac{g_{4,3}}{a}\Pi_{2,i}^m] - \frac{g_{4,4}}{a}\Lambda_{5,i}^m$$

$$\Lambda_{5,i}^m = -a(g_{4,1} + g_{5,1})g_{2,3}\Pi_{1,i}^m - (g_{4,3} + g_{5,3})\Pi_{2,i}^m + ag_{5,2}\Pi_{4,i}^m$$

$$-[1 + hB_3^m(e_{6,6} + F_{7,8})]\Pi_{5,i}^m$$

$$\Lambda_{6,i}^m = \Pi_{6,i}^m - ag_0(a)g_{6,1}\Lambda_{1,i}^m - ag_0(a)g_{6,2}\Lambda_{4,i}^m$$

$$\Lambda_{7,i}^m = \Pi_{7,i}^m - ag_0(a)g_{7,1}\Lambda_{1,i}^m - ag_0(a)g_{7,2}\Lambda_{4,i}^m.$$

Note that the order of calculation is: first $\Lambda_{5,i}^m$, then $\Lambda_{4,i}^m$, $\Lambda_{1,i}^m$, $\Lambda_{2,i}^m$, $\Lambda_{3,i}^m$, $\Lambda_{6,i}^m$, and finally $\Lambda_{7,i}^m$.